DESCRIPTION OF THE BAKKEN FORMATION'S ROCK PROPERTIES OF THE WILLISTON BASIN, NORTH DAKOTA
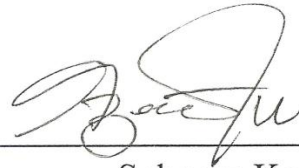
A Thesis Presented to

the Department of Earth and Atmospheric Sciences

University of Houston

In Partial Fulfillment

of the Requirements for the Degree

Master of Science

By

Sebnem Kocoglu

May 2013

DESCRIPTION OF THE BAKKEN FORMATION`S

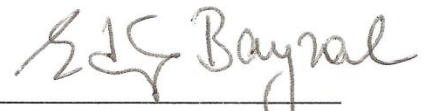# ROCK PROPERTIES OF THE WILLISTON BASIN,

NORTH DAKOTA

_____
Sebnem Kocoglu

APPROVED

_____
Dr. John P. Castagna

_____
Dr. Robert Stewart

_____
Dr. Edip Baysal

_____
Dean of Natural Sciences and Mathematics

ii

Acknowledgements

Every person who stayed with me during this journey is very valuable for me. I am grateful to have you all in my life.

First and foremost, I would like to express my sincere appreciation to my advisor, Dr. John Castagna, for his guidance. Your experience and knowledge were always helped me. Also, I would like to thank my co-advisor, Dr. Robert Stewart, for providing excellent data, and his continuous friendly support on my research. My dear teacher and committee member Dr. Edip Baysal, thank you very much for your friendship and support. I appreciate his valuable assistance in the preparation and completion of this study .Thank you very much to AGL laboratory assistant and my friend Bode Omoboya for all the information and friendship.

All my friends who have been with me during my journey thank you very much. I did not feel homesick even I was thousand miles away from home. I am glad you were here.

Dear Mom, Dad, and rest of my family, I cannot find a word to describe my appreciation and gratitude for you. I was able to continue with your love and support. Thank you for believing in me.

My very special thanks go to the one person, Volkan Bilgin. I would not be able to come this far without you. I am really grateful you were with me since from the beginning, and I am thankful that you will be with me until the end.

DESCRIPTION OF THE BAKKEN FORMATION'S ROCK PROPERTIES OF THE WILLISTON BASIN, NORTH DAKOTA

An Abstract of a Thesis

Presented to

the Department of Earth and Atmospheric Sciences

University of Houston

In Partial Fulfillment

of the Requirements for the Degree

Master of Science

By

Sebnem Kocoglu

May 2013

Abstract

It is possible to determine rock properties by utilizing seismic inversion techniques. The inversion technique is the most frequently used, by which the seismic interpreters derive lithology and physical properties.

In this study, the 2D pre-stack seismic data was obtained from the analysis of Ross Field of the Williston Basin located in North Dakota. The Williston Basin has been used as a production area for numerous years, which makes this particular area one of importance, since there has been an increase in production using hydraulic fracturing and horizontal wells. The relationship between rock properties and well performance is very important in this kind of unconventional reservoir. The lateral changes in rock properties are also important to determine well locations. Via AVO analysis and inversion, rock properties were observed in the unconventional reservoir.

The Bakken Formation is one of the main hydrocarbon-prone formations in the Williston Basin. This formation has generated approximately 200 to 400 billion barrels of oil and boasts a low permeability system. Three distinct members (the Upper Shale Member, the Middle Mixed lithology Member, and the Lower Shale Member) are present in this location and in this study.

The Bakken Formation members have been analyzed according to their physical properties, obtained by inversion and LMR cross-plotting methods.

Table of Contents

List of Figures

Introduction

Seismic inversion method has been an effective way for defining reservoir rock properties for many years. It is mostly needed to see the subsurface clearly in order to define rock properties and reservoir characterizations (Russell, 2005). Although the physical properties of a formation cannot be identified using a seismic section, the inversion method enhances the resolution and adds log results to the seismic section, thus allows for geoscientists to make further speculations about the properties of the formation (Russell, 1991).

The oil and gas exploration in North Dakota had been mainly focused on conventional reservoirs. After discovery of the unconventional Bakken shale, oil and gas production dramatically increased from 2005 to 2011. The oil production rates are specifically important due to the tightening world liquid fuels supply and demand balances, as well as the increasing price volatility. Why It is speculated that the Bakken can help eradicate these economical pitfalls because oil production spiked 87% between 2005 to 2011, from 3 MMbbl/d to 400 MMbbl/d. However, due to the depletion of conventional reservoirs in North Dakota, the oil and gas exploration has been oriented towards unconventional reservoirs (Mason, 2012).

A plethora of successful wells have been discovered within the Bakken Formation in Ross Field, North Dakota. In this study, horizons and inversion analysis are based on the

actual depth of the Bakken Formation; therefore, utilizing the Bakken Formation as a reference, it allows for the new wells that should be drilled to be discovered.

The purpose of this study is to unearth information about rock properties within the Bakken Formation by using AVO analysis and seismic inversion methods. Since the previous AVO analysis gives inaccurate information on the Bakken Formation, pre-stack seismic inversion was used to make it more effective.

Chapter 1

Study Area and Geological Background

1.1 Study Area and The Williston Basin

The study area is located in North Dakota, United States of America, specifically within the Williston Basin. The Williston Basin covers around 300,000 square miles (777,000 km^2) from North Dakota and Montana in the USA to Manitoba in Canada (Figure 1.1).
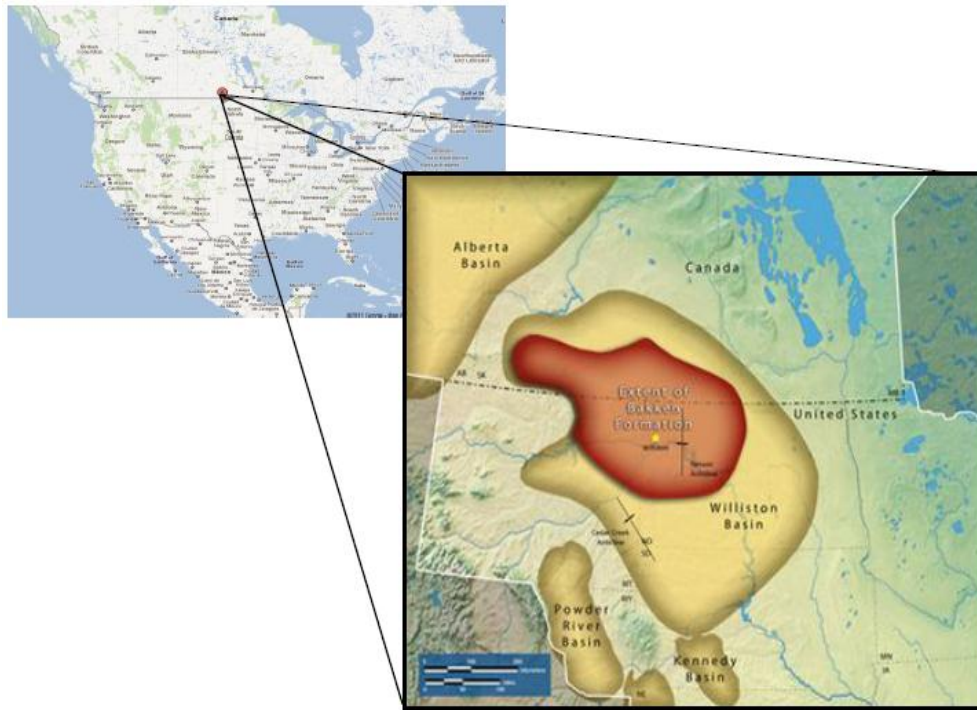
Figure 1.1Survey Location with Google map view and extension of the Bakken formation and Williston Basin. (Source: http://www.undeerc.org/bakken/bakkenformation.aspx)

In the Williston Basin, the deepest basement location is near North Dakota. There are two major anticlines in the basin, which are the Nesson and Cedar Creek. There are two types of resource systems: conventional and unconventional. Unconventional systems are mostly utilized in North Dakota. A staggering 94% of oil locked within shale formations are tight formations (Hayes, 1984). Tight formations have low porosity and low permeability, thus, wells are drilled vertically and horizontally; oil flows with difficulty in tight formations. Using the horizontal well, water and sand is pumped down the hole with a high pressure and creates open fractures that are known as hydraulic fracturing. Artificial permeability is created in tight rock with hydraulic fracturing (Carl T. et al, 2010), thus, reservoir rock has high permeability and high porosity.
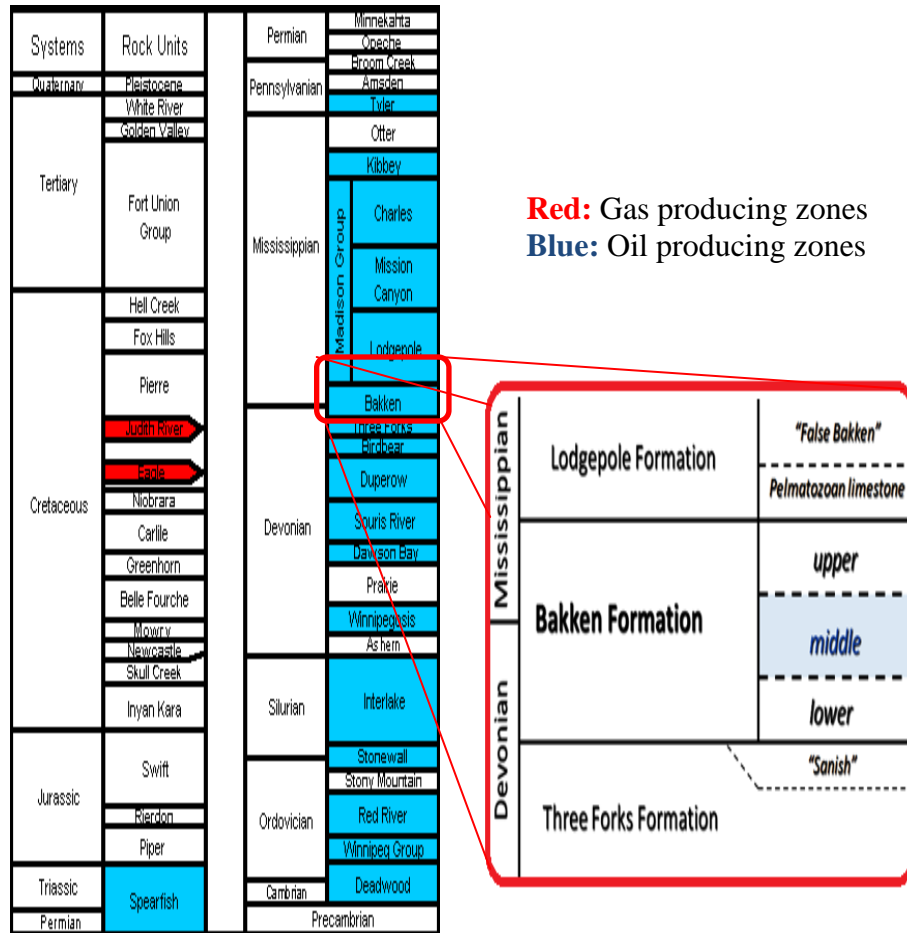
Figure 1.2 Generalized stratigraphic column of the Williston Basin (Modified from source: https://www.dmr.nd.gov/ndgs/Resources/WBPetroleumnew.asp)

1.2 Geology of the Bakken Formation

The Bakken Formation overlies the Three Forks Formation and is overlain by the Lodgepole Formation. The Bakken formed in North Dakota, USA in the Early Mississippian age. It is approximately 200,000 square-miles (520,000 km^2) in area of the subsurface of the Williston Basin (Pitman et al., 2001). The formation is completely on the subsurface with no surface outcrop. The formation was discovered in the early 1950s, but since technology was not as developed, the production period had to wait until the 1980s. Although technology did not allow for the production to begin until the 1980s, the Bakken Formation was known and described as one of the biggest resources in the USA. According to the USGS report in 2008, the estimated amount of technically recoverable oil ready to be produced in the Bakken Formation was approximately 3 − 4.3 billion barrels by the end of 2007.

The Bakken Formation overlies the Three Forks Formation and underlies the Lodgepole Formation. The Lodgepole Formation is the base unit of Mississippian Age. The oil and gas from the Lodgepole Formation produce hot and low salinity waters together (Manz, 2008) and it also consists of shale and dolomite. The Three Forks Formation consists of dolomite, shale, siltstone, mudstones, and anhydrite (Karasinski, 2006).

The Upper and Lower Members of the Bakken are organic-rich shale, whereas the Middle Bakken is formed of a mixture of clastics and carbonates. The Middle Bakken usually represents the reservoir and it consists mainly of sandstone and dolomite. In North Dakota, the Bakken Formation has a maximum thickness of 150 ft. (46 m) which

can also be seen in the well sites within the well log analysis located in Chapter 3. In the west of the well location lies the Nesson anticline within the north-south direction. The upper and lower shale members depict very high gamma rays, high sonic slowness, and low resistivity. Within the Bakken Formation, porosity and permeability are 5% and 0.04 mD on average, respectively. This shows that the permeability of the formation is low compared to the oil reservoirs (Pitman et al, 2001).

Chapter 2

Red Sky Seismic Survey and Data Set

2.1 Data Set

2D 3C Red Sky Seismic Survey Data and all well logs owned by Hess Company were obtained from the Allied Geophysical Laboratory (AGL). The data set used in this study includes two seismic lines: 1001 and 2001 seismic lines and ten well logs. The study field located in North Dakota is called Ross Field as depicted below (Figure 2.1).
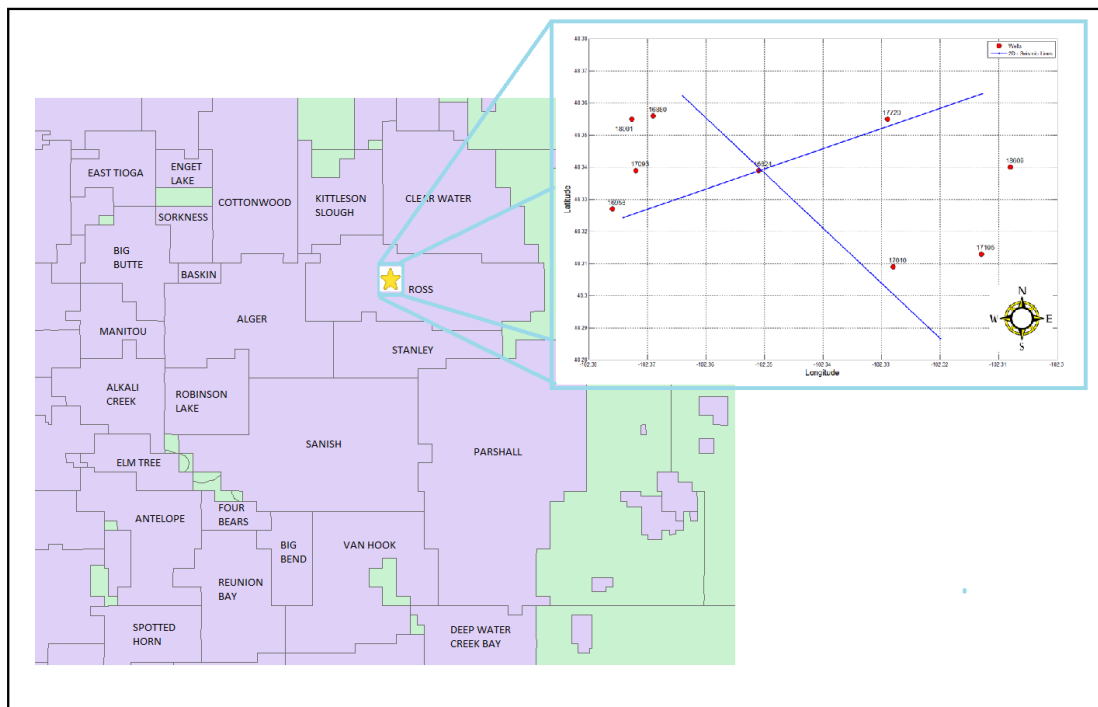
Figure 2. 1 Ross field and data sets locations.

Along the first seismic line (1001 seismic line) oriented NW to SE, there are 265 shots with a 110 ft. (34 m) interval and 486 receivers with a 55 ft. (17 m) interval. Along the second seismic line, (the 2001 seismic line), oriented SW to NE, there are 179 shots with a 110 ft. (34 m) interval and 330 receivers with a 55 ft. (17 m) interval. During the seismic data collection, receivers on both of the seismic lines were continuously recording. In other words, while only one shot was fired along one line, the receivers on both of the lines were collecting data. Therefore, the two seismic lines provide nearly three-dimensional data, albeit in poor quality. The low quality of the data is due to the lack of sufficient number of inline and crossline. The shot gathers for both lines are depicted in Figure 2.2. In order to attenuate the unwanted signals, seismic data processing was applied using Echos seismic processing software.

(a)

(b)

(c)
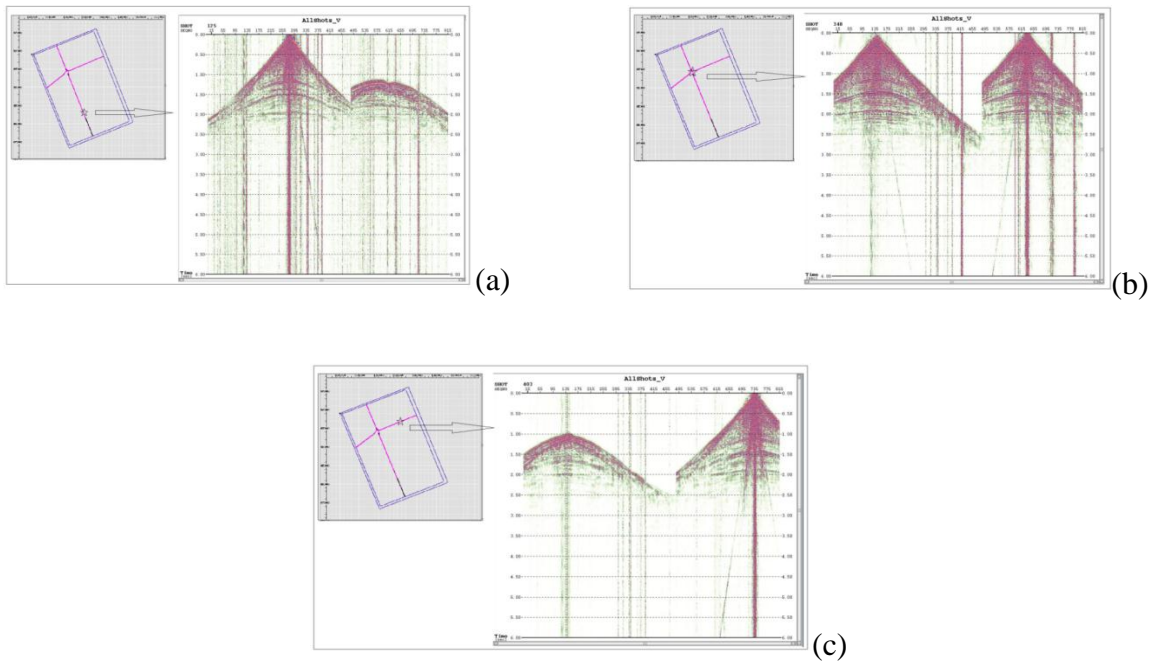
Figure 2. 2 Receivers response from both seismic lines in different shot locations

2.2 Data Preparation

Seismic data are two-dimensional and include three components: vertical component (Z), transverse component (Y), and radial component (X). Three different receivers collecting data for the three components were placed at every shot point to successfully collect the data. For each shot, three traces were stored by one station. As mentioned before, all receivers were recorded at every shot.

Among all three components, only the vertical component (Z) is required for further analyses. The vertical component was separated from shot gathers. In order to do that, one must take one of the three traces that were captured and cleaned along the trace. After the separation, the shot-gathers have vertical components only to be used for further analyses. Initially, the dataset and geometry were created in 3D. After separation of the two seismic lines, the dataset and geometry were changed into 2D.

2.3 Geometry Definition and Static Corrections

Observer logs and supported survey (SPS) files were used to create geometry. Each line, receiver, shot, and channel was uploaded in the program with their X&Y coordinates using SPS files. The created geometry is shown in Figure 2.3 using a Quality Control (QC) map. Common Depth Point (CDP) model was created after creating 2D geometry. The geometries were determined as a crooked line for both seismic lines. The crossline was taken at a wider angel to avoid placing CDPs out of the 2D lines.
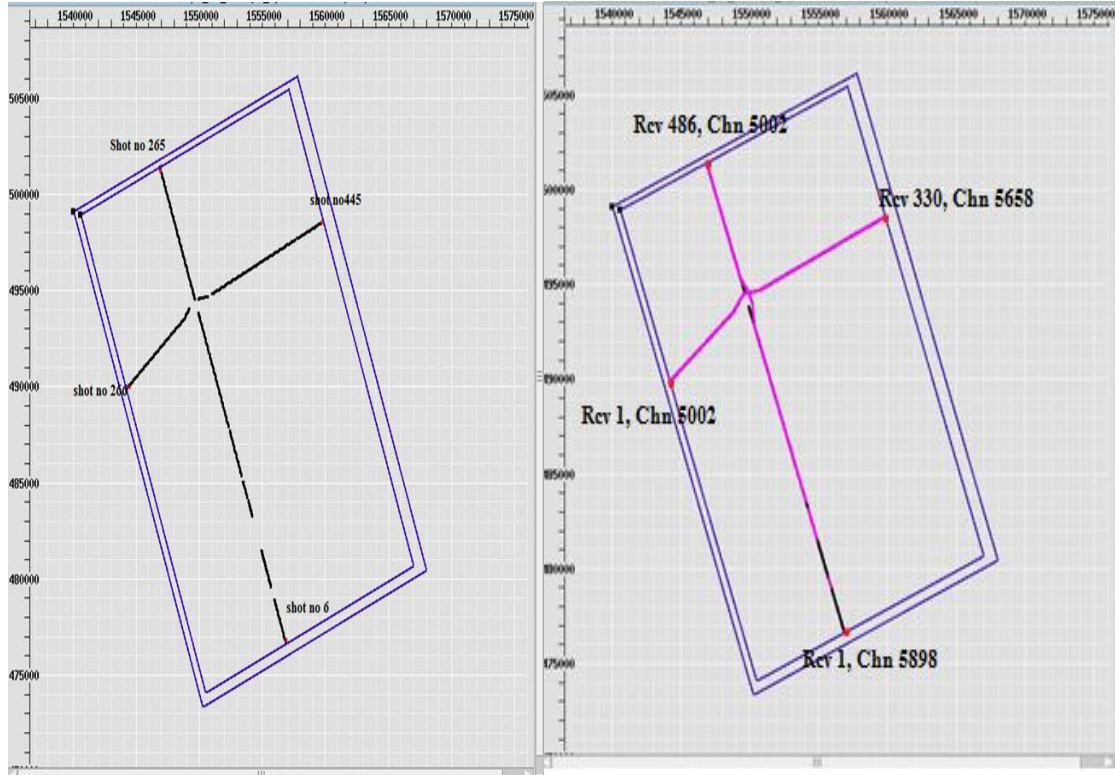
Figure 2. 3 Shot and receiver geometry

2.4 Seismic Processing

Before seismic processing, a suitable work flow that fits the purpose of this study was defined. The work flow relies on the corrected dataset, therefore, before the initiation of the seismic processing work flow, every shot location was analyzed, and thus eliminating the incorrect and poor traces. Additionally, void fire shots were also removed from the data by taking observer logs into consideration. The detailed seismic processing work flow is given in Figure 2.4.

11
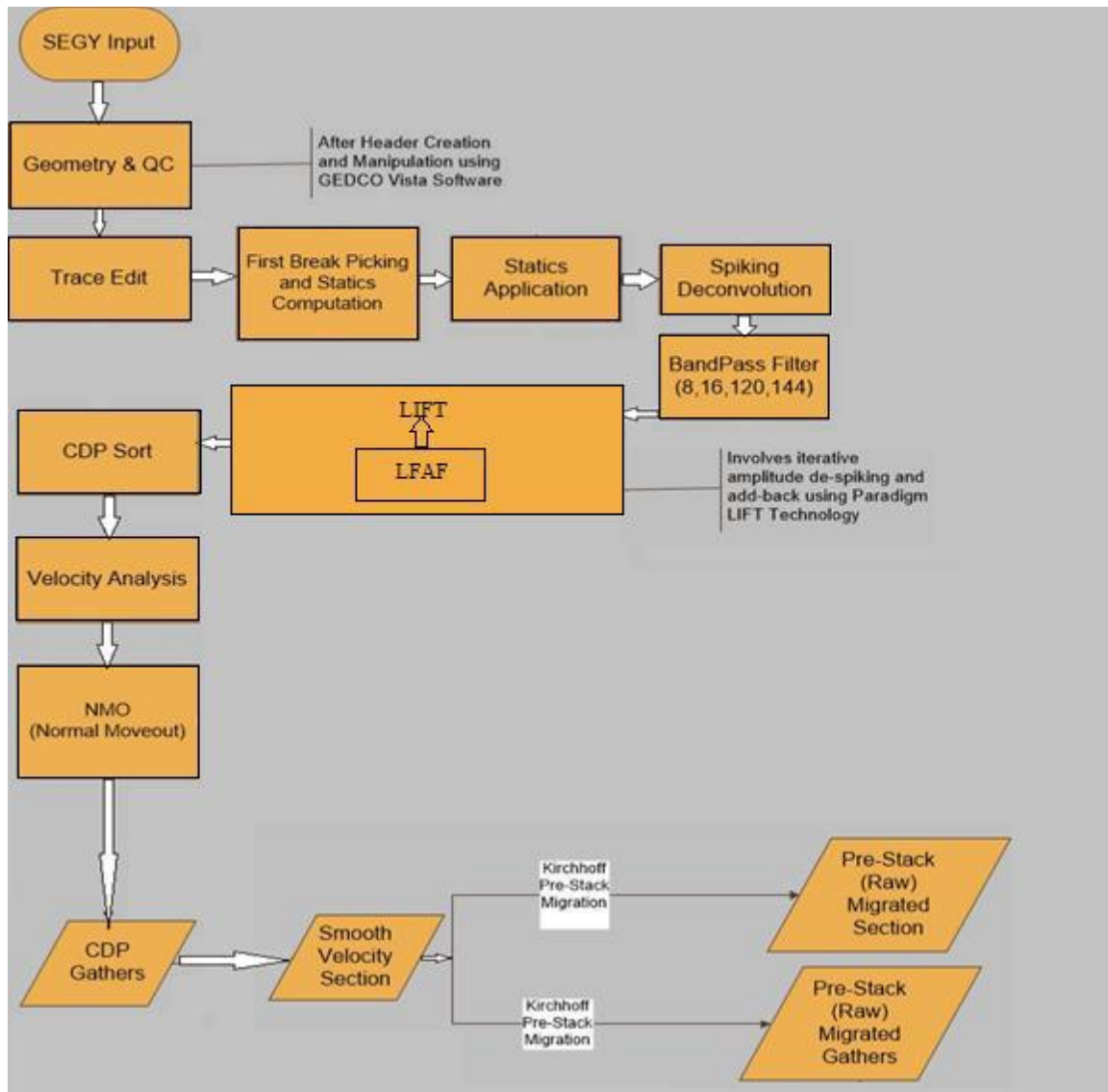
Figure 2. 4 Seismic processing work flows

After trace editing, first arrivals were auto picked for both seismic lines and combine with the elevation values to obtain an input for the static correction. The elevation values observed between 2150 ft. (656 m) and 2280 ft. (695 m), which indicate that it is above the sea level. Datum was fixed at 2300 ft. (701 m).

12

Primarily, wave-shape deconvolution was applied to get rid of unwanted or repeating wavelets (Figure 2.5). The main reason for applying the wave-shape deconvolution is so the data from multiple reflections can be saved. This method is only utilized to convert a wavelet to the whole data. It converts signatures from phase to minimum phase (Echos-Paradigm, 2011). Spiking deconvolution was applied after the wave-shape method to transform the wavelets minimum phase to zero phase (Figure 2.5).
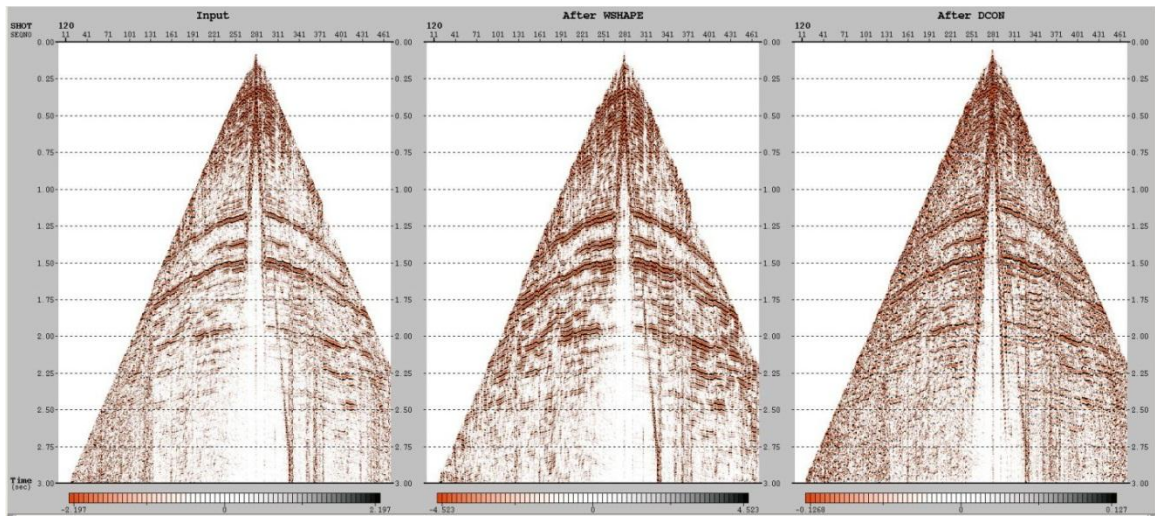
Figure 2. 5 Shot gather after wave-shape and deconvolution applications

Bandpass filter (8, 16,120, and 140 Hz) was applied to remove the high frequency noise. Next, Leading Intelligent Filter Design (LIFT) was applied to the data set in order to increase signal-to-noise ratio and conserve the amplitude integrity of seismic signal. Basically, this method separates the data to a signal model and noise, and then noise is suppressed and integrated to the signal model to create the output (Figure 2.6).
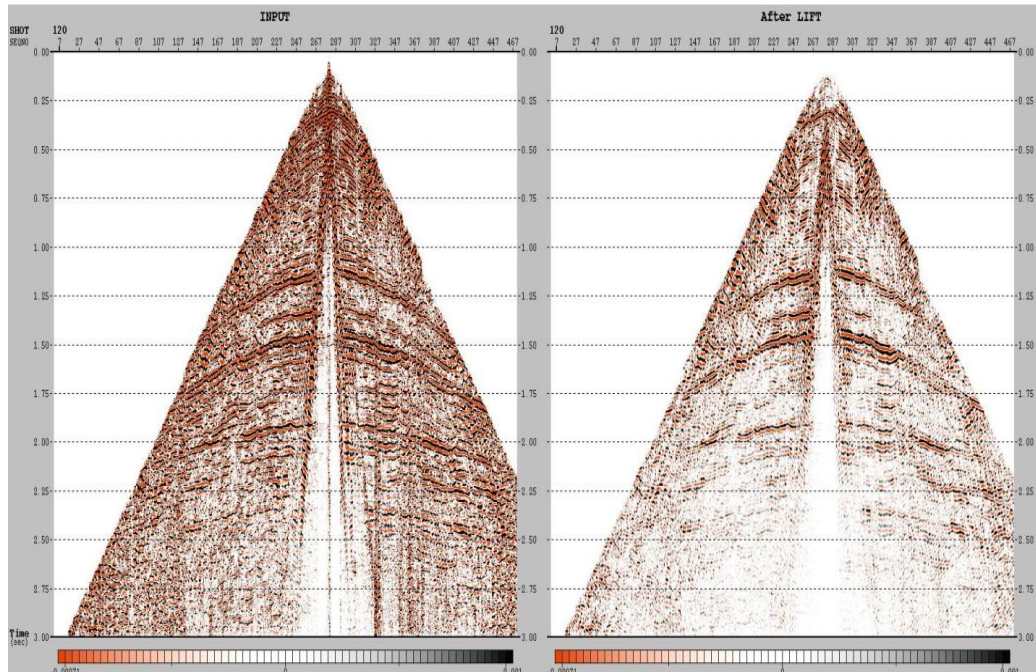
Figure 2. 6 Shot gather before and after LIFT application.

After the processes mentioned above, the data were sorted to CDP. Inline 1001 has 973 CDPs, and inline 2001 has 652 CDPs. Sorted data velocity analysis was applied on CDPs. Velocity picking was done at every ten CDP, then Normal Move-out Correction (NMO) was applied. NMO correction was utilized to remove the effect of the difference in a reflection arrival time caused by the source to receiver distance (offset). After all this process, all the output was stacked (Figure 2.7).

14
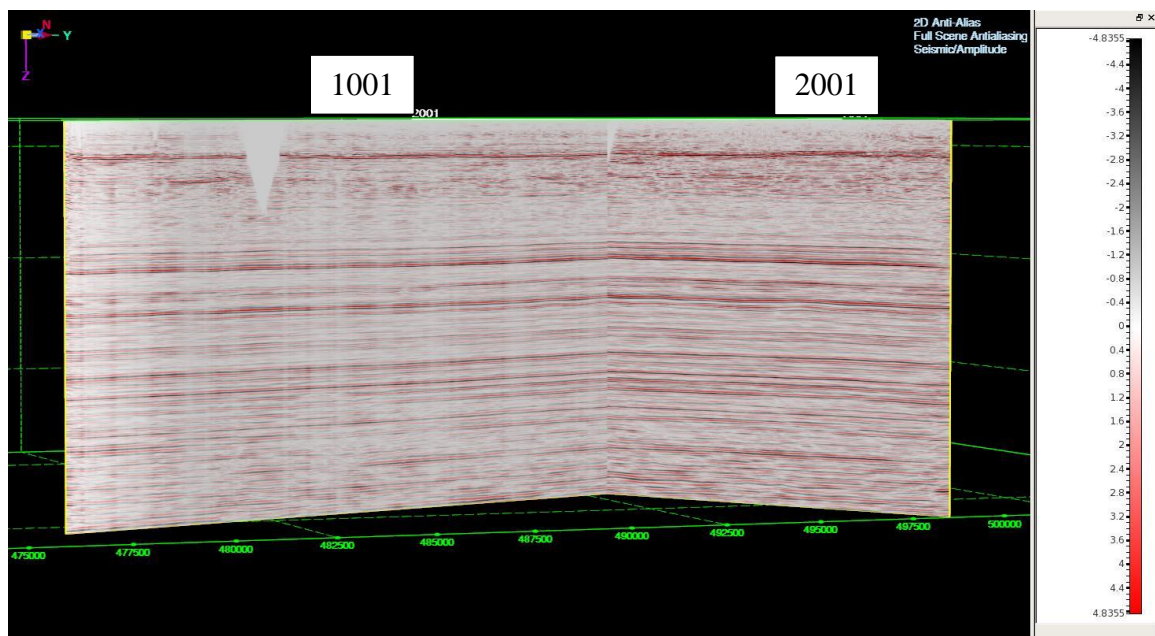
Figure 2. 7 Stacked data for seismic lines 1001 and 2001.

Chapter 3

Well Log Analysis and Interpretations

3.1 Well Log Data Sets

As previously mentioned, the study area is located in Ross Field, North Dakota and east of the Nesson Anticline. Well location is depicted in Figure 3.1. In the study area there are ten different wells. Well 1 is RS-BLACK STONE-156-91- 1011H-1; Well 2 is RS-VEDAA-156-91- 0336H-1; Well 3 is RS-NELSON-156-91 1423H-1; Well 4 is RS-STATE B-156-91- 1609H-1; Well 5 is RS-APELESE-156-91- 1522H-1, Well 6 is RS-HOWELL-156-91- 1207H-1; Well 7 is RS-RED CROWN-156-91- 2536H-1; Well 8 is RS-F NELSON-156-91- 2413H-1; Well 9 is PALERMO 2-18H; Well 10 is NELSON FARMS 1-24H (Figure 3.3).
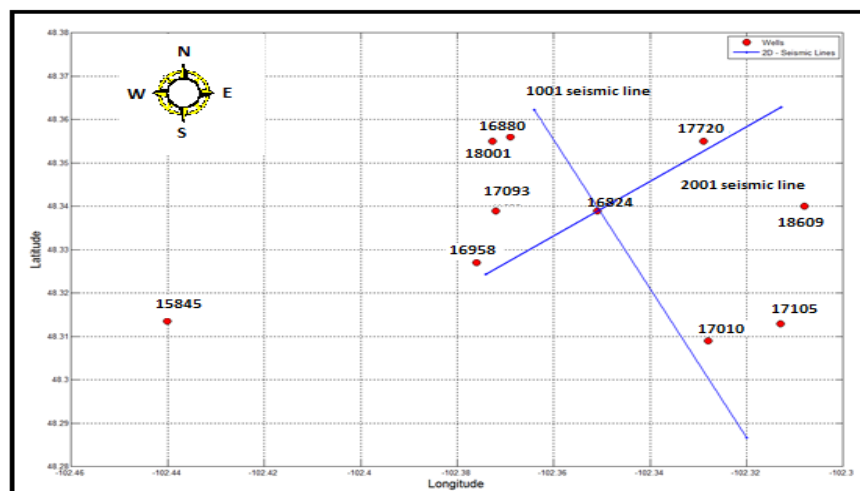
Figure 3. 1 Well locations in the study area, Ross field.

All the wells used in this study have horizontal and vertical components. However, not all of these wells have information from the Bakken Formation. Additionally, velocity, density, and gamma ray log information are not available for all the wells. Therefore, in order to figure out properties of the Bakken Formation all the available information from the available wells tried to be combined. The reason for the analysis is to characterize the Bakken Formation in its well log and to receive an accurate result in the oncoming created models.

3.2 Log Data Analysis

The well logs were analyzed in terms of its density, velocity, Vp/Vs ratio, depth, and thickness, Young's Modulus and Poisson's ratio. All the information deduced from log data analysis will be used to describe the Bakken Formation and will be compared to the results of the inversion method.

The well RS-NELSON-156-91 1423H-1 used for the seismic inversion method indicates characteristic properties of the Bakken Formation. Therefore, this log suite can be used for identification of the formation (Figure 3.2). The Upper and Lower Bakken shale gave very high gamma ray response while the Middle shale shows low gamma ray response. The well log data provides information not only for the Bakken Formation but also overlying Lodgepole Formation and underlying Three Forks Formation.
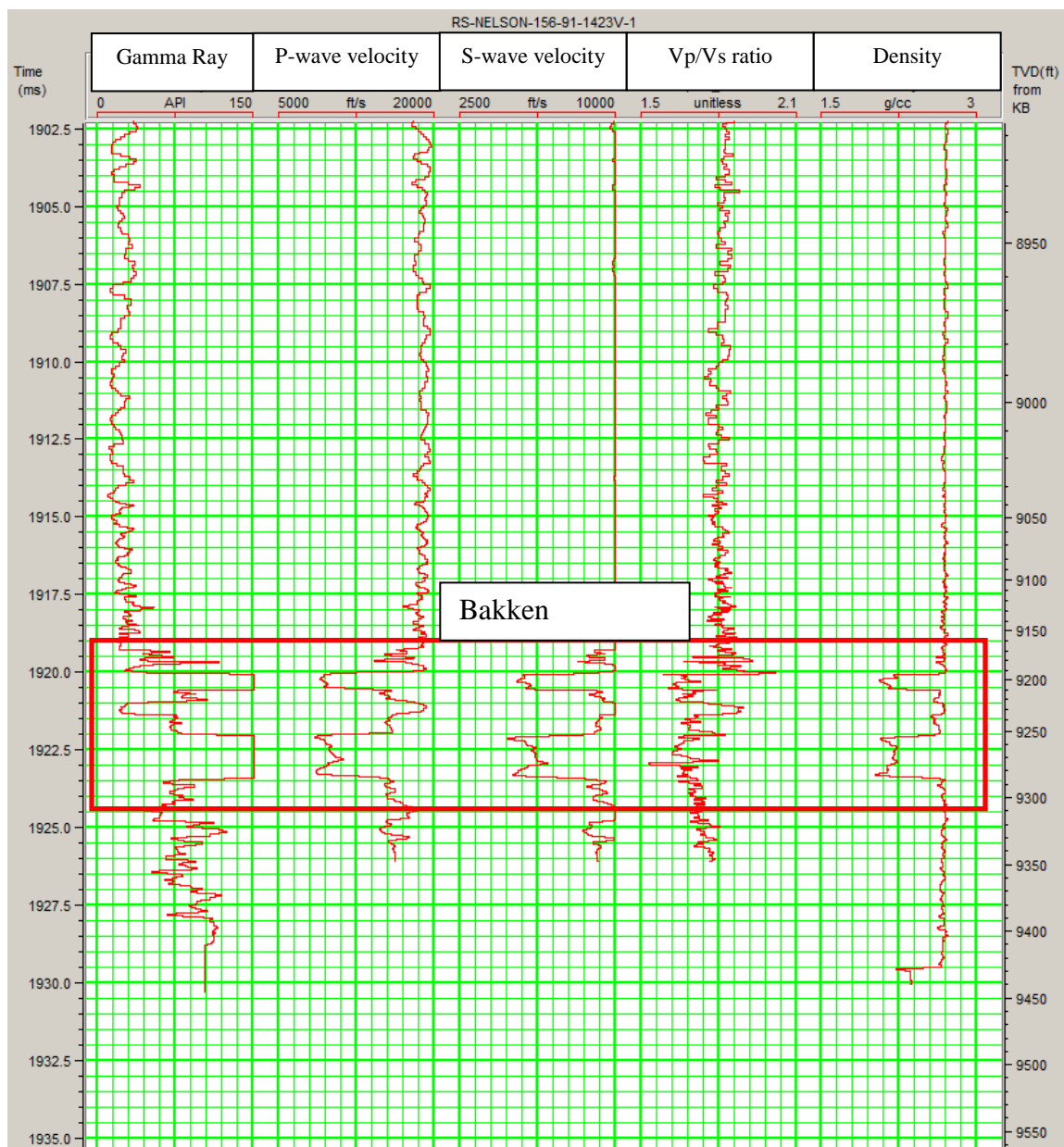
Figure 3. 2 Well log (RS-NELSON-156-91 1423H-1) suites.

18

3.2.1 Depth and Thickness

In general, the Bakken Formation is divided into three members: the Upper Member, the Middle Member, and the Lower Member. However, in most of the wells, except two, depth and thickness values for the Middle and the Lower Members are not separated and are given as a single member – the Middle Member. For the sake of comparison, the depth and thickness values are shown for the Upper and the Middle Members. Depth and thickness values of the formation in the study area are summarized in the following table (Table 3.1).

Well Name from Ross Field	Well No Ross Field	Depth(ft)	Thickness (ft)		
			Total Bakken	Upper Bakken	Middle and Lower Bakken
RS-BLACK STONE-156-91- 1011H-1	18001	9280	46.16	22.72	23.44
RS-VEDAA-156-91- 0336H-1	16880	9247	34.32	18.20	16.12
RS-NELSON-156-91 1423H-1	16824	9300	111.57	18.00	93.57
RS-STATE B-156-91- 1609H-1	16958	9340	54.80	21.20	33.60
RS-APELESE-156-91- 1522H-1	17093	9320	54.52	16.30	38.22
RS-HOWELL-156-91- 1207H-1	17720	9296	232.26	148.00	84.26
RS-RED CROWN-156-91- 2536H-1	17010	9323	117.23	17.80	99.43
RS-F NELSON-156-91- 2413H-1	17105	9238	116.00	16.00	100.00
PALERMO 2-18H	18609	9057	41.73	20.23	21.50
NELSON FARMS 1-24H	15845	9595	93.20	13.20	80.00

Table 3.1. Depth and thickness of the Bakken Formation in Ross Field.

The depth and thickness values along with the locational information (coordinates) of the wells were uploaded to Matlab and three-dimensional volume of the formation were created (Figure 3.4). Subsequently, cross-sections along the seismic lines were created in order to observe unidirectional depth and thickness of the Bakken Formation (Figure 3.5&3.6).
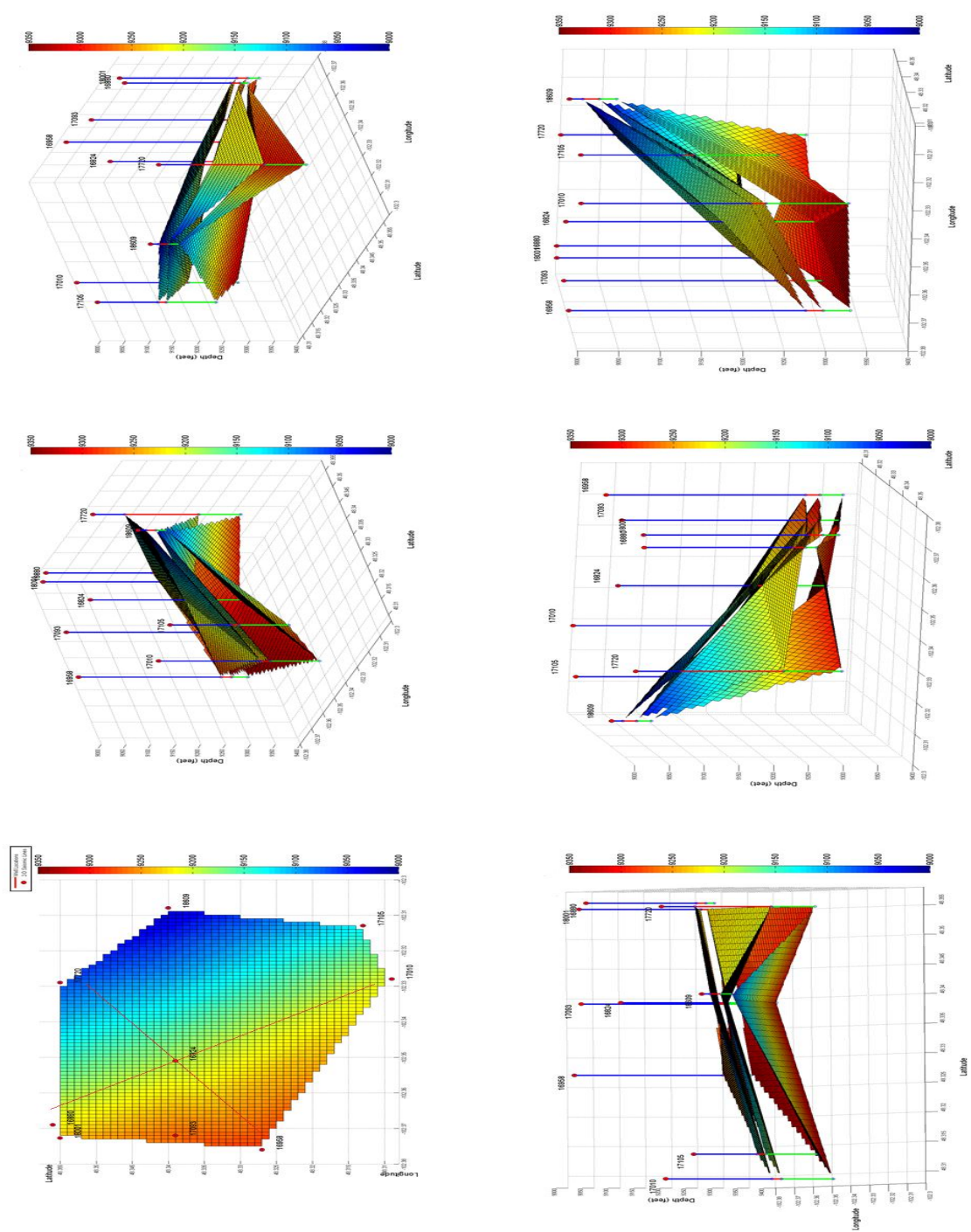
Figure 3. 3 Well logs' depth and thickness changing.

The depth of the Bakken Formation generally varies from 8000 to 10,000 ft. (2400 m to 3050 m). Three dimensional volume results indicated that the Bakken Formation is deeper in the southeast and it became shallower towards the northeast. The difference between the deepest and the shallowest points of the Bakken Formation in the study area is around 150 ft. (46 m).

The difference in depths of the 1001 and 2001 seismic lines from the cross-sections of the 3D volumes are shown in Figures 3.5 & 3.6. According to the Bakken Formation's depth change, by taking 1001 seismic line as a reference, the formation gets thicker throughout the northwest and continually gets deeper. The average Bakken depth is 95ft. (29 m) in southeast and 120ft. (36 m) in Northwest. When we observe the 2001 seismic line, it was seen that the Bakken Formation gets deeper and thinner towards the southeast direction. It is 230 ft. (70 m) towards the northeast, while it is 60 ft. (18 m) towards the southwest. This means that the thickness of the Bakken becomes 3.8 times thicker towards the northeast direction.
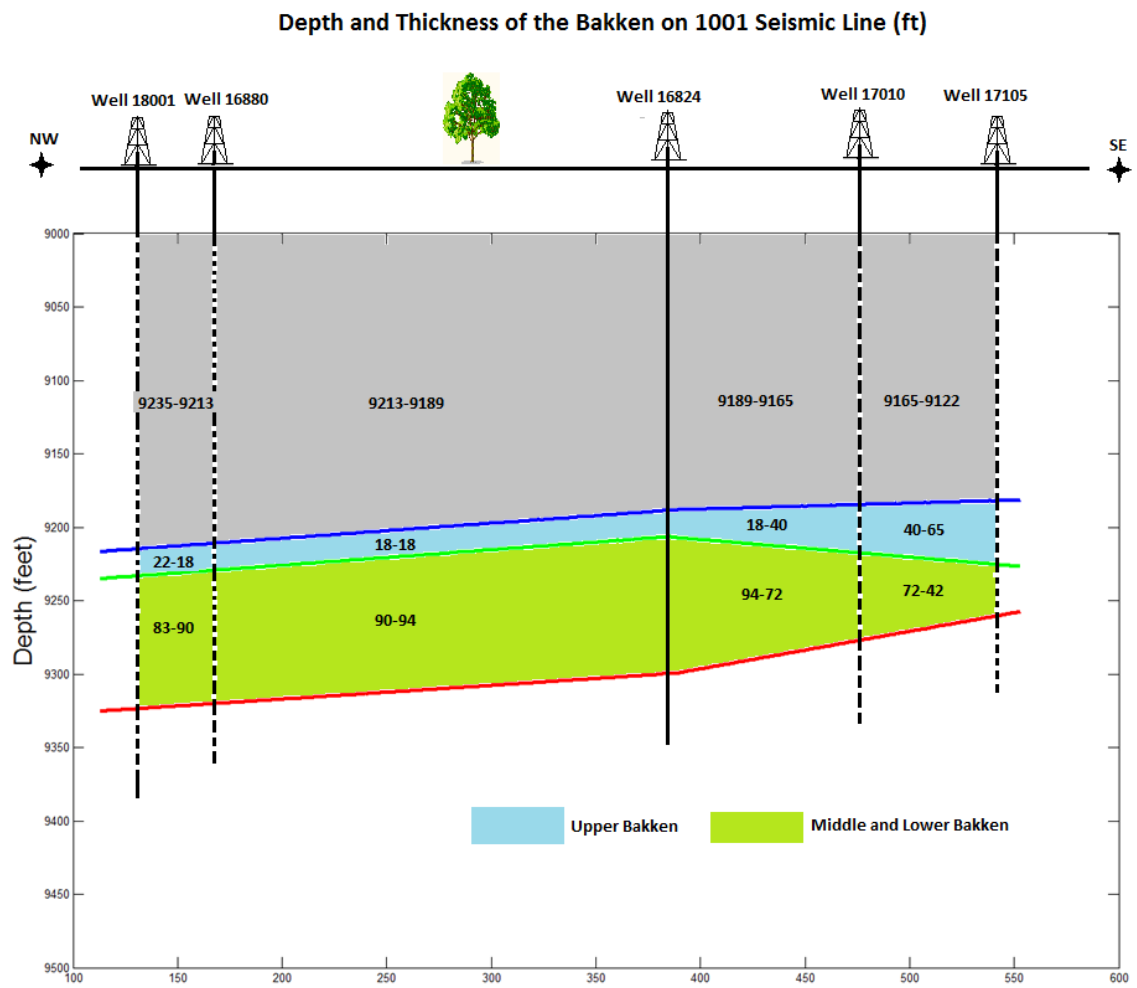
Figure 3. 4 Depth and thickness section from 1001 seismic line
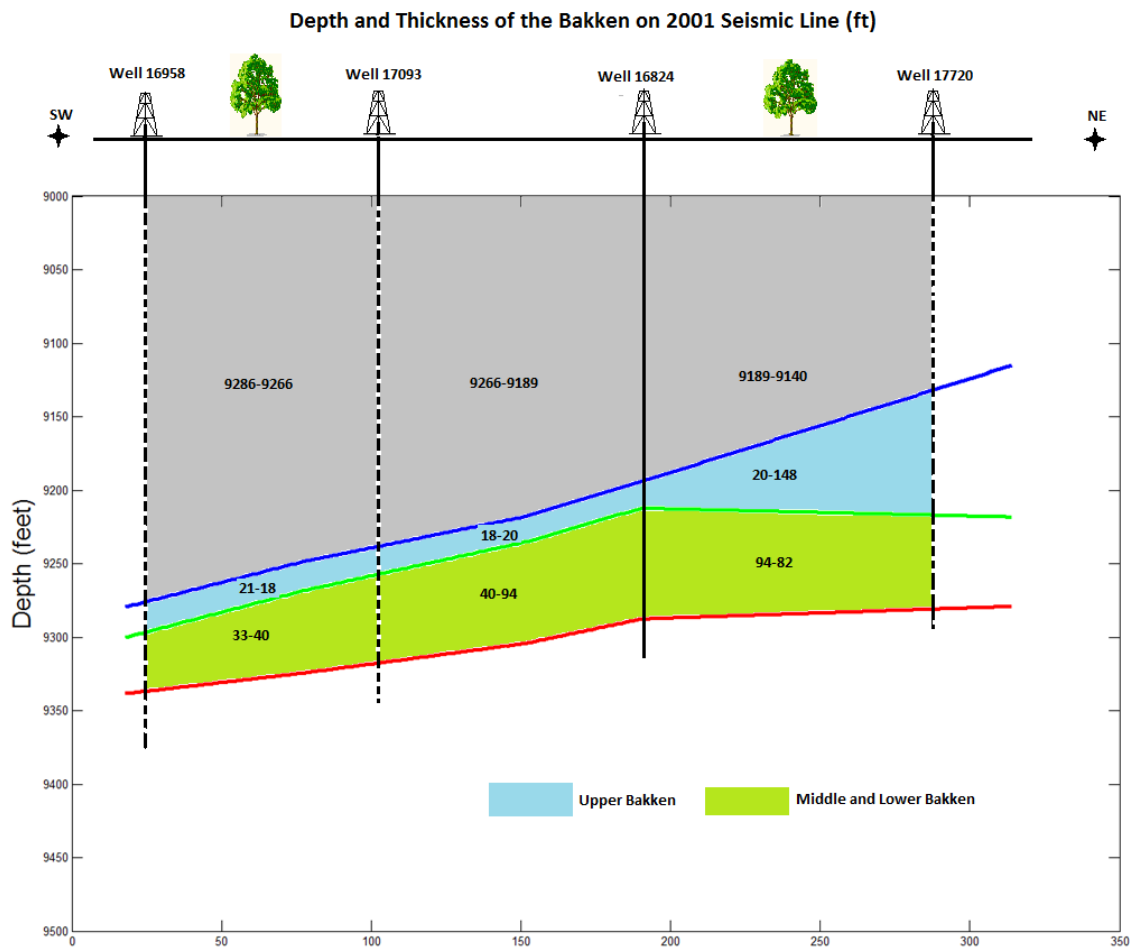
Figure 3. 5 Depth and thickness section from 1001 seismic line

3.2.2 Density

The Bakken Formation can be seen in detail in the well RS-NELSON-156-91 1423H-1 (well no 16824) and the well NELSON FARMS 1-24H (well no 15845). The Upper Member, Middle Member, and Lower Bakken values were drawn according to their average values. Amongst three members in the Bakken Formation, the Upper and the Lower Bakken Members have lower densities compared to that of the Middle Bakken Member. However, the density of the Middle Bakken Member is still lower than the Lodgepole and the Three Forks Formations. The results from both logs are approximately the same. Detailed density log values are shown in Figure 3.7 and 3.8. The average density values at 16824 are as follows: the Lodgepole 2.66 g/cm^3, the Upper Bakken 2.23 g/cm^3, the Middle Bakken 2.62 g/cm^3, the Lower Bakken 2.18 g/cm^3, and the Three Forks 2.68 g/cm^3. The average density values at 15845 are as follows: the Lodgepole 2.68 g/cm.^{3}, the Upper Bakken 2.18 g/cm^3, the Middle Bakken 2.63 g/cm^3, the Lower Bakken 2.21 g/cm^3, and the Three Forks 2.67 g/cm^3.
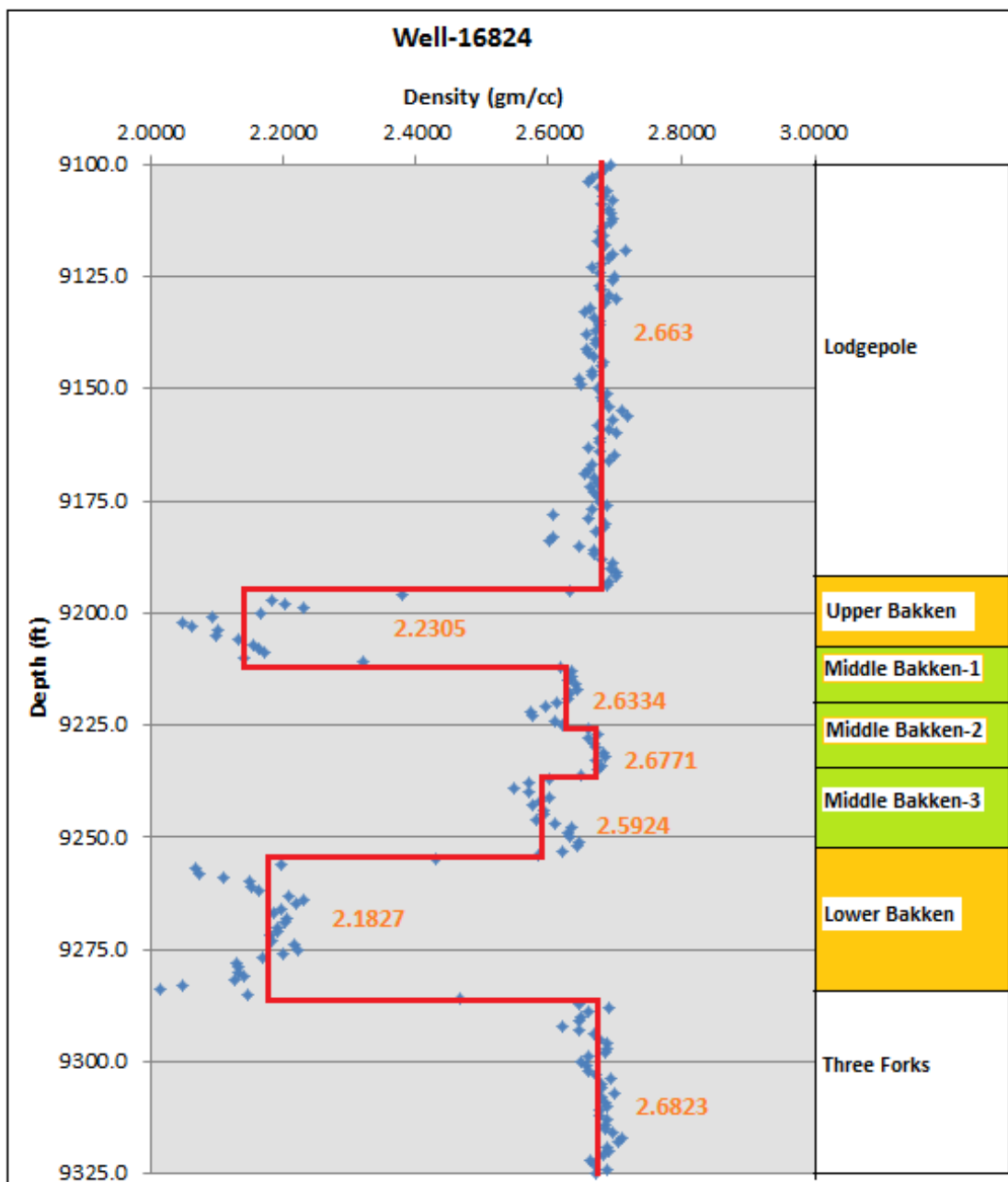
Figure 3. 6 Well 16824 density changes. Dots are real data, solid line is average
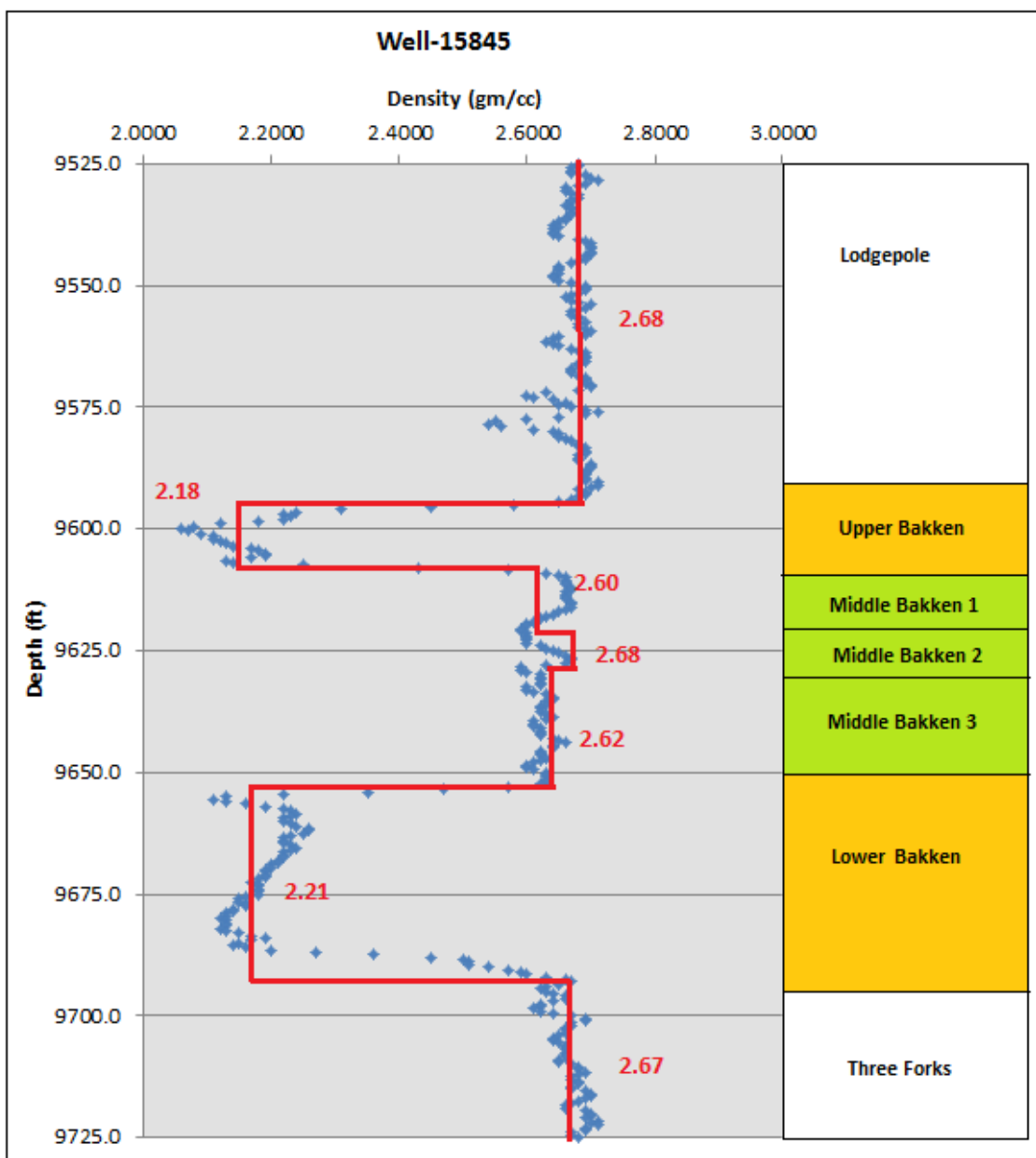
Figure 3. 7 Well 15845 density changes. Dots are real data, solid line is average

3.2.3 Velocity

Both P- and S-wave velocities for wells 16824 and 15845 are drawn in Figure 3.9 and 3.10. The points show the real well log values, whereas the solid line shows the average value. Velocity values for the Upper and the Lower Bakken are fairly lower and quite similar. In these members, the velocities are lower than those of Lodgepole and the Three Fork Formations at Well 16824, S-wave velocity drops 45% from 10460 ft/s (3188 m/s) to 5821 ft/s (1774 m/s) and P-wave velocity drops 51% from 18543 ft./s (5652 m/s) to 9254 ft./s (2821 m/s). At Well 15845, S-wave velocity drops 43% from 10472 ft/s (3192 m/s) to 5962 ft/s (1817 m/s) and P-wave velocity drops 48% from 18920 ft/s (5767 m/s) to 9890 ft/s (3014 m/s). According to the values of these two wells, average S-wave velocity is found to be 5900 ft/s (1798 m/s), and the average P-wave velocity is found to be 18600 ft./s (5669 m/s). Velocity values are higher in the Middle Bakken, compared to the Upper and the Lower Bakken. There are three different kinds of velocity change in The Middle Bakken due to the lithological variation. This can be seen in both of the wells. But if we take the average of the P-wave velocity in the Middle Bakken Member, it is 16000 ft/s (4877 m/s), while it is 9000 ft/s (2743 m/s) in the Upper and the Lower Bakken. S-wave velocity is 9600 ft/s (2926 m/s) in the Middle Bakken and 5900 ft/s (1798 m/s) in the Upper and the Lower Bakken.
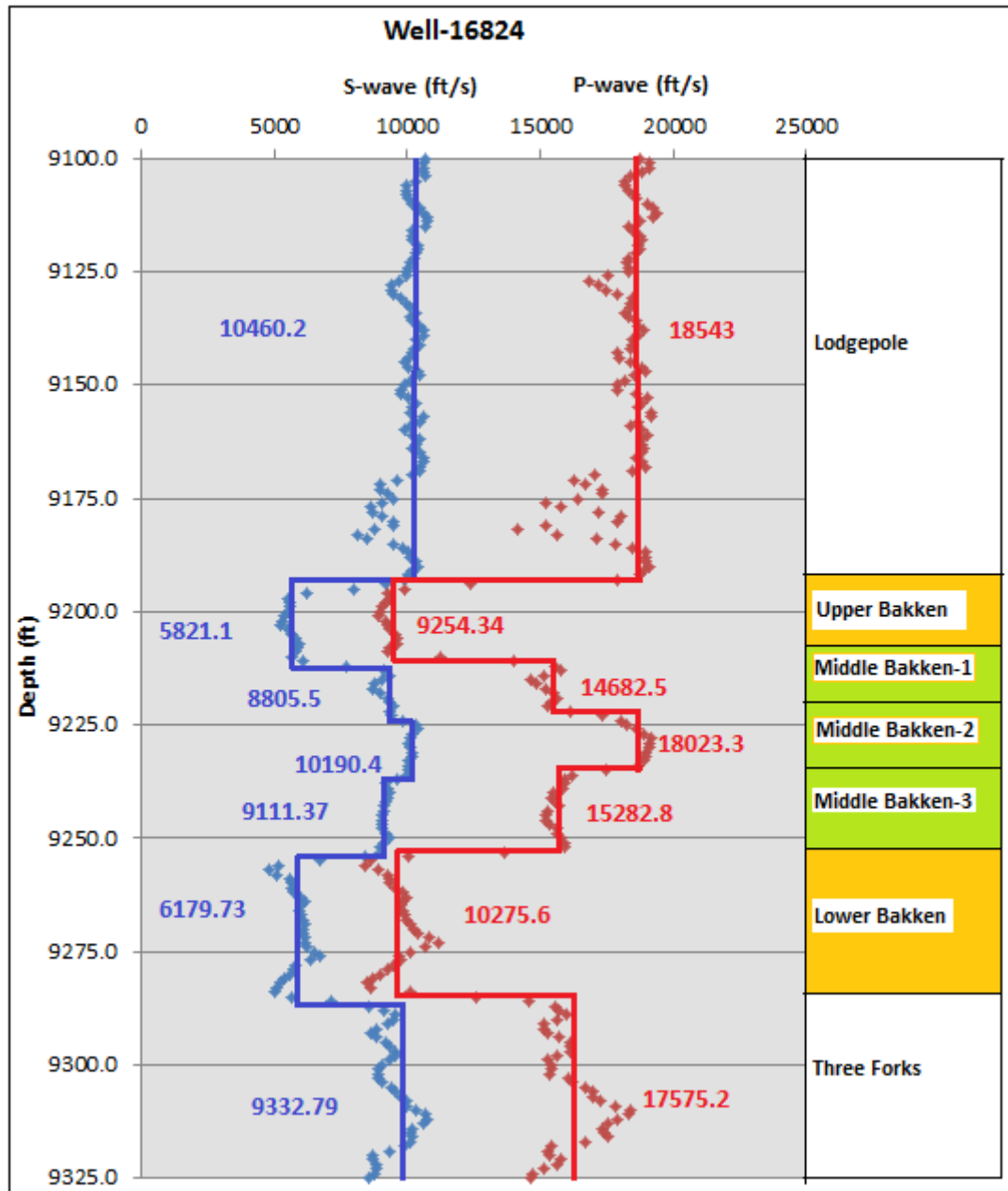
Figure 3. 8 P- and S-wave velocities for well 16824. Dots are real data, solid line is average velocities
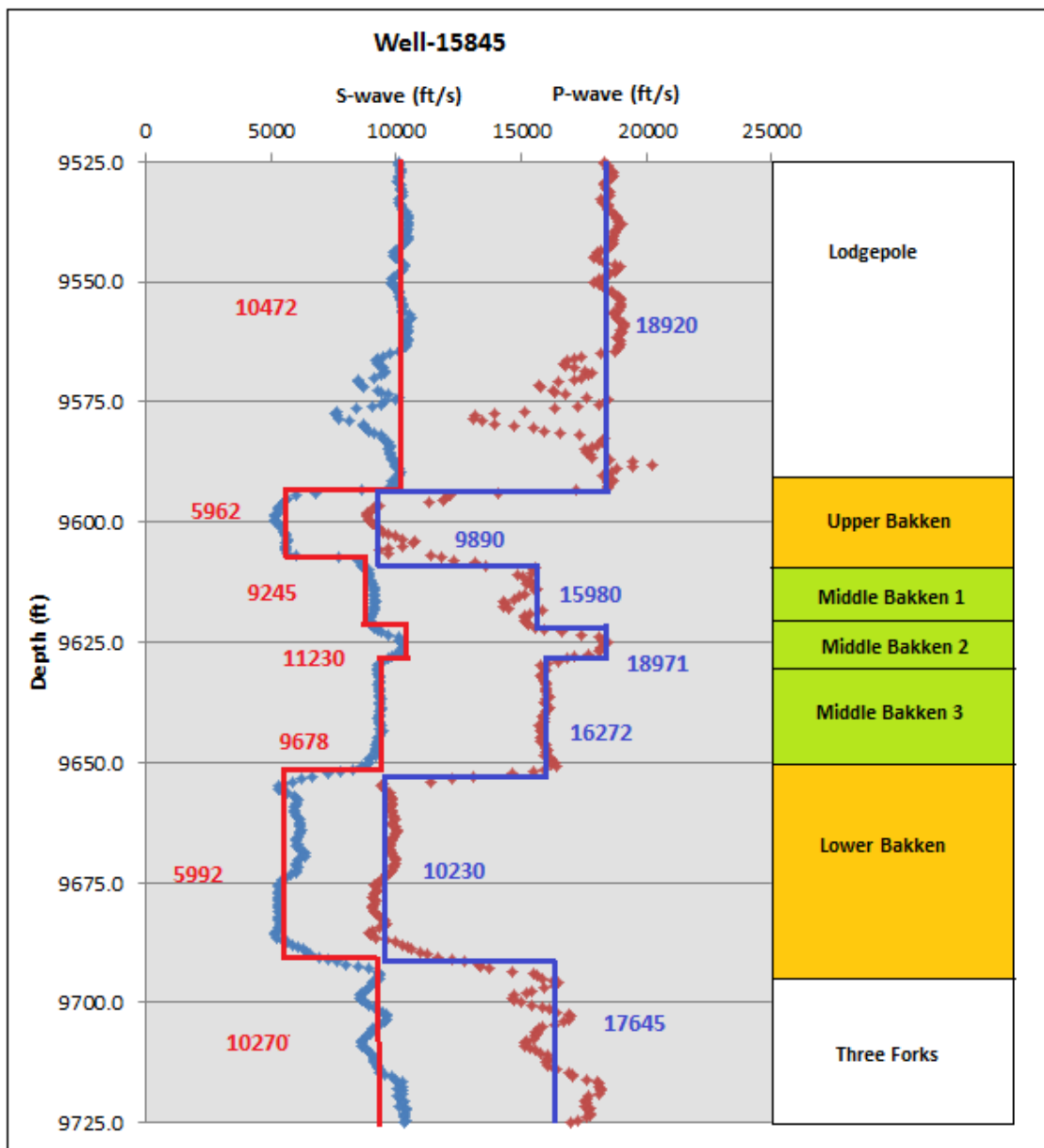
Figure 3. 9 P- and S-wave velocities for well 16824. Dots are real data, solid line is

average velocities

3.2.4 Vp/Vs Ratio

The ratio of P- and S-wave velocities gives the Vp/Vs ratio. At well 16824, the Vp/Vs ratio was measured at well log, whereas, at well 15845 the Vp/Vs ratio was calculated. It is known from previous geophysical research that Vp/Vs ratio is compatible with lithology. According to Tatham and McCormack (1991), Vp/Vs ratio changes between 1.7 and 3.0 for shale, between 1.78 and 1.84 for dolomite, between 1.59 and 1.76 for sandstone, and between 1.84 and 1.99 for limestone. A greater interval is taken for Vp/Vs ratio of shale. This value increases, while the clastic sequence inside the porous increases.

The Vp/Vs ratios of both well logs are drawn in Figures 3.11 and 3.12. The dots indicate the real well log data, while the solid lines show the average velocity value. The Upper and the Lower Bakken can be observed easily as these members are mainly shale. Although the Middle Bakken Member 1 &3 are also mainly shale, due to clastic carbonate contents, the Vp/Vs ratio is higher compared to the Upper and the Lower Bakken. The core results depict that the Middle Bakken has shale and dolomite and the Vp/Vs ratio support this result.
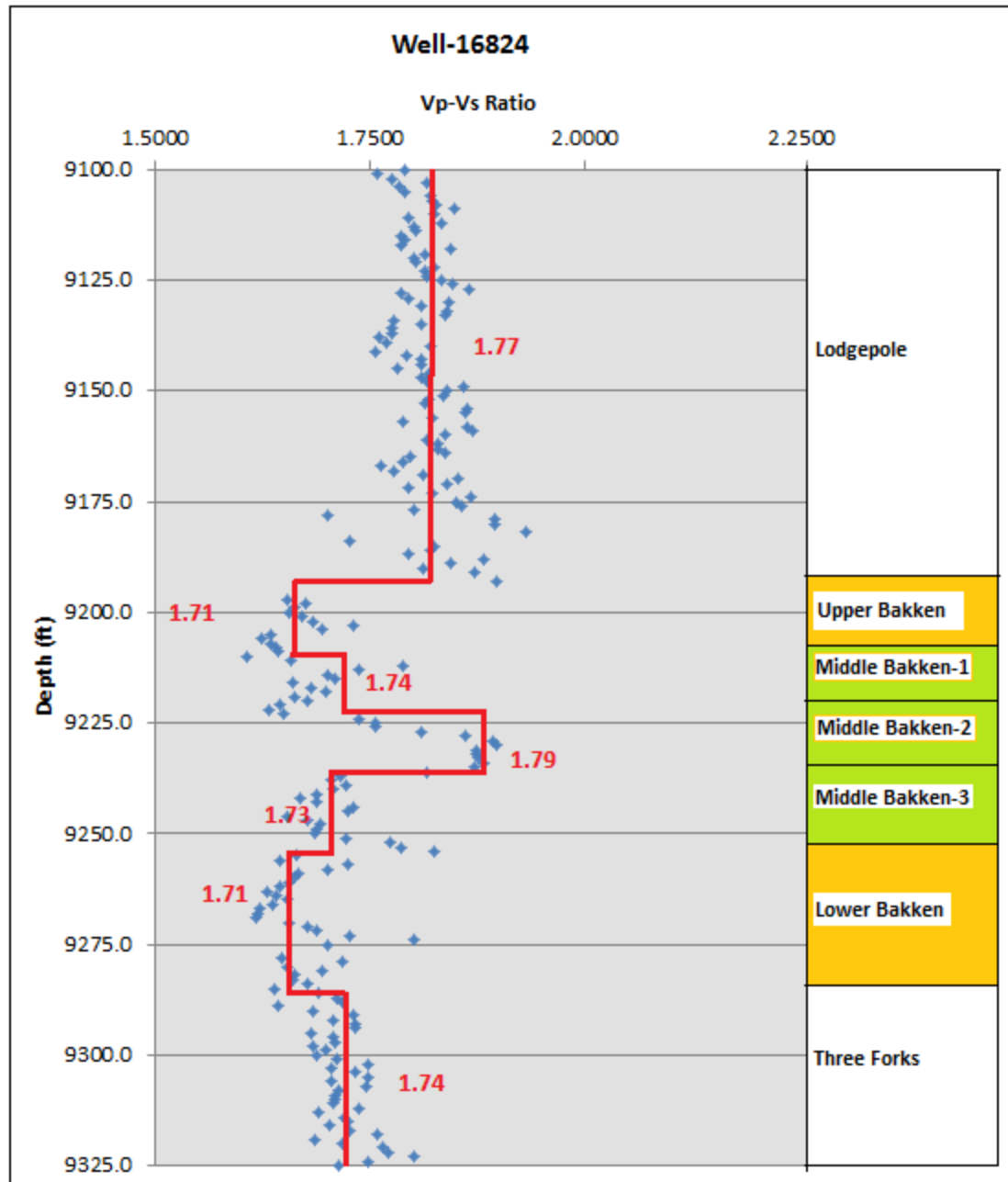
Figure 3. 10 Vp/Vs ratio, well 16824. Dots are real data; solid line is average Vp/Vs ratio
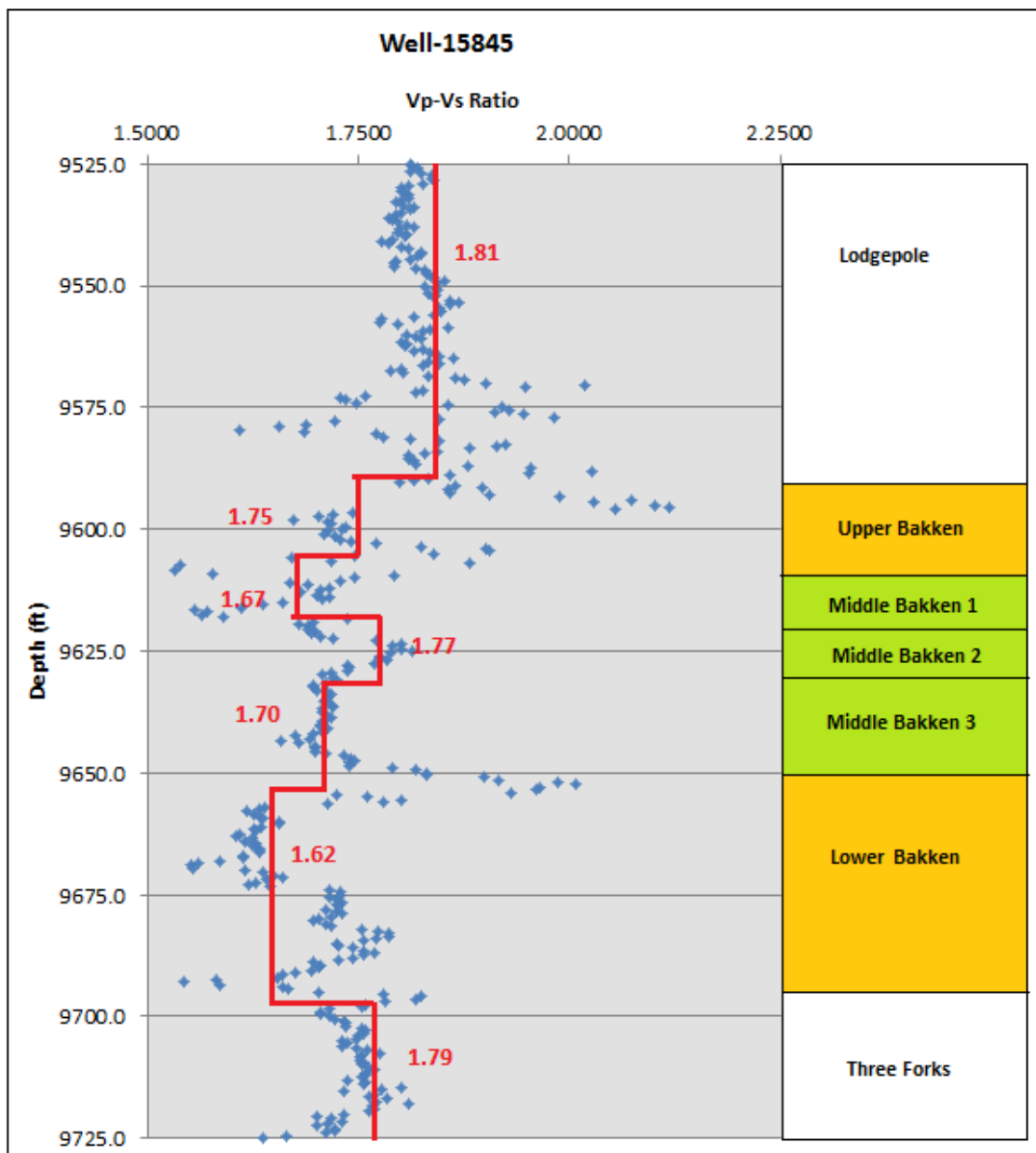
Figure 3. 11 Vp/Vs ratio,well 15845. Dots are real data; solid line is average Vp/Vs ratio

3.2.5 Young's Modulus and Poisson's Ratio

Young's Modulus can be best explained as the ratio of stress over strain (Sheriff, 2002). The Young's Modulus was calculated according to the following formula using Vp and Vs values (Eq. 3.1).

$$E = \frac{\rho Vs^2\ (3Vp^2 - 4Vs^2)}{Vp^2 - Vs^2}$$
Eq. 3.1

Poisson's Ratio on the other hand, is the ratio of lateral strain over axial strain (Mavko et al., 2003). The Poisson's Ratio is calculated based on the following formula using Vp, Vs, and density values.

$$V = \frac{1}{2}\frac{(Vp/Vs)^2 - 2}{(Vp/Vs)^2 - 1}$$
Eq. 3.2

Figure 3.12& 3.13 show the Young's Modulus values for both well log data. The average values for both well 16824 and well 15845 are shown by the solid lines. The Young's Modulus values of the Upper and the Lower Bakken shales are lower compared to that of the Middle Bakken and the other formations. The Lodgepole, the Three Forks and the Middle Bakken show similar values.

Figures 3.14& 3.15 show Poisson's Ratios for both wells. The Lodgepole and the Three Forks Formations have similar Poisson's Ratio values. The Middle Bakken has similar but slightly smaller ratio compared to those two formations while the Upper and the Lower Bakken shale show lower results compared to other formations.

Figure 3.17 shows the cross-plot of Poisson's Ratio and Young's Modulus. This cross-plot gives completely different values for the Upper and the Lower Bakken shales in comparison to all the other formations. On the cross-plot, three distinct clusters can be identified. The first cluster delineated by a solid red circle shows the Upper and the Lower Bakken shales. Decreasing Poisson's Ratio along with increasing Young's Modulus indicates change from more brittle to more ductile characteristic. The second cluster delineated by a solid blue circle show the Lodgepole and the third cluster delineated by a solid green circle shows the Three Forks Formation and the Middle Bakken.

Figure 3. 12 Young's Modulus result for well 16824. Dots are real data, solid line is average.
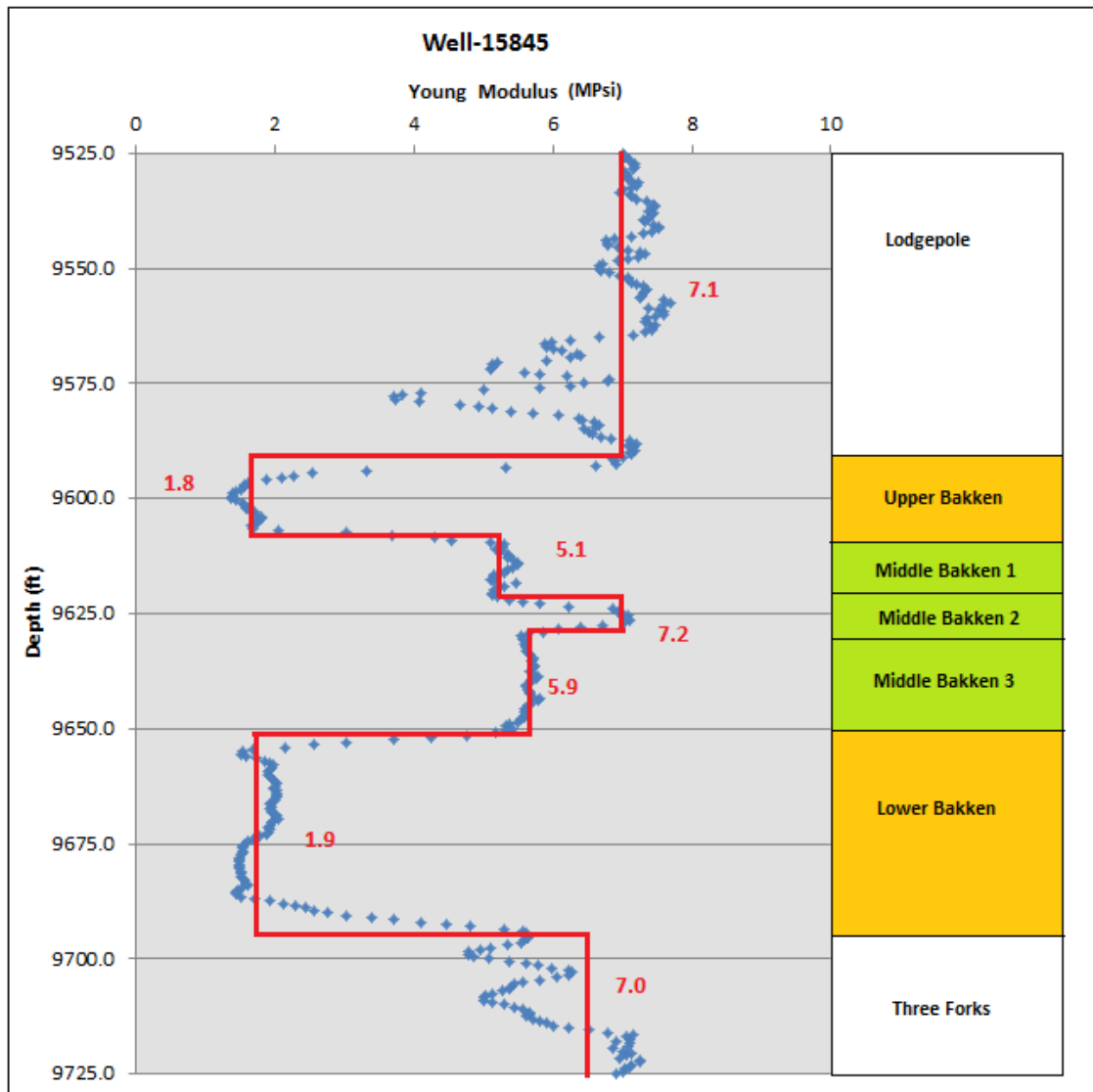
Figure 3. 13 Young's Modulus result for well 15845. Dots are real data, solid line is
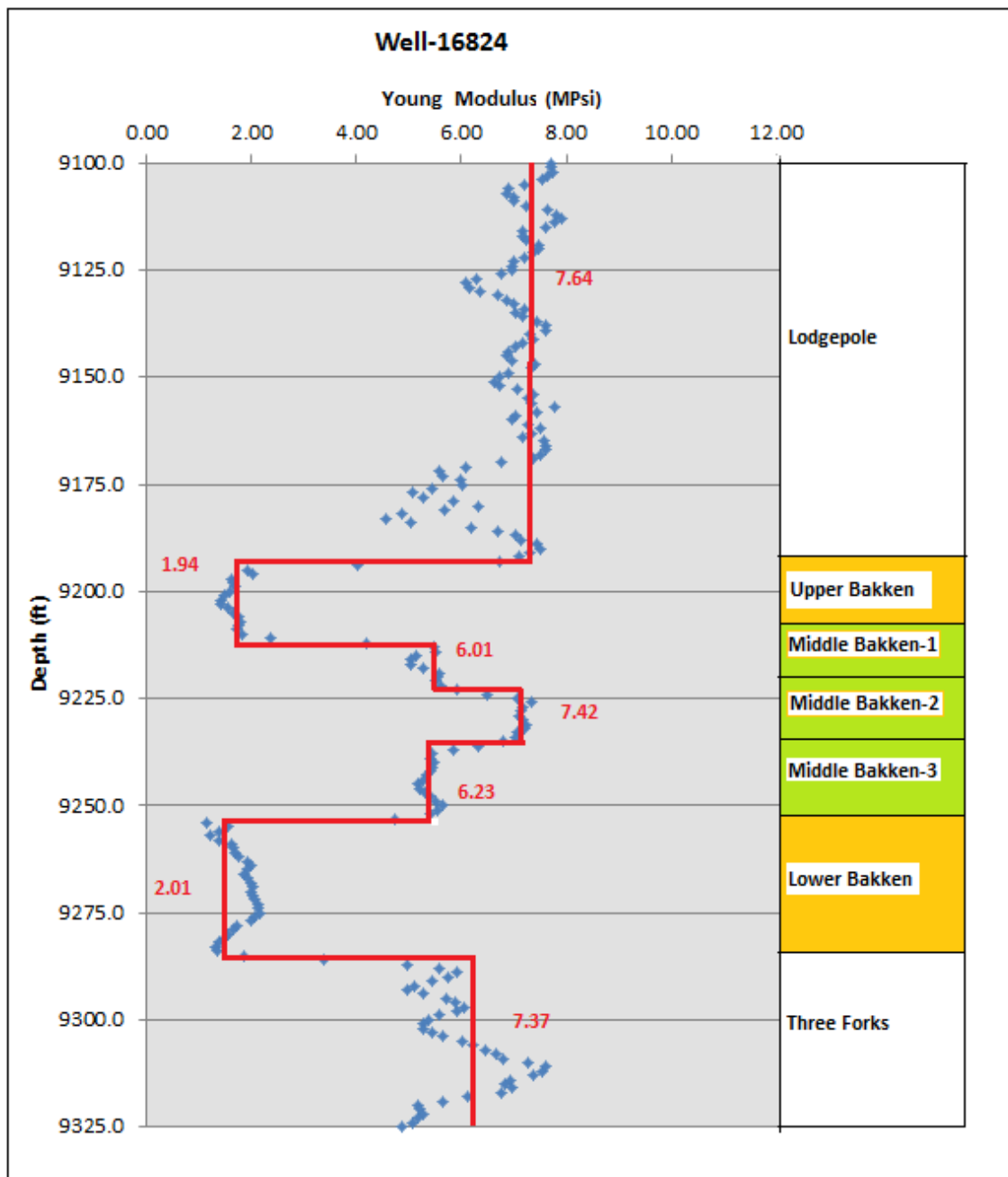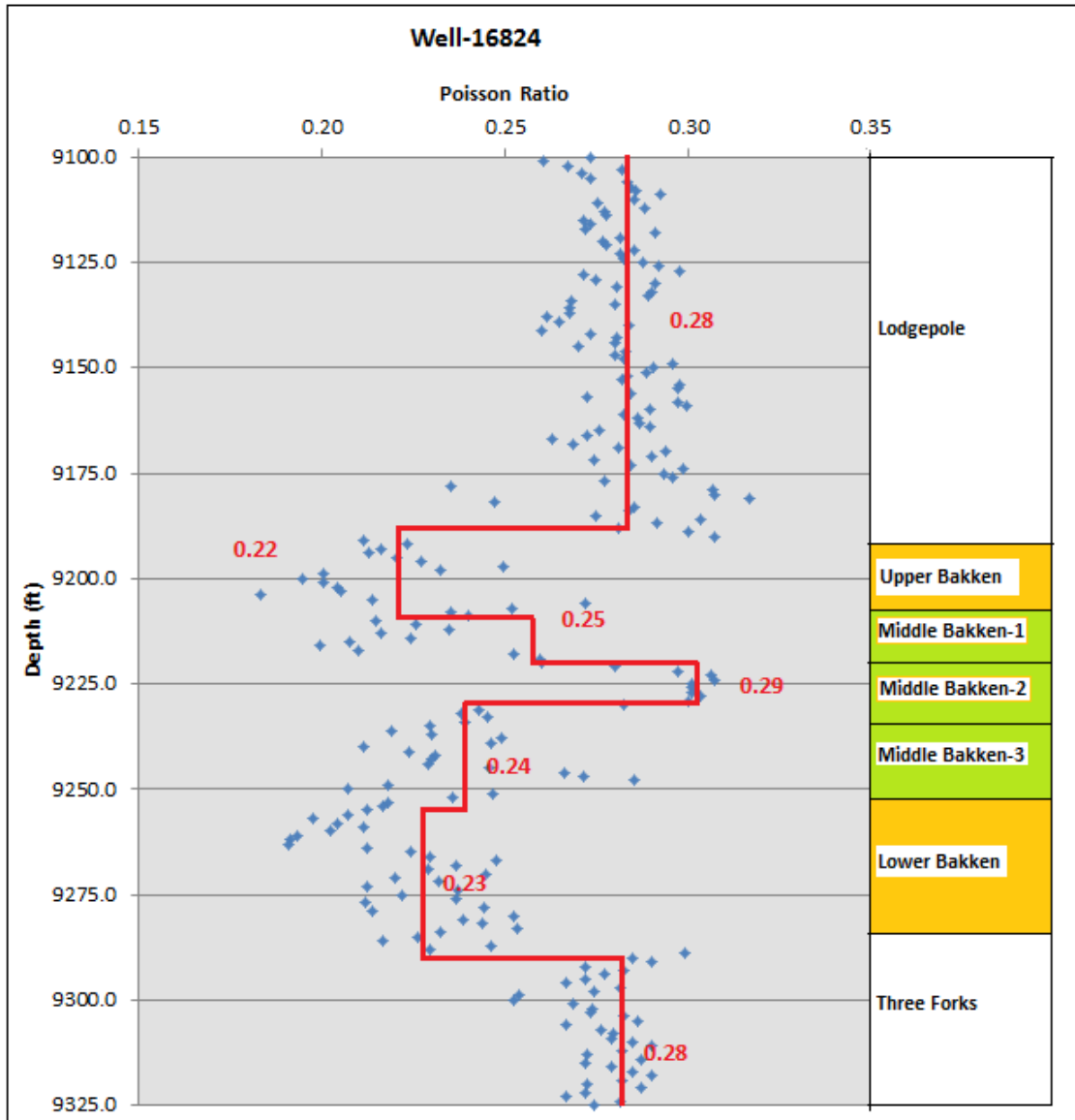
average.

Figure 3. 14 Poisson's Ratio result for well 16824. Dots are real data, solid line is average.
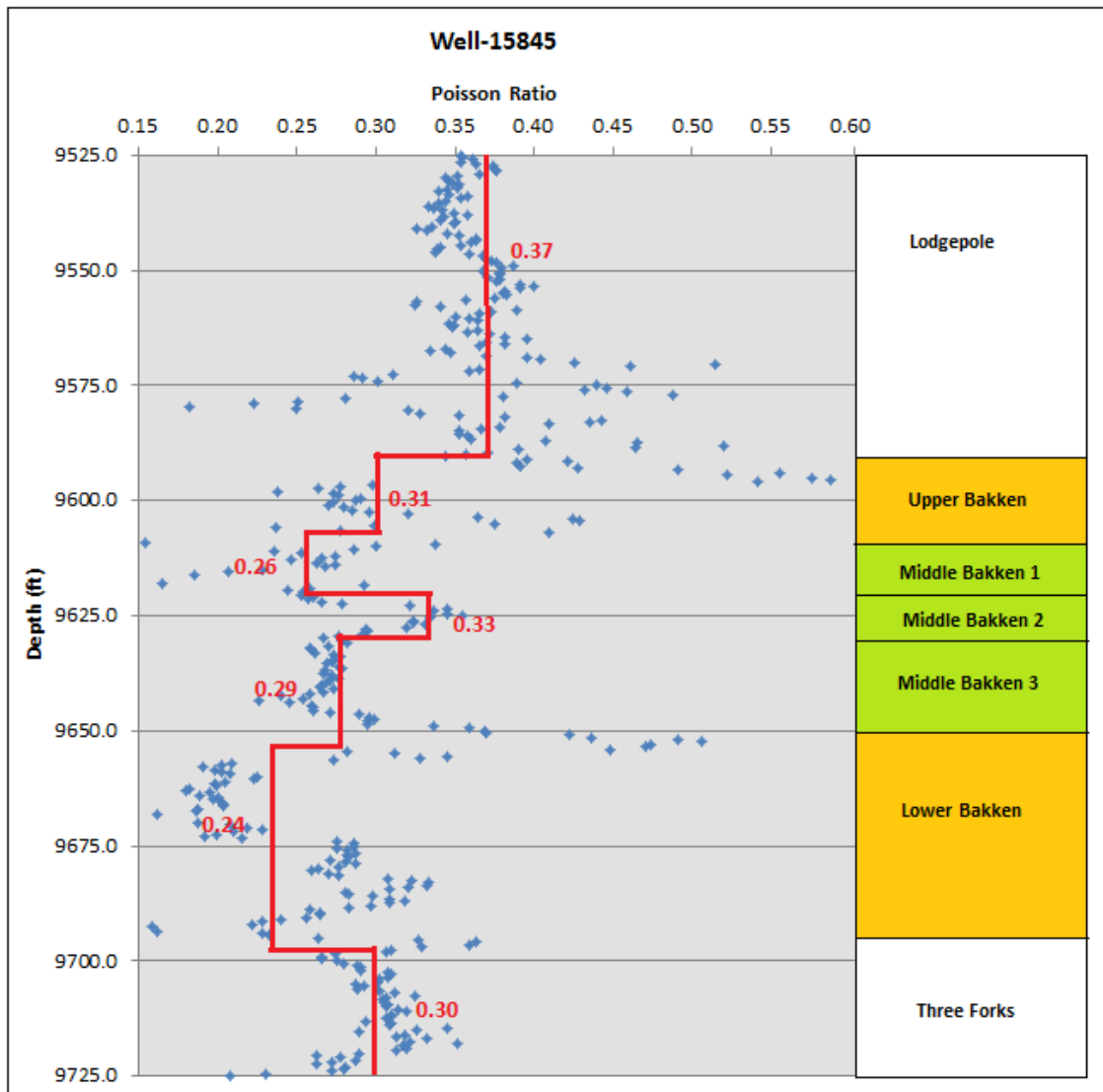
Figure 3. 15 Poisson's Ratio result for well 16824. Dots are real data, solid line is

average.
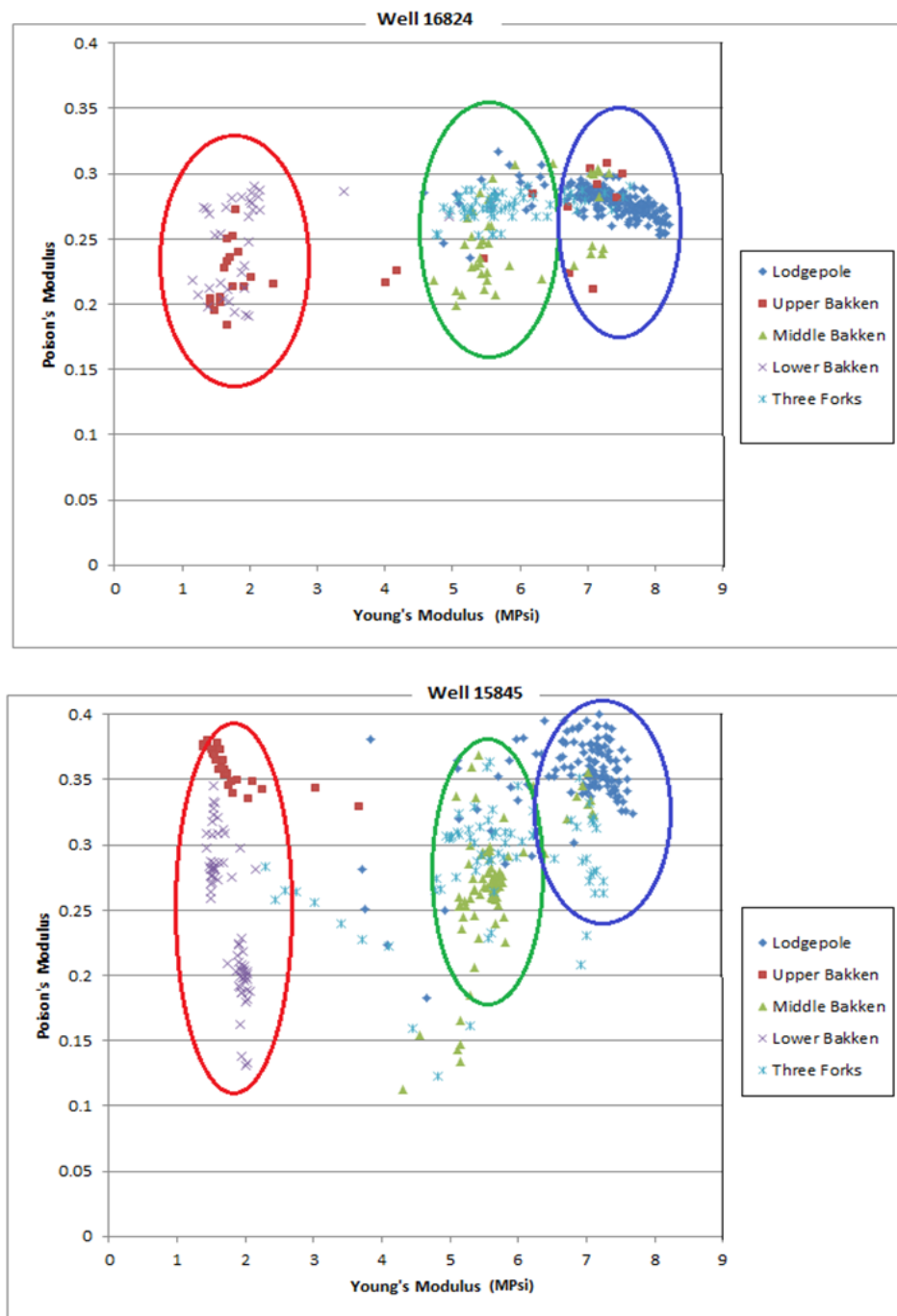
Figure 3. 16 Cross-plots of Young's Modulus versus Poisson's Ratio for both well logs.

39

3.3 Summary

Well log data were acquired from Ross Field, North Dakota. All of those data were interpreted by taking depth and thickness, density, velocities, Vp/Vs ratio, Young's Modulus, and Poisson's Ratio into consideration. It was analyzed by comparing the Upper Bakken, the Middle Bakken, the Lower Bakken, the Lodgepole (above The Bakken Formation), and Three Forks Formation (below The Bakken Formation). On average, the thickness of the Bakken Formation is around 60 ft. (18 m) while the depth of the formation is around 9000 ft (2743 m). It has been found that Bakken Formation gets thicker and deeper towards the NW direction. The Upper and the Lower Bakken shales show similar characteristics and can be separated more clearly using well log data. The Upper and the Lower Bakken shales have lower density and lower P- and S-wave velocities. The Middle Bakken shale has higher Vp/Vs ratio compared to the Upper and the Lower Bakken shales. However, using Vp/Vs ratio is not sufficient for defining the Middle Bakken.

3.4 Well Log Preparation and Seismic Well Tie

The reason for using only one well log in order to create the AVO analysis and pre-stack inversion is the fact that there is only one well (RS-NELSON_156-91-1423H-1) on the seismic section and it crosses only one seismic section in the study area. First of all, the well log was defined with its X and Y coordinates using Hampson & Russell Software.

The well log suite includes density, gamma ray, resistivity, and sonic log (P- and S-wave) measures.

It is important for the study to correlate well log and seismic section correctly in order to focus on the Bakken Formation and to receive accurate results. Therefore, seismic well tie was used in order to obtain seismic section time and well log depth correlation. The check-shot values were correlated with the program in order to receive the correct correlation (Figure 3.17). Also, for the recommended seismic event and seismic well tie that was obtained using sonic logs and gamma ray log to express the target zone properly, composite trace was created. The average traces related to the composite trace well location are shown in blue (Figure 3.18). While creating the composite trace, the average of nine traces near well location was utilized. Automatic time shift and manual stretching were used to express event location with time and depth. In manual stretching, wavelet was extracted to get accurate results. The most suitable wavelet extracted using different parameters is used to correlate time event and well log depth. The correlation coefficient is 0.768 while the used wavelet is 1850-1930 ms. time section with 200 ms. wavelength. These correlation results are the highest of all the trials.

The P-wave log created by these correlation processes was used in all AVO and pre-stack inversion analysis.
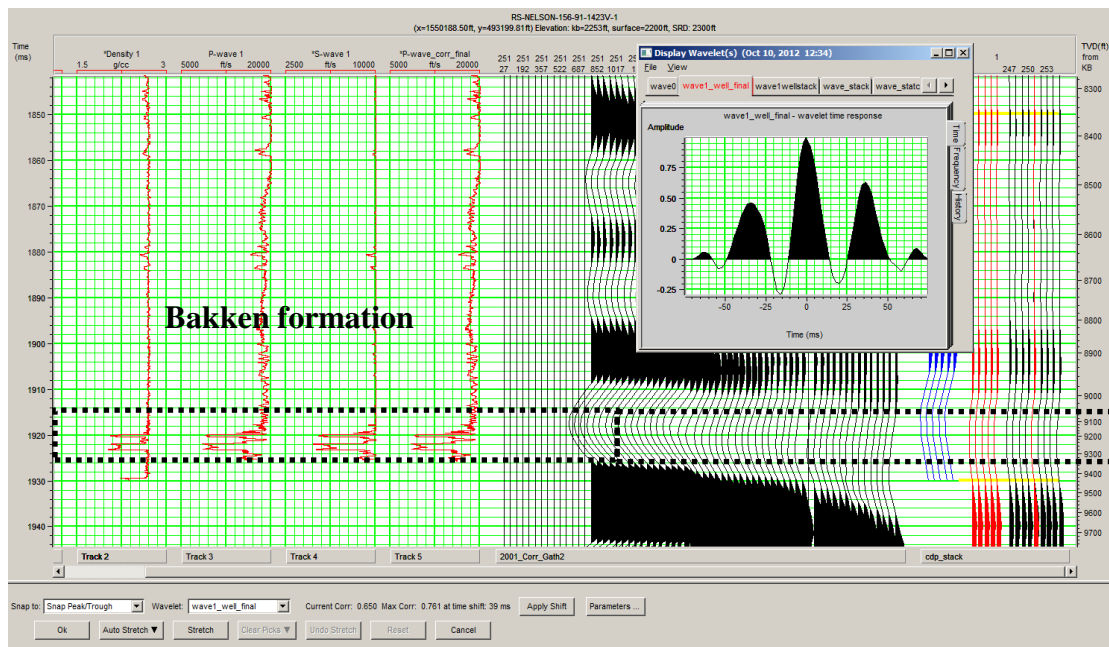
Figure 3. 17 Seismic well tie and correlation wavelet
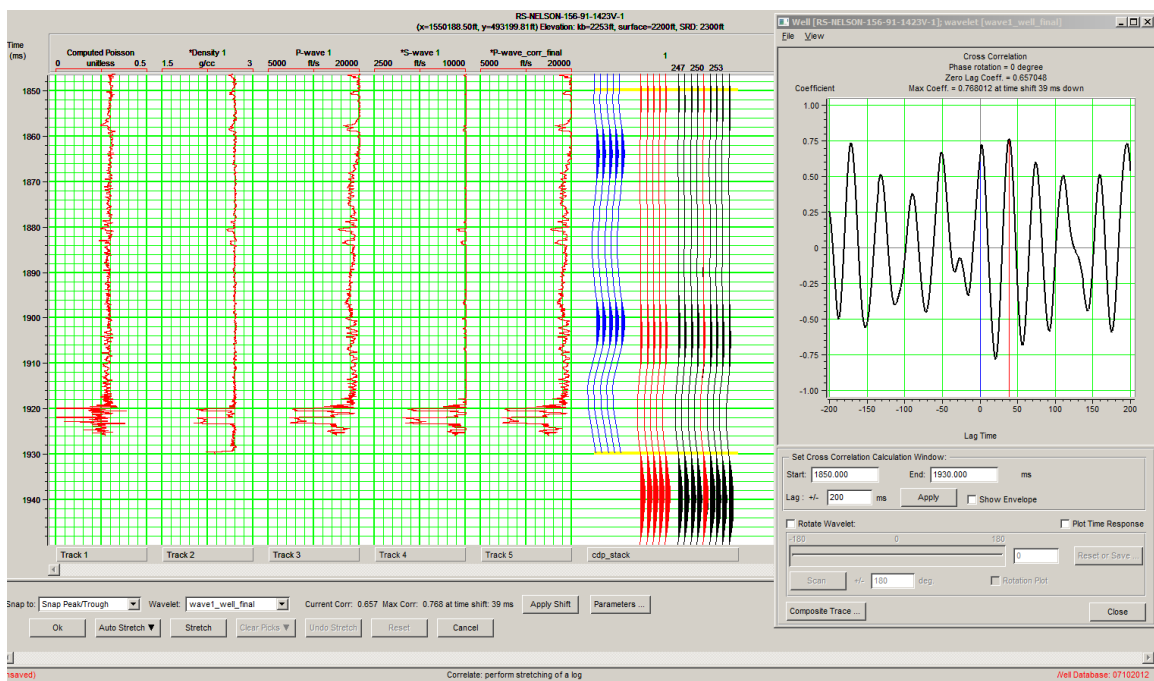
Figure 3. 18 Well log correlation window with cross correlation calculation window
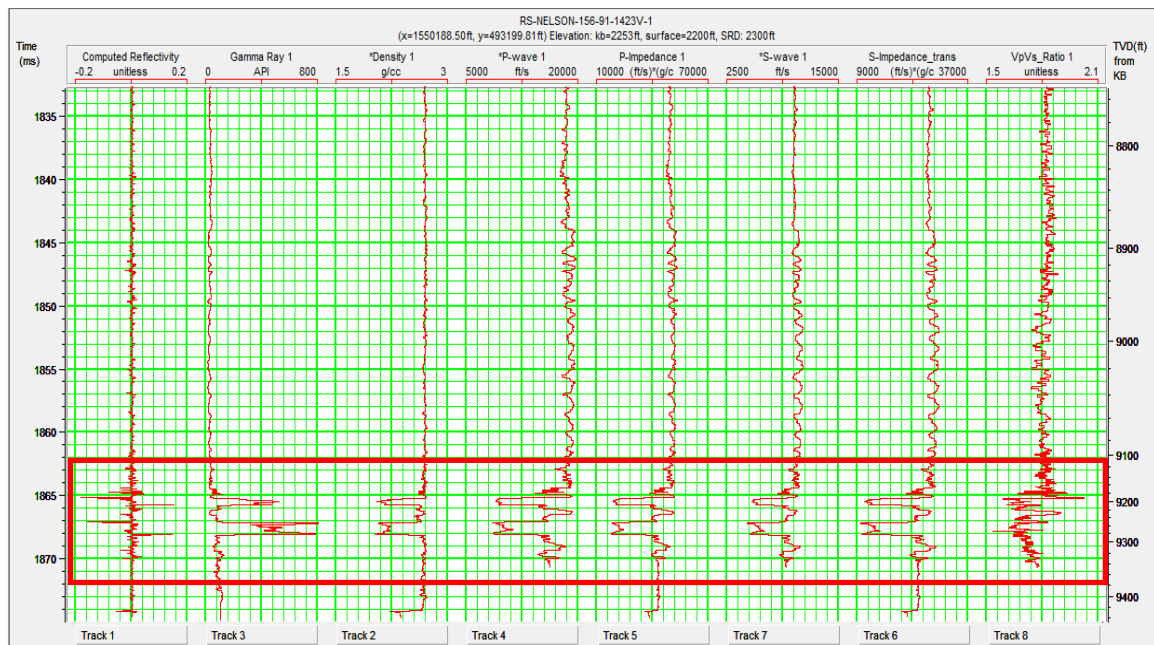
Figure 3. 19 Well log suites with calculation acoustic impedance and shear impedance

Chapter 4

AVO Analysis and Applications

4.1 AVO Analysis

AVO (Amplitude Variation versus Offset) analysis was founded in the 1980s and became one the most powerful reservoir characterization assistant. In 1984, W.J. Ostrander proved that gas sand reflection coefficients would create different anomalies with incremental offsets and direct hydrocarbon affects to be seen by making use of these anomalies. The AVO was developed because of well drilling in the previous years, while the assumptions were made by depending on the bright spots and on the structures that made the researchers suspect oil was present, which proved to be unsuccessful. With this development, the possibility of hydrocarbon reservoirs being real has increased (Castagna and Swan, 1997).

AVO is based on Zoeppritz equation: two different formations are divided into reflection and refraction with respect to the incident angle of seismic wave energy. The reflected seismic wave amplitude changes where the change of angle of incidence occurs. This change underlies the amplitude versus the offset analysis (Hampson and Russell, 1999).

According to the Shuey's approach, the wave is reflected from two different layers with respect to an angle that creates reflection coefficients depending on their rock elasticity, or in other words, acoustic impedance. AVO gradients are represented by amplitude

values with respect to offset average, which further supports the AVO response (Castagna and Swan, 1997).

According to the Shuey;

$$R\ (\theta) = R_0 + G\ sin^2\ (\theta) \qquad \text{Eq. 4.1}$$

where R (θ) is the reflection coefficient at an incident angle θ,

R_0 is the zero offset reflection coefficient, and

G is the AVO gradient.

Just like P- and S-waves show changes in different lithologies, they show changes by being affected with pore fluids inside the formations. These changes create different AVO anomalies together with showing differences in two boundaries, reflection coefficient and impedance values. In connection to this, AVO anomalies have been sorted for any possible hydrocarbon indicator (Russell and Hampson, 2005).

There are three main AVO classes according to the research of Rutherford and Williams in 1989. The diagram, showing all the AVO classes, can be seen in the Figure 4.1. AVO classes are created by generalizing gas sand. The general features are:

Class I: Sand has higher impedance compared to the shale above, and it shows large positive reflection coefficient. It starts with high amplitude and decreases in amplitude over time when the offset or the angle of incidence rises.

Class II: Sand has almost the same impedance value with the shale above, and the reflection coefficient is close to zero and it is positive. The impedance difference between the two formations is minimal. It starts with low amplitude and becomes higher while the offset or the angle of incidence rises.

Class III: Sand has lower impedance compared to the shale above, and it shows large negative reflection coefficient. It starts with high amplitude and it gets higher while the offset rises.

Taking Class III as a reference, Castagna and Swan have created Class IV in 1997.

Class IV: It is similar to Class III and while the offset increases, amplitude value decreases.

These classifications are shown, according to their increasing offsets and reflection coefficients and changes in Vp/Vs, schematically in Figures 4.1 and 4.2.
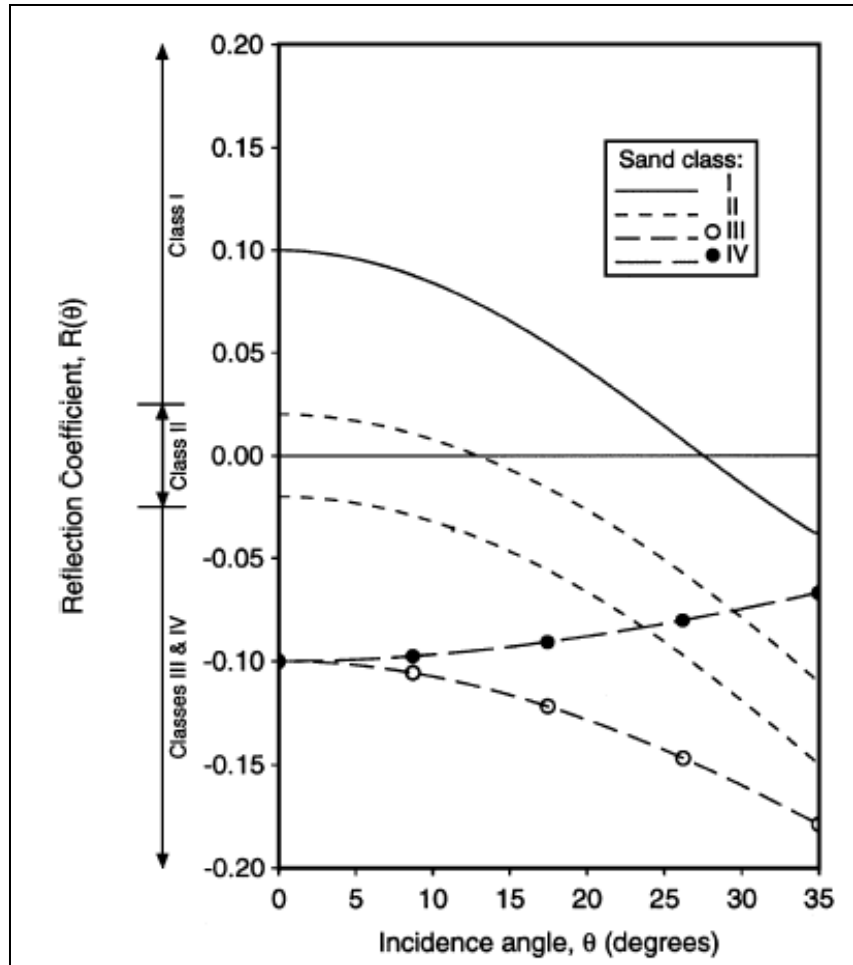
Figure 4. 1 Classifications of AVO response (Rutherford and Williams, 1989).

47
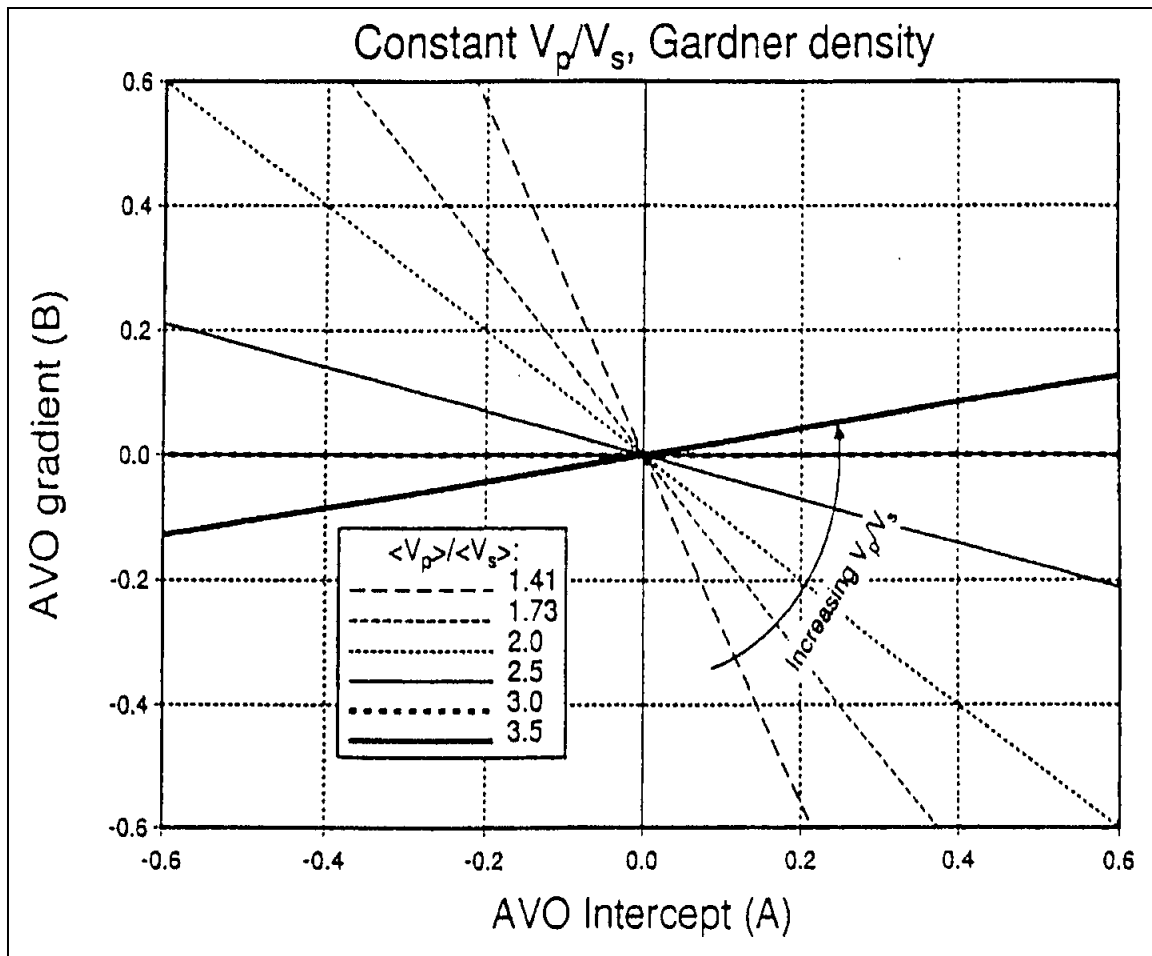
Figure 4. 2 AVO intercept (A) and gradient (B) cross-plot (Castagna & Swan, 1997).

Class	Relative Impedance	Quadrant	A	B	Amplitude vs. Offset
I	Higher than overlying unit	IV	+	-	Decreases
II	About the same as the overlying unit	II, III, or IV	+ or -	-	Increase or decrease; may change sign
III	Lower than overlying unit	III	-	-	Increases
IV	Lower than overlying unit	II	-	+	Decreases

Figure 4. 3 AVO behavior for gas sands (Castagna and Swan, 1997).

The geology of the study area contains dolomite in the Upper and Lower Bakken shales and the Middle Bakken, as previously mentioned. When AVO analysis is performed on the dolomite area under gas saturation, it reacted like sandstone. Therefore, sandstone classification chart (Figure 4.2) can be used for dolomite under gas saturation in AVO analysis. The fluid effect in sandstone suggests different AVO results, but the fluid inside the dolomite gives similar AVO effects for oil, gas, and brine (Li et al, 2003). Therefore, applying azimuthal AVO (AVA) would be most appropriate for carbonate reservoirs.

Even though AVO is the practical solution to utilize, it gives argumentative results in the characterization of carbonate rock properties or carbonate rock reservoirs. The reason for this being, although fluid affects rock properties in carbonate rocks, they give similar responses to AVO (Li et al, 2003). Accordingly, defining a dolomite reservoir, depending on Lambda-rho and Mu-rho, would offer a more accurate result. In this study, AVO analysis was made and the values of gradient and intercept are compared with Lambda-rho and Mu-rho values.

4.2 AVO and AVA Analysis Applications

The pre-stack applied 2D CDP gathers were ready to be used in AVO analysis. 2D CDP gather data was analyzed by using Hampson-Russell software AVO tool. In order to do this, P-wave velocity, created in process stage, was utilized with volume data. AVO analysis began by using CDP gathers that indicate velocity change.

Seismic reflections should be aligned with the velocity volume in addition to the CDP gathers for the AVO analysis. Trim statics were applied to correct this alignment and created proper results in the CDP gathers utilized. While applying trim statics on all data, event locations were picked specially, thus, the reflections of Bakken Formation between 1.850 ms – 1.950 ms, were flattened.

In the AVO analysis, a single well was uploaded in AVO. Since there is only one well on the seismic section, AVO analysis was conducted using a single well. The previously interpreted well, RS-NELSON_156-91-1423H-1, was introduced in this stage. The 200 ms wavelet, from the interval 1.850-1.930 ms extracted from the previous correlation process is used, making the well log correlation ready for analysis. Single well overlies on 251st CDP on the 2001 seismic section and 300th CDP on the 1001 seismic section (Figure 4.4).

The angle gather was prepared after the log is set to seismic data. Like in CDP gather, velocity volume was added to the angle gather before applying trim statics. The maximum angle at the zone of interest is found to be 30 degrees (Figure 4.5).

The trim statics applied angle gather was ready for AVO analysis (Figure 4.7). First, gradient analysis was made depending on the offset and the angle. In order to do this, trim statics applied CDP gather and angle gather, as well as, depending on the offset and the angle, synthetic models were created by using the Zoeppritz equation. Different gradient analysis was conducted for every synthetic model. The gradient analysis results of amplitude vs. angle, and intercept vs. gradient was in line with Class IV(Figure 4.8).

The next step in AVO analysis was creating the AVO attribute volume. First, a horizon is picked in the zone of interest in order to follow amplitude changes, followed by the AVO attribute volumes, which are viewed as intercept and gradient.

Even though some information is obtained from the intercept and gradient volumes about the Bakken Formation, no detailed results could be concluded for the three formations. The results were improved also by using Lambda-Mu Rho and pre-stack inversions, in order to receive more detailed information.
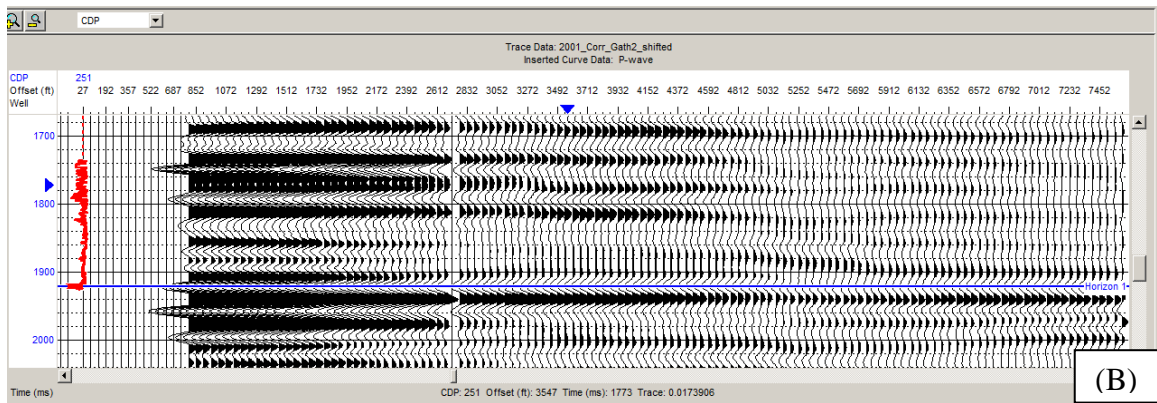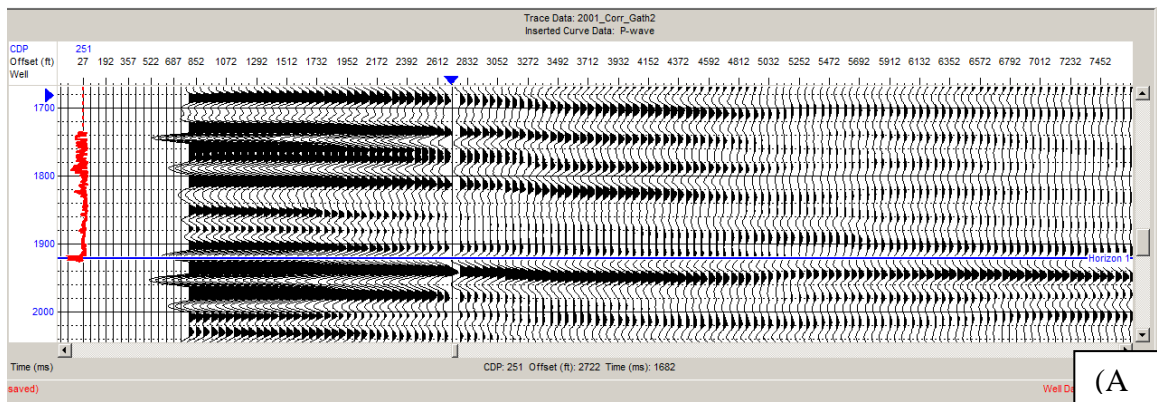

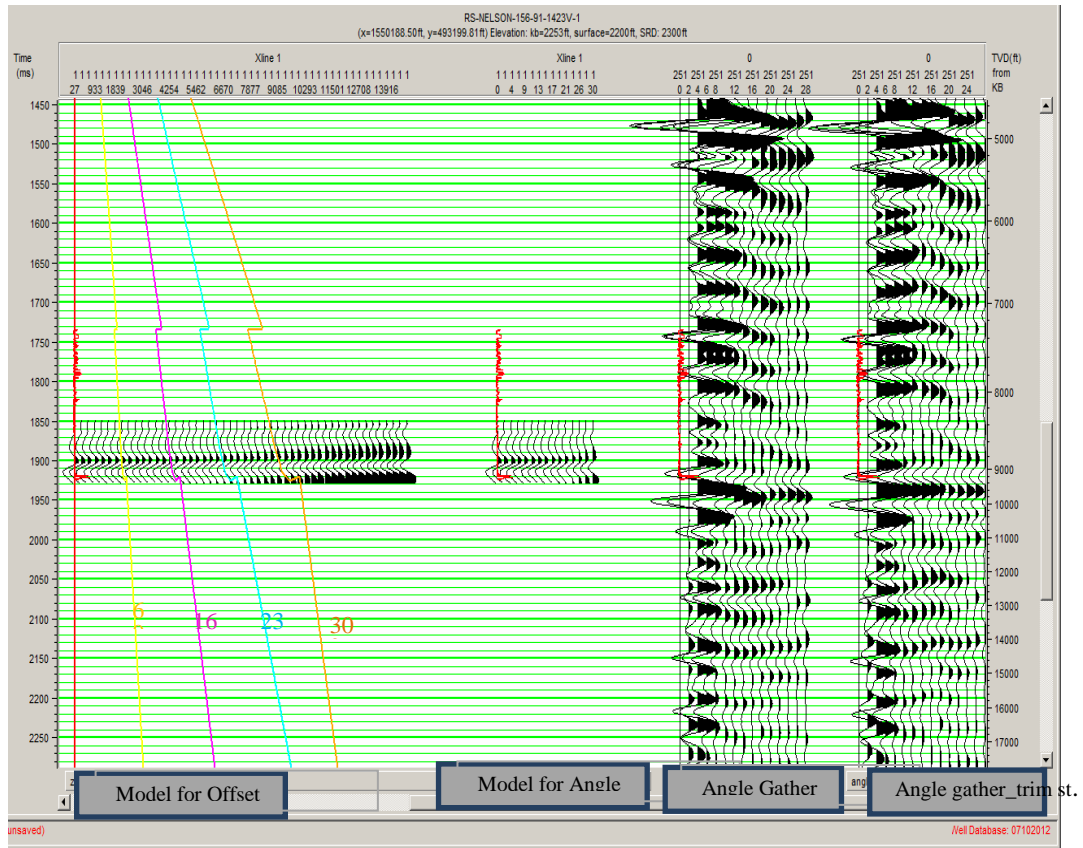Figure 4. 4 CDP gather before (A) and after (B) trim statics applied.

Figure 4. 5 Angle gather determined from the model of the offset. Suitable angle is 30^0
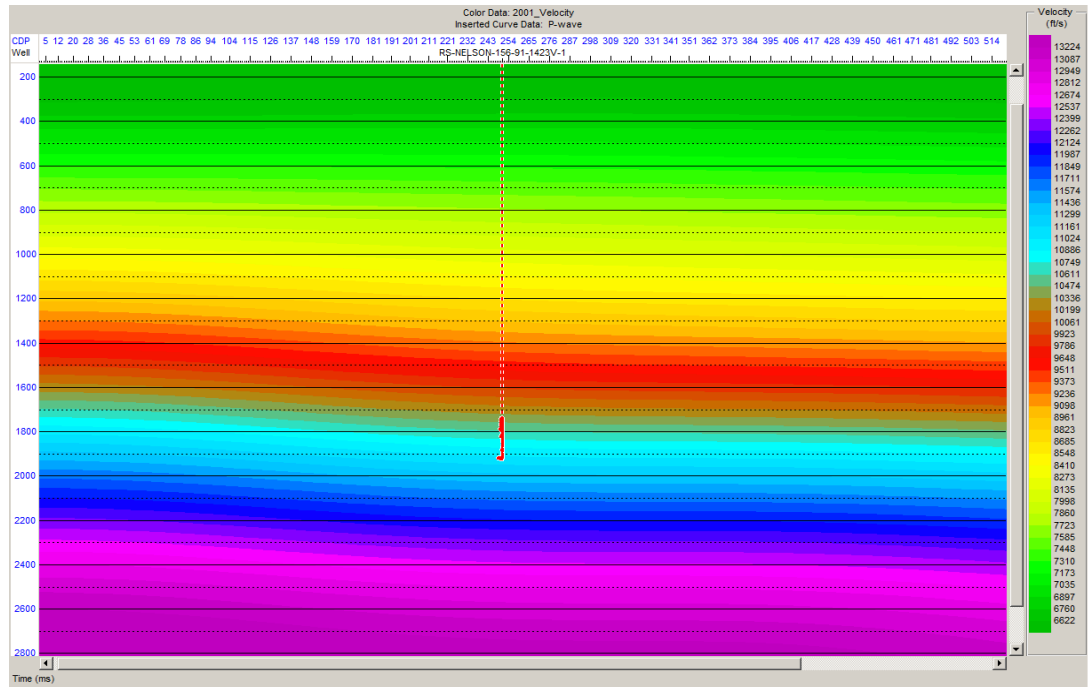
Figure 4. 6 Velocity volume (RMS velocity)
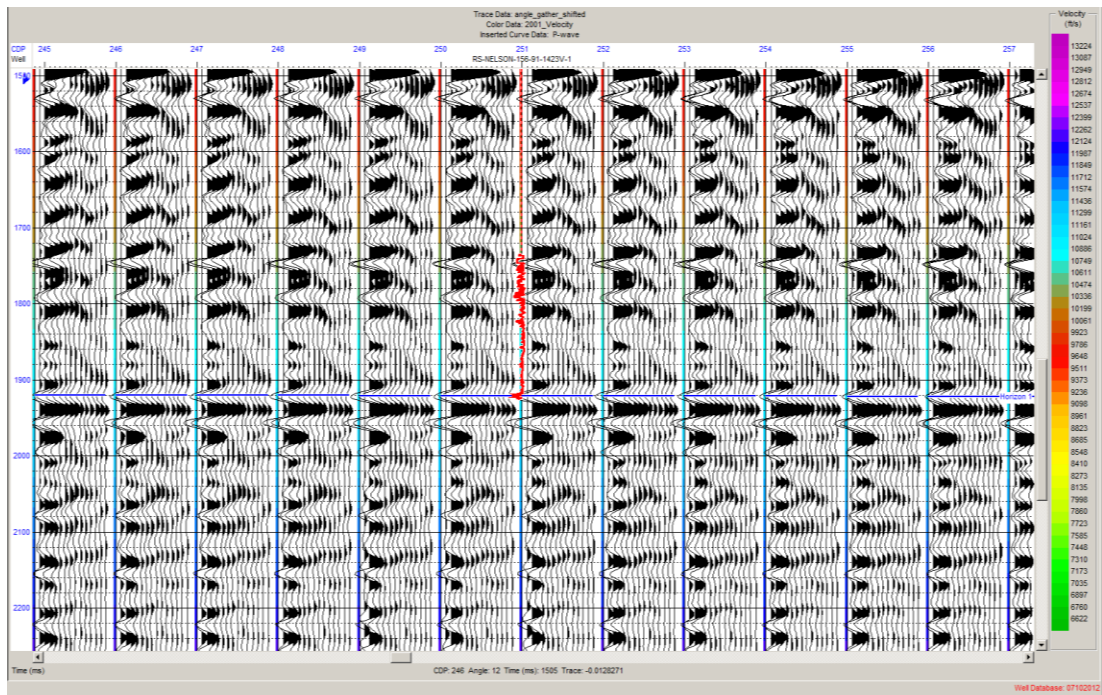
Figure 4. 7 Angle gather (trim applied) with velocity volume

Figure 4. 8 Gradient analysis for angle gather (a), model angle gather (b), and model

offset gather (c). negative gradient and positive intercept Class IV.

(a) Intercept volume attribute

(b) Gradient volume attribute

Figure 4. 9 Intercept and gradient volume

Gradient vs intercept cross-plot

AVO cross-plot on seismic section

Figure 4. 10 AVO cross-plot based on Class IV and attribute volume.

56

Chapter 5

Simultaneous Inversion and Applications
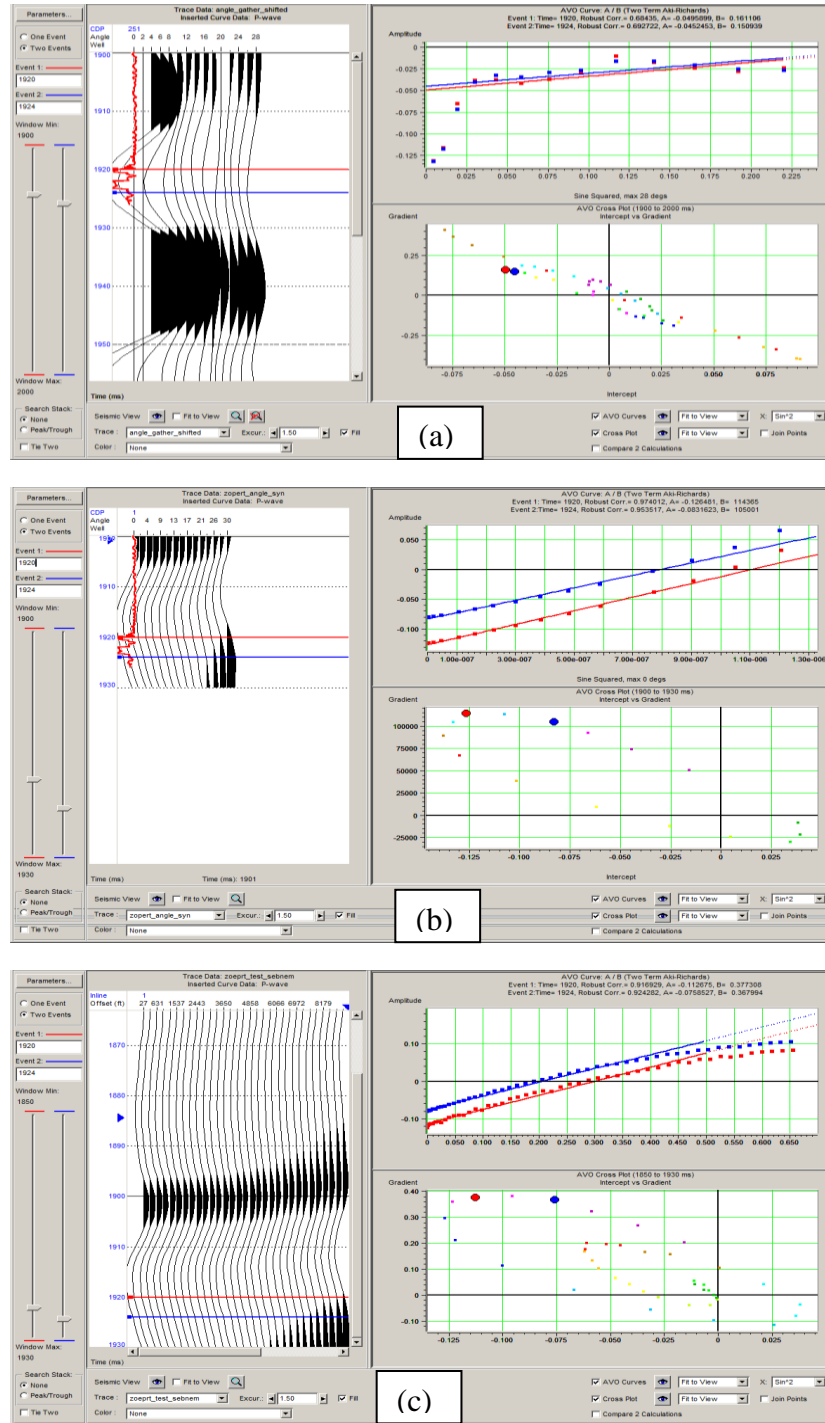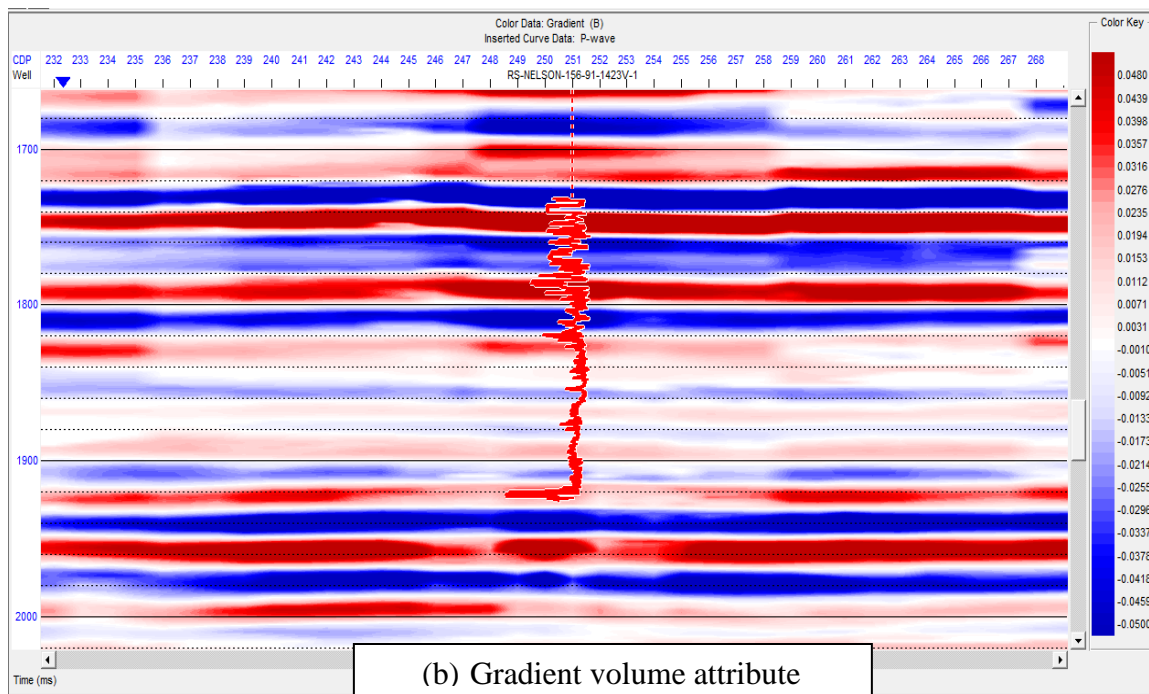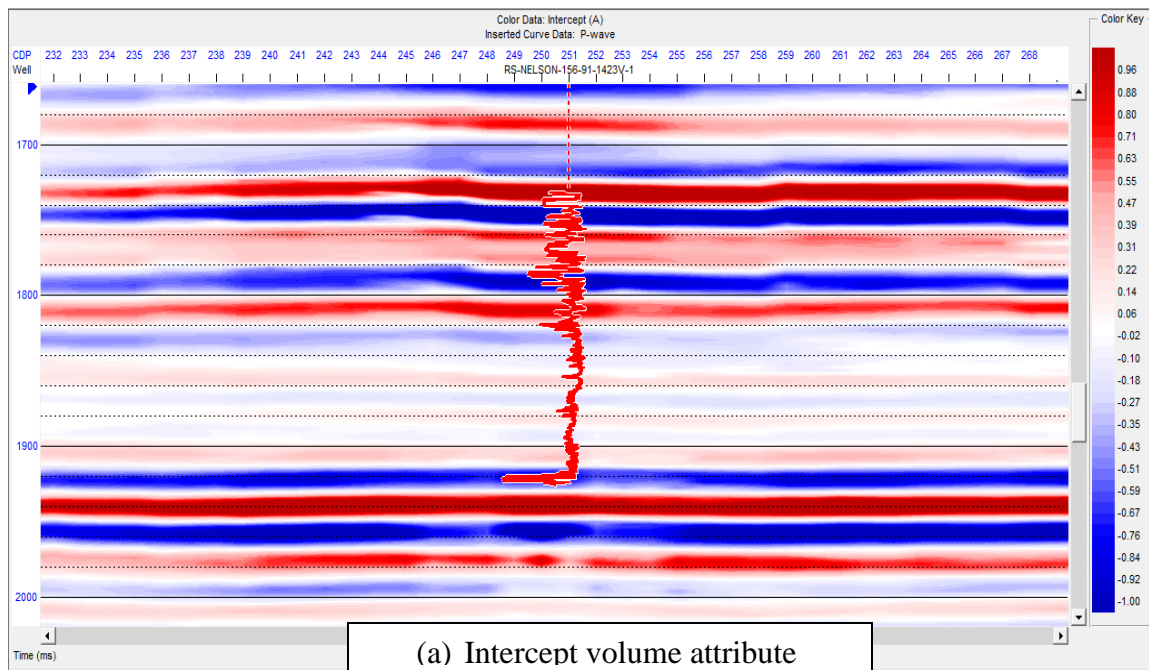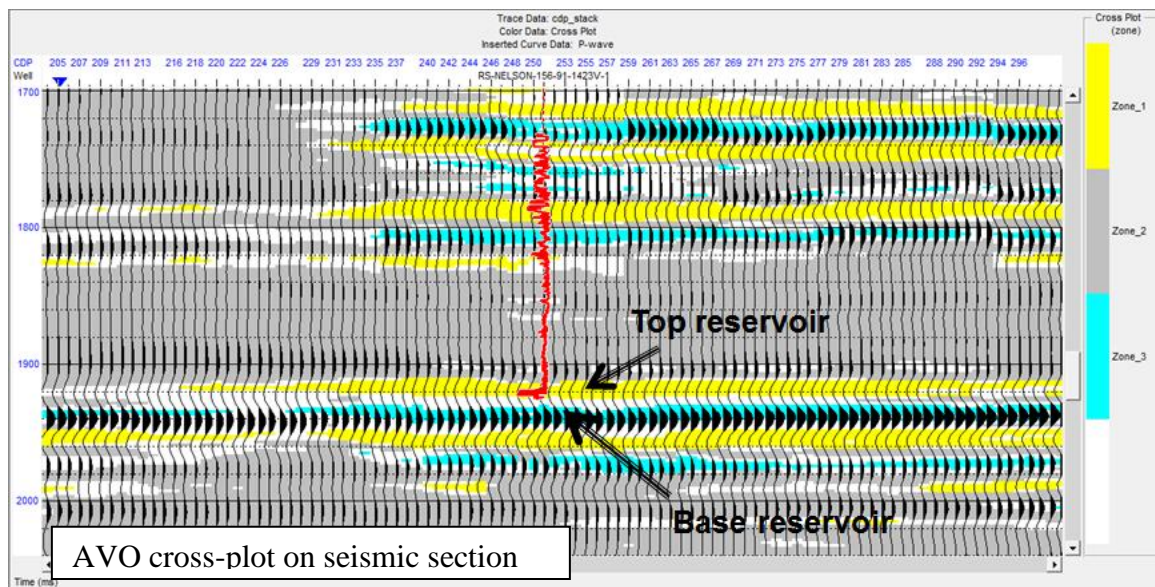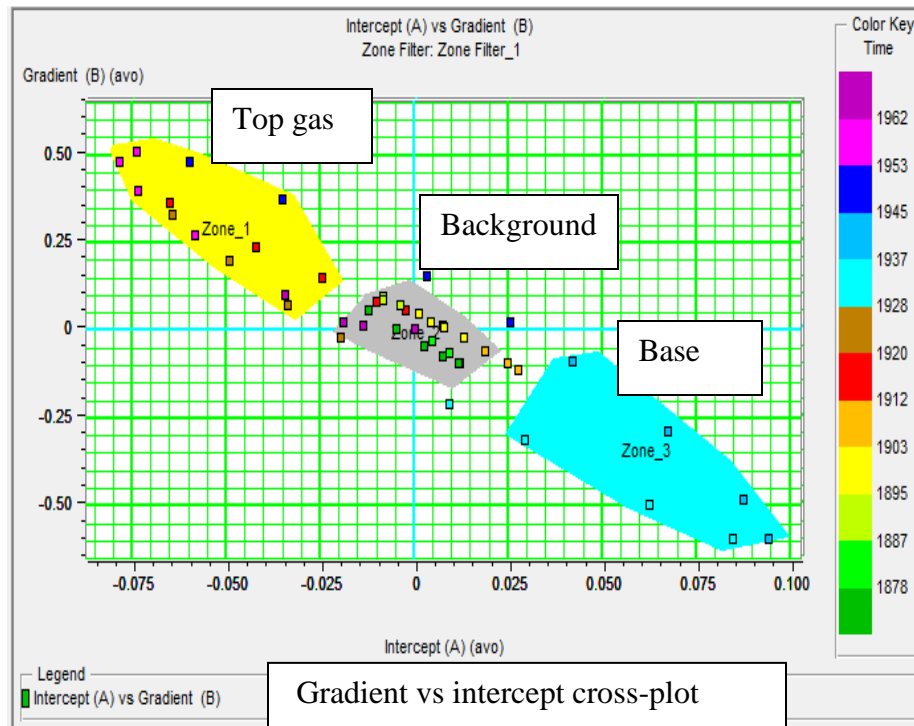
5.1 Seismic Inversion

Seismic inversion is one of the most effective ways used for oil and gas exploration in geophysics. It is used to define the rock properties of reservoirs by transformation of reflections. Pre-stack or post-stack inversions can be done by using well log and seismic data. In this study, rock properties in the zone of interest were defined by using pre-stack simultaneous inversion.

Inversion can be defined as earth model creation by using seismic data and well log information. Russell (2005) explains inversion as, "the process of extracting from the seismic data, the underlying geology which gave rise to that seismic".

Like applying forward modeling, seismic response can be created from the real earth model; however while applying inversion, the opposite is done. The realistic earth model can be created by using seismic section and subsurface information (Hampson-Russell Software, Strata Workshop, and June 2012).
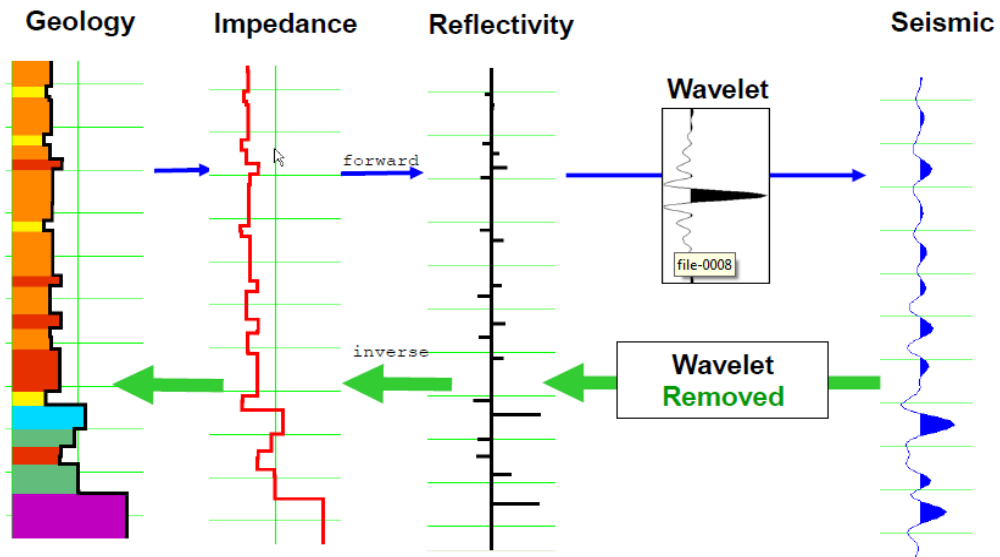
Figure 5. 1 Forward modeling and Inverse modeling (Hampson-Russell Software, Strata
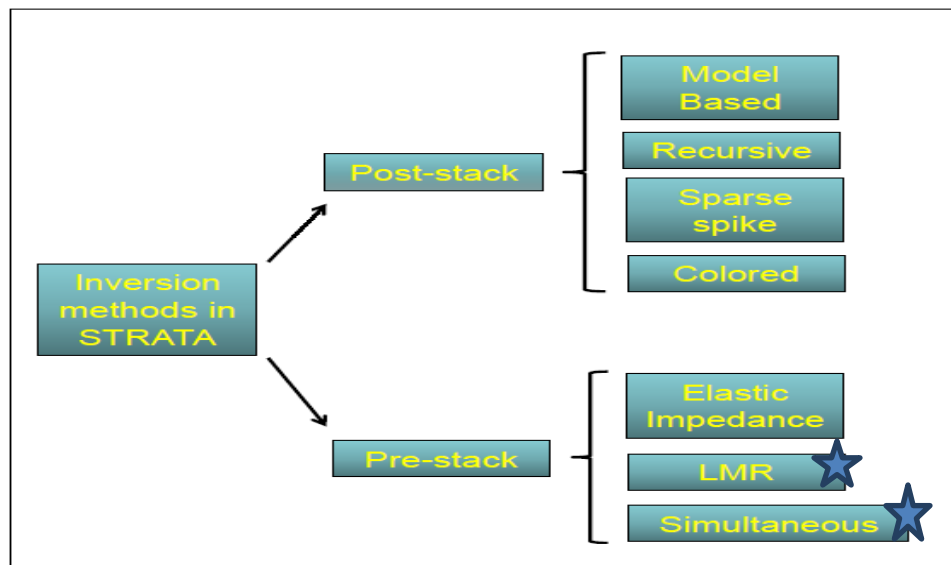
Workshop, and June 2012)

Figure 5. 2 Seismic inversion techniques that can be applied in Hampson and Russell.

Stars show inversion methods used in this study. (Hampson-Russell Software, Strata

Workshop, June 2012)

The forward graphical model can be analytically defined as;

$$S(t) = W(t)*R(t)+N(t)…..Eq\ 5.1$$

where S(t) is a output seismic trace

W (t) is the wavelet created for the seismic model

R (t) is a reflectivity

N (t) is a noise

The equation 5.1 that was expressed in frequency domain can be shown as a forward modeling in time domain as:

$$S(w) = W(w).R(w)+N(w)…..Eq\ 5.2$$

Since noise can be removed easily, reflectivity can be analytical definition of the process of inversion as:

$$R(w) = S(w)/W(w)…..Eq\ 5.3$$

Post-stack inversion and pre-stack inversion are the two types of inversion. When post-stack inversion fails, pre-stack inversion is applied on the seismic data where the differences of formations are very low in P-impedances.

Elastic inversion, LMR analysis, and simultaneous inversion are the three types of pre-stack inversion. Since elastic inversion did not offer an accurate result in this study, LMR analysis and simultaneous inversion were used.

Simultaneous inversion creates P-impedance, S-impedance, and density outputs by using multiple offset or angle seismic stack data and their wavelets.

Acoustic impedance (AI) is obtained by using density (ρ) and P-wave velocity and it is expressed as such:

$$AI = \rho * Vp \ldots . . Eq\ 5.4$$

Vp/Vs change in the S-wave data inversion is not effective as it is in the AVO data; however, the impedance data collected from inversion prove to be very useful (Russell, 2005).

When it is not possible to get information about geological layers in the area by only looking at seismic data, impedance data give information about rock properties in the area.

Impedance data include all the valid information from logs and seismic, it especially helps to steer away from all the complications, such as, wrong stratigraphy due to wavelets (Savic et al, 2000).

It is possible to obtain realistic information about the characteristics of the reservoir and lithology.

Since the vertical resolution was made to reach the maximum level, the tuning effect would not be a problem and it would provide one with more information.

It should be stated that a successful inversion result depends on how well correlation and extracted wavelet were. Interpretations can be made by outputs obtained from inversion and combining them with other information such as, well suite.

5.2 Pre-stack Inversion Applications

Inversion process was conducted with the trim statics that was applied to the angle gather, after the AVO analysis. Angle gather was used in the inversion process as it was done in the AVO analysis. In order to do pre-stack simultaneous inversion, the STRATA module in Hampson-Russell Software was used. Trim statics was applied to the angle gathers, which, those angle gathers were uploaded to the software. The well log data from the database are needed in order to create impedance volume that was used in the process correlation or extract wavelets, which are not needed with the help of well log data.

After the desired data were created in STRATA, inversion analysis was performed on the well location. The inversion analysis on direct log and seismic section gave results with their original impedance logs. It also depicted how much error it would provide while comparing synthetic and original composite traces. The inversion parameters were also modified in order to minimize the error percentage from a higher percentage. In order to have better results in the upcoming inversions, the parameters were modified multiple times.

Inversion parameters were extracted by changing P-impedance (Zp) versus S-impedance (Zs) cross-plot, and density versus P-impedance (Zp) cross-plots in the process of modification (Figure 5.3). After all the tests were performed, the best correlation was found to be 0.63. As the most suitable parameters were found, simultaneous inversion can be seen.

After all the analysis was conducted, P-impedance, S-impedance and density models were created by using angle gather. While creating the model, Bandpass filter was applied on the data. The views P-impedance, S-impedance, density, P-wave, and S-wave of final acoustic impedance models were created for the area worked on, after the pre-stack inversion.

Following the steps mentioned above, all the anomalies were observed clearly and the impedance volumes were compared with original well data. LMR analysis was performed right after pre-stack inversion to support the results.
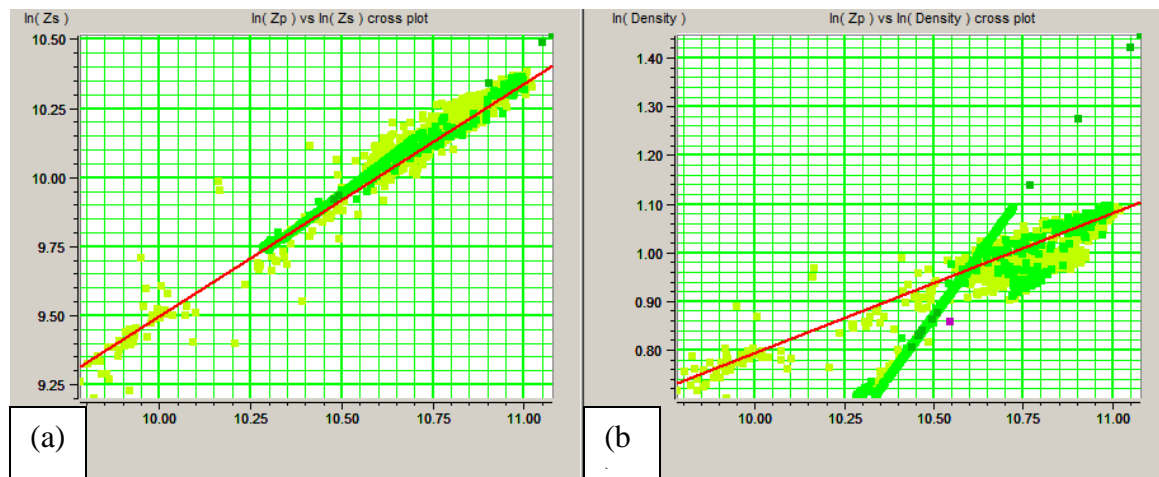

Figure 5. 3 Cross-plots for inversion analysis. (a) Zp vs. Zs, (b) Zp vs. ρ
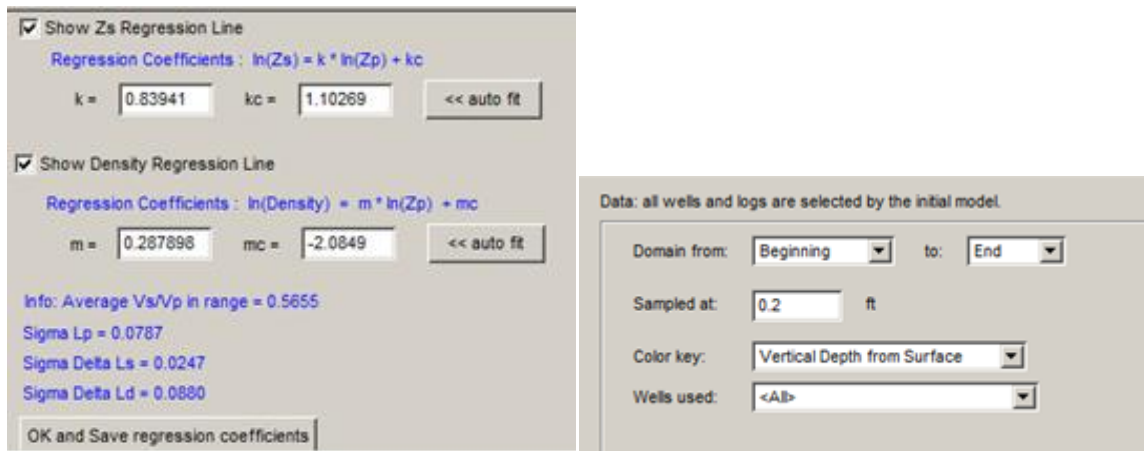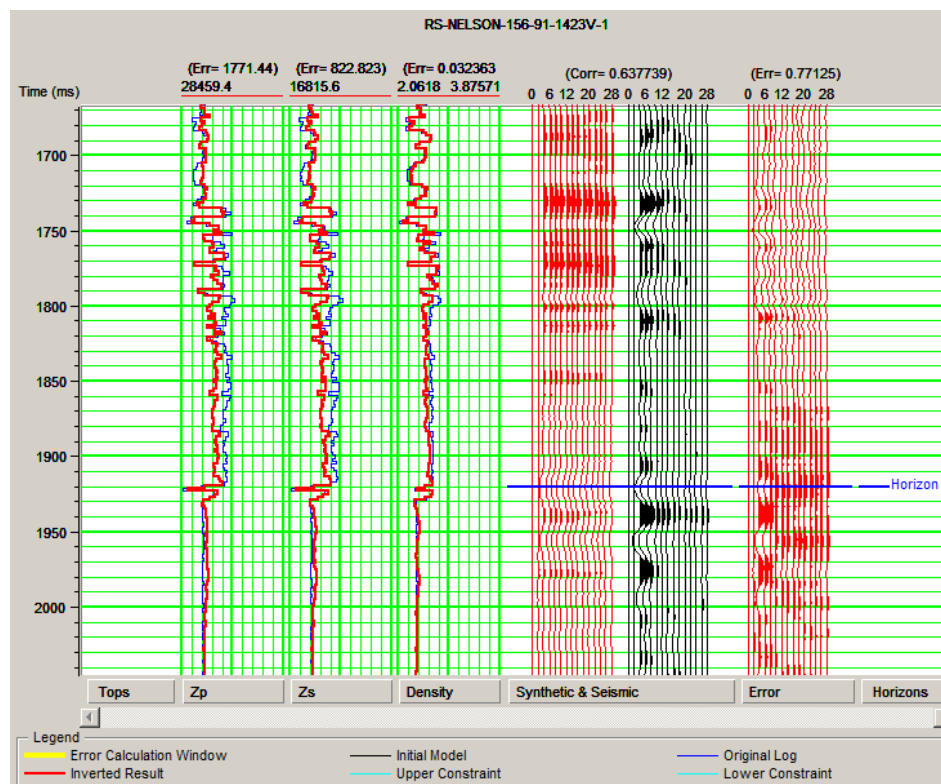
Figure 5. 4 Extracted inversion parameters

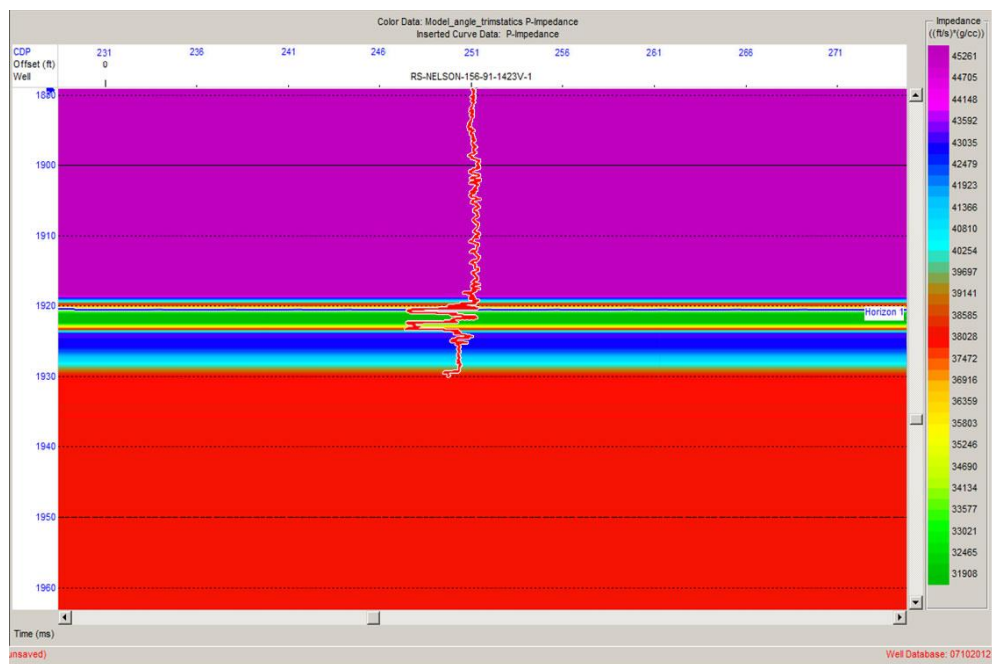Figure 5. 5 Inversion correlation error analysis.

Figure 5. 6 Initial model of P-impedance for 2001 seismic line

Figure 5. 7 Initial model of S-impedance for 2001 seismic line

64

Figure 5. 8 Initial model of density for 2001 seismic line

Figure 5. 9 Initial model of P-wave velocity for 2001 seismic line

Figure 5. 10 Initial model of S-wave velocity for 2001 seismic line

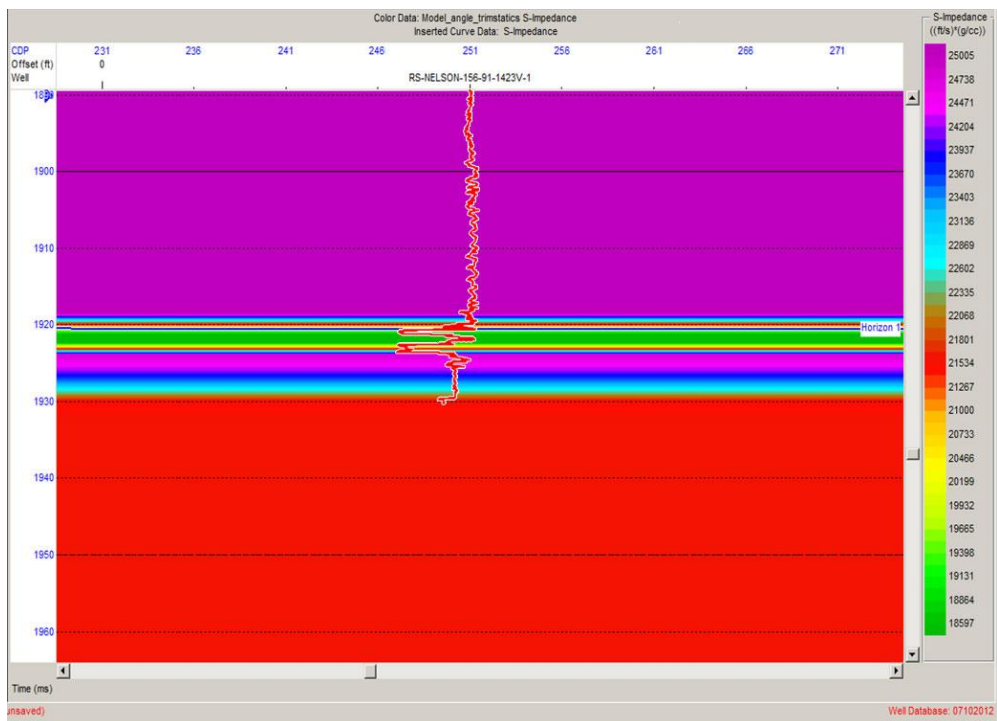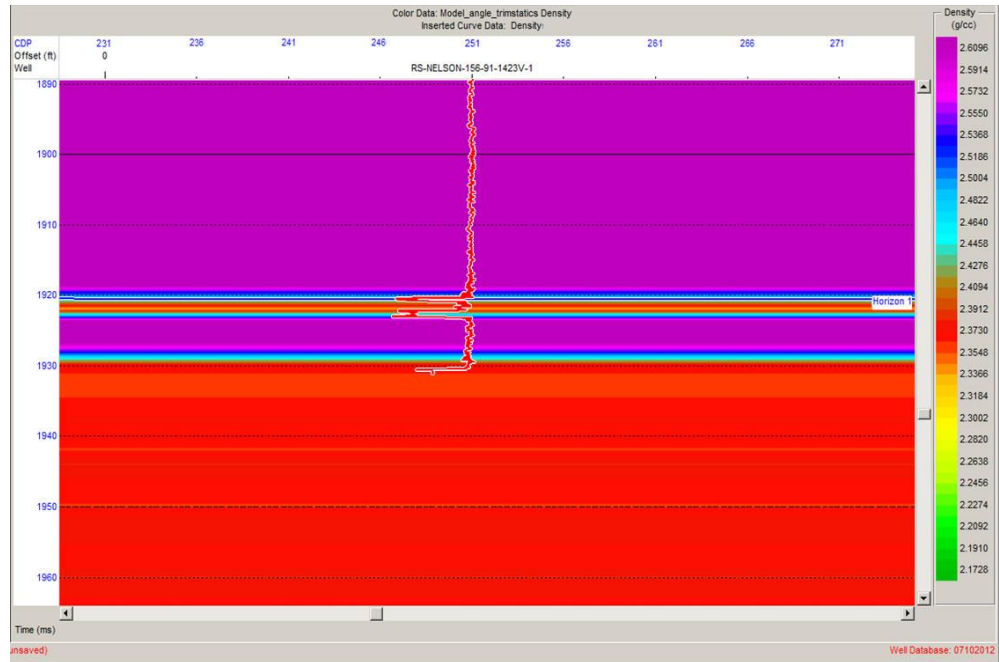Figure 5. 11 Initial model of P-impedance for 1001 seismic line

66

Figure 5. 12 Initial model of S-impedance for 1001 seismic line

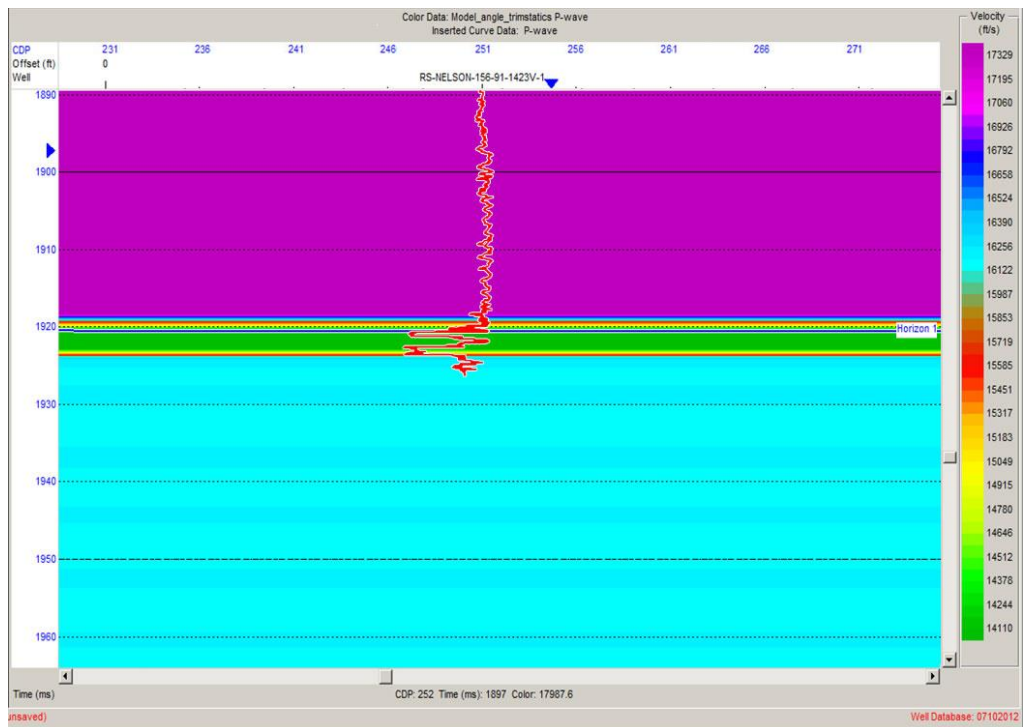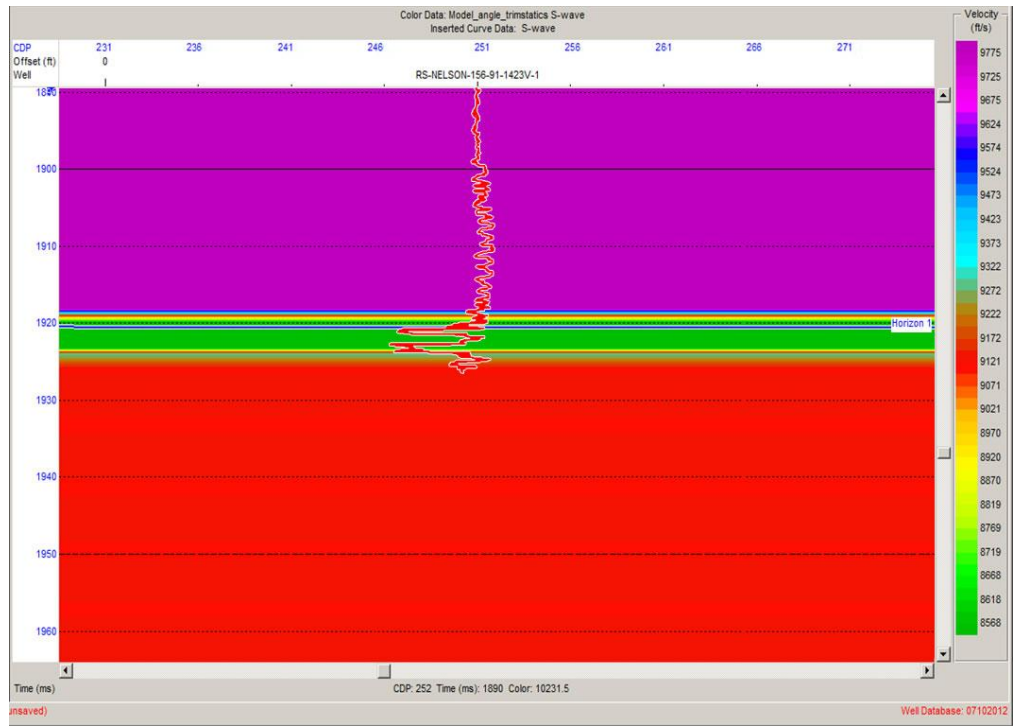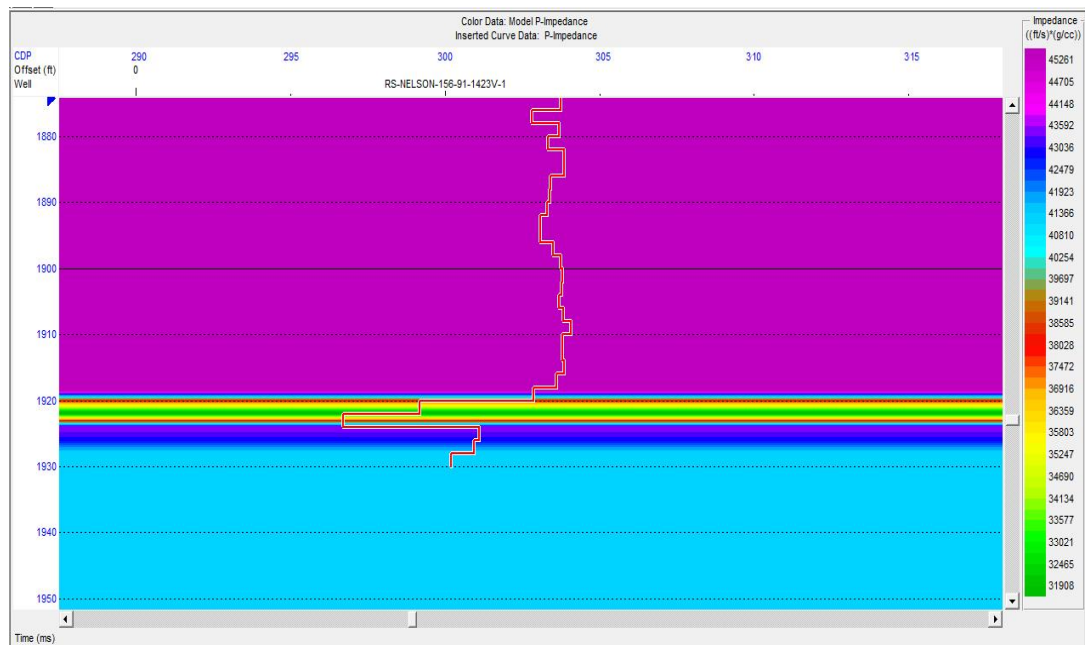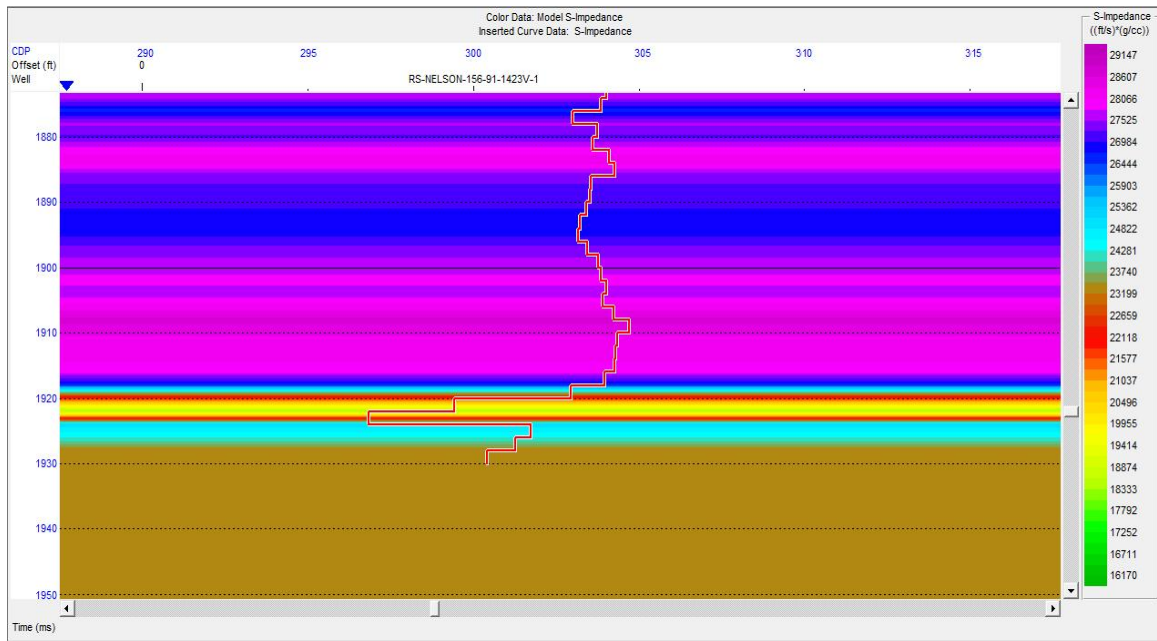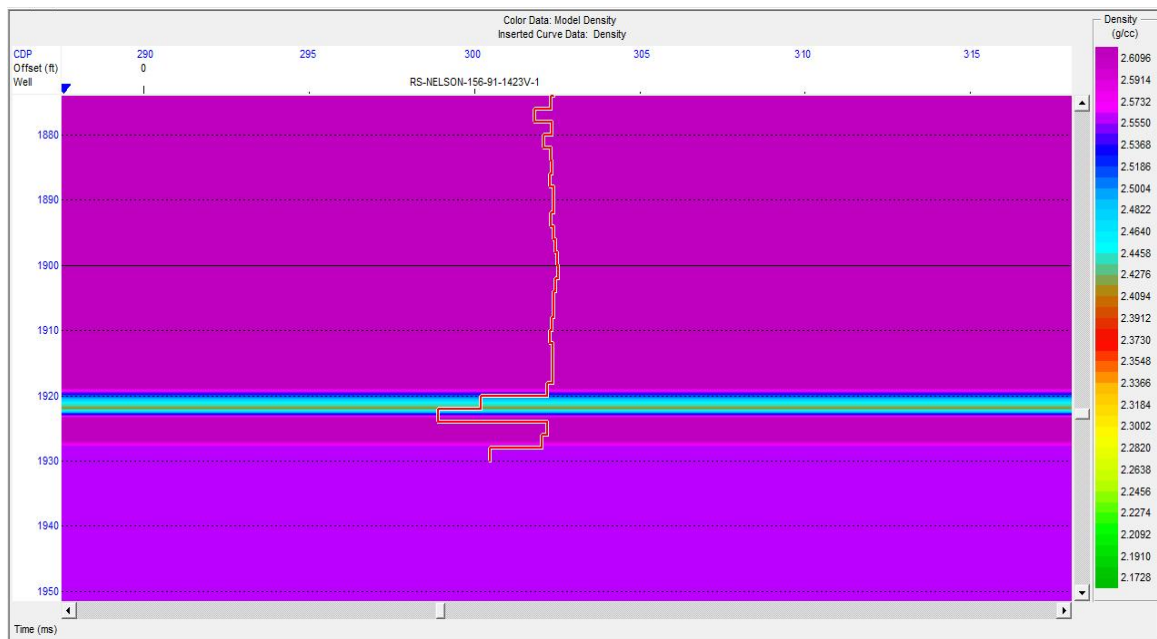Figure 5. 13 Initial model of density for 1001 seismic line
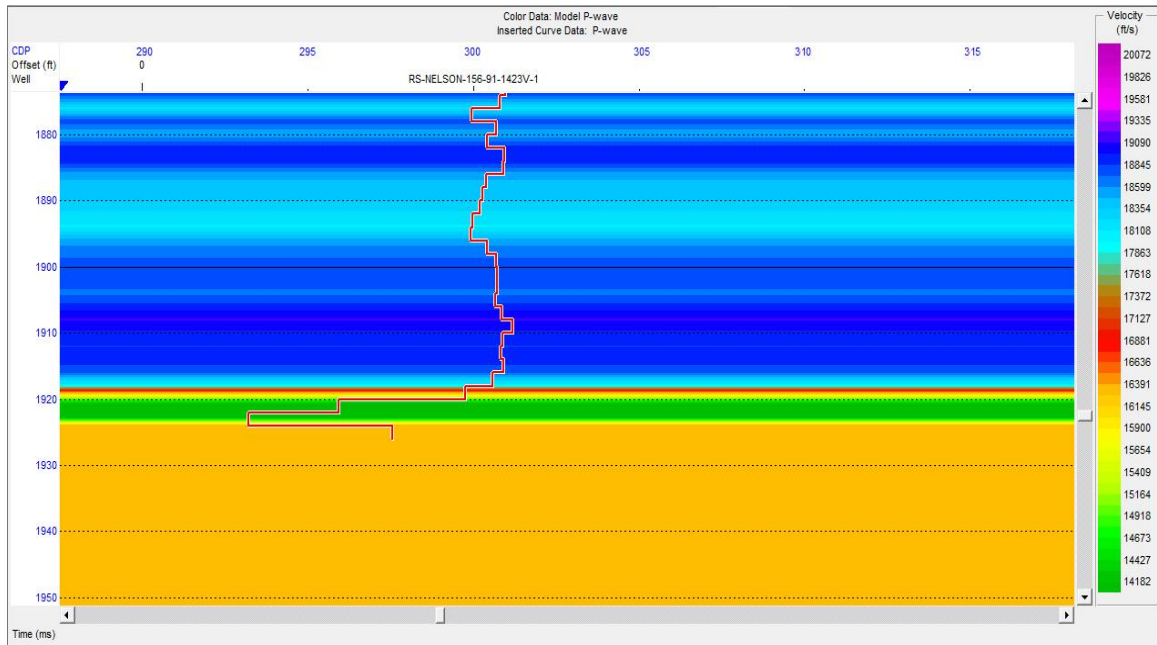
Figure 5. 14 Initial model of P-wave for 1001 seismic line
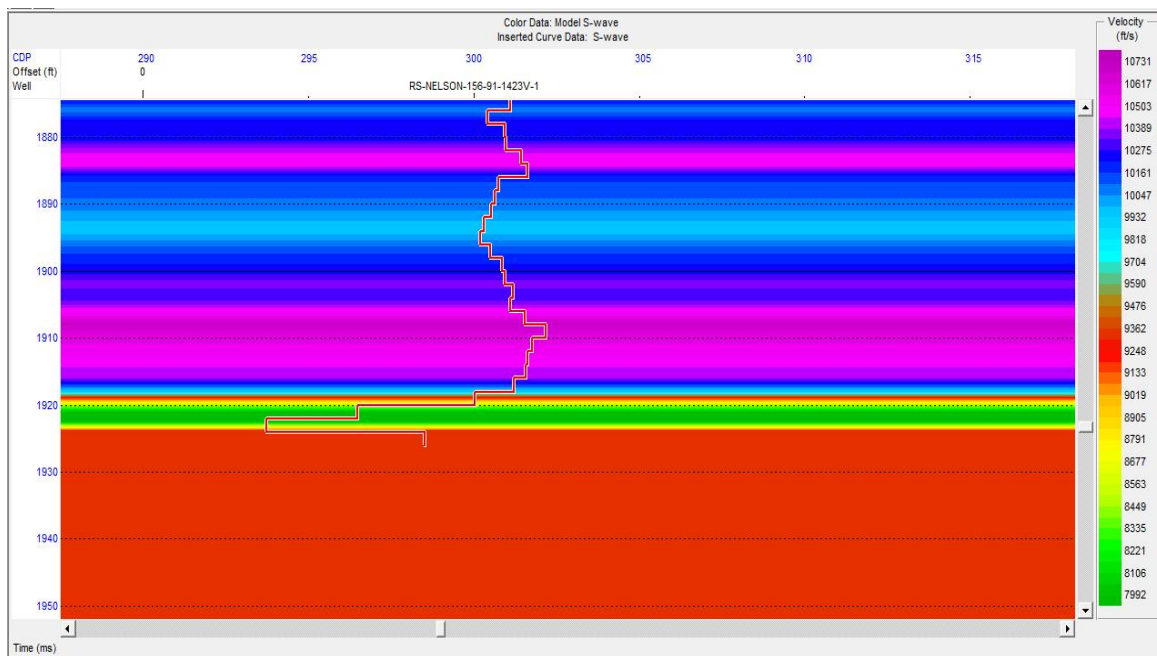
Figure 5. 15 Initial model of S-wave for 1001 seismic line

Chapter 6

Lambda, Mu-Rho Analysis

6.1 Introduction

Lamé Parameters (LMR, Lambda, Mu, and Rho) are commonly used to determine the type of reservoir rock or reservoir fluid. It is possible to detect and determine the characteristics of focused reservoir by using models which are obtained from derived Lamé parameters. In addition, using LMR responses, it is possible to differentiate shale zones.

Goodway (2001) describes that Lamé parameters (λ incompressibility and μ rigidity) can be used for seismic reservoir characterizations together with rock density. Rigidity, incompressibility, and density parameters show different values within different lithology, which is needed to be effective to conduct sensitive analysis in order to determine pore fluids inside the reservoir.

6.2 Theory and Method

P-wave velocity (Vp), S-wave velocity (Vs), and density (ρ) changes are vital elements in reservoir characterization practice. Rock properties inside the reservoir are determined with regards to those changes. Goodway, Chen, and Downton (1997) expressed the Lamé parameters by using below formulas:

$$Vp^2= (\lambda+2\mu)/\rho \text{ and } Vs^2=\mu/\rho \qquad \text{Eq. 6.1}$$

It can be formulized by correspondence of λ and μ with velocity that derive from Vp and Vs formulas:

$$\lambda= Vp^2.\rho-2Vs^2.\rho \text{ and } \mu=Vs^2.\rho \qquad \text{Eq 6.2}$$

The study expressed reservoir properties in the inversions. These properties include not only velocity properties, but also with impedance changes. If we apply impedance changes, S-impedance (Is) and P-impedance (Ip), to the Vp − Vs formula above, one can surmise:

$$Ip^2= (Vp.\rho)^2= (\lambda+2\mu)\rho \text{ and } Is^2= (Vs.\rho)^2=\mu\rho \qquad \text{Eq. 6.3}$$

If one were to extract Lambda-Rho ($\lambda\rho$) and Mu-Rho ($\mu\rho$) values from the equation above, it can be assumed as the following:

$$\lambda\rho= Ip^2-2Is^2 \text{ and } \mu\rho=Is^2 \qquad \text{Eq. 6.4}$$

70

As it can be seen from the equation above, it is challenging to calculate impedance or to conclude intercept and gradient in AVO analysis, since density is unknown or could not be estimated from the logs. However, it is possible to find LMR density as a log from unknown seismic; therefore, one can surmise both $\lambda\rho$ and $\mu\rho$ to be directly related with impedance; it can be used to determine rock properties (Goodway, 2001).

Incompressibility, unlike rigidity, is not a physical property. One can state that incompressibility changes while rigidity remains unaffected according to the rock matrix in connection to the pore fluid. The ratio of the two values (λ/μ) gives information about rock properties and pore fluid (Goodway et al., 2010).

Goodway (2001) and Perez and Tonn (2003) created cross-plot templates of the ratio of Lamda-rho and Mu-rho that would give information of rock properties (Figure 6.1-6.2).
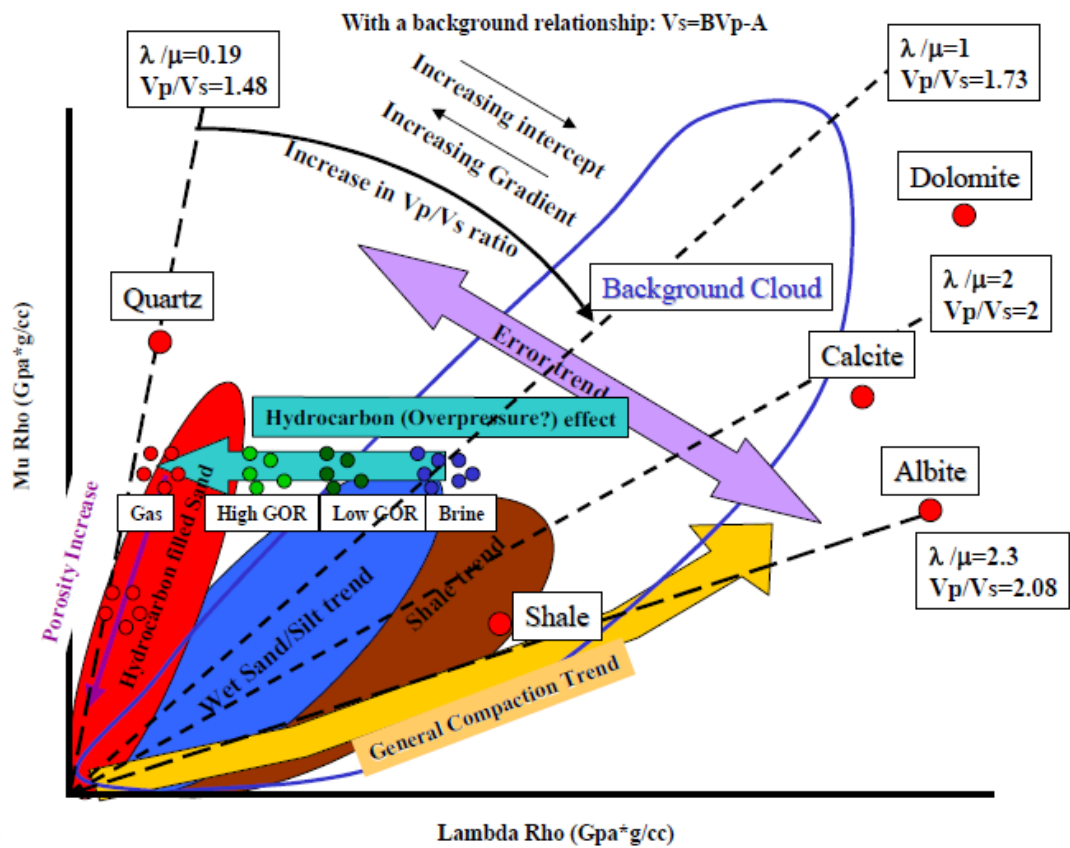
Figure 6. 1 LMR cross-plot classification (Perez and Tonn, 2003)
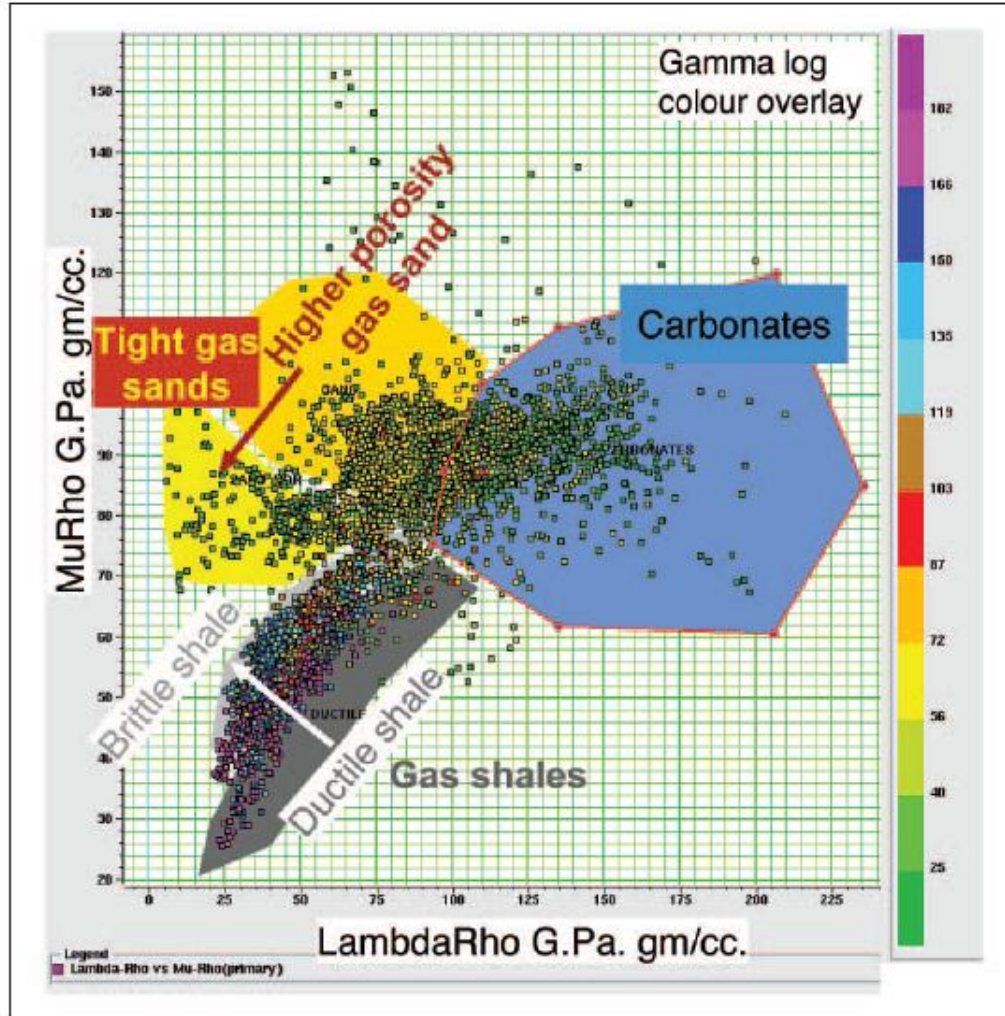
Figure 6. 2 LMR cross-plot analyses from Goodway et al. (2010). This figure shows an example analyzing cross-plot using template.

According to the LMR classification, grain inside the formation, in regards to large quantities, would not be affected from stress if incompressibility is more than rigidity. This generally can be found in laminated shale. If $\lambda=\mu$, then the grain shape is affected from stress and it is organized randomly. This situation usually can be found in sand, therefore, if the ratio of $\lambda\rho/\mu\rho$ gets smaller, there will be a transition from shale to sand.

6.3 LMR Cross-plotting

As explained in theory and method, cross-plot techniques have been chosen in order to conduct LMR analysis. While preparing a LMR cross-plot, three different steps have been used to create them.

In the first stage, Lambda-Rho and Mu-Rho values are calculated from the measured P-wave, S-wave logs, and density values by using equation and drew log. With these new logs, it was seen like the originals, Lambda-Rho and Mu-Rho values follow the Bakken Formation trend. The cross-plot was drawn by using these values. Gamma ray was used as the color key. It has been found that the Upper and Lower Bakken have high gamma rays, and the Middle Bakken has low gamma rays. Considering this, the Upper and Lower Bakken zones have been marked with red on the cross-plot in order to show their highest gamma ray values. Instead, the Middle Bakken zone has been marked with blue in order to show the lowest gamma ray values.

The second cross-plot stage was done by using Lambda-Rho and Mu-Rho values which derived from the seismic section. In order to determine the zones, only one trace from the seismic session was used. It was difficult to differentiate all the members of the seismic obtained Lamé parameters because it was not possible to see the Bakken members of the seismic section with details. Consequently, the Upper and Middle Bakken were derived together, which the green color indicates and the red color for the Lower Bakken.

In the third and the last stage, the two cross-plots were combined, and Lambda-Rho and Mu-Rho values were used to achieve a clearer result. Lambda-Rho and Mu-Rho values

have derived by final impedance results that were found by using seismic and log values together to obtain from simultaneous inversions. From the obtained results, LMR cross-plotting was created. Since the last cross-plot had the seismic and log values together, it was selected to utilize the data in this analysis. The color key on the cross-plot was chosen to be gamma ray. Similar to the second stage, the Upper and Middle Bakken were marked with a green color, and the Lower Bakken was marked with a red color.

In the cross-plots, gamma ray was used as the color key. As it is known from the geology of the area worked on, the Upper and Lower Bakken consisted of shale, and the Middle Bakken consisted of organic contents. The Total Organic Content (TOC) in the Bakken Formation is 11%. The total organic content carries traces of source rock potential. It can be used to determine TOC in the well logs. As a result, it can be obtained by using density, sonic, and gamma ray evaluations. In the gamma ray measurements, gamma spectrum changes with respect to potassium, uranium, and thorium inside the rock. The reflections of uranium on gamma rays are similar to TOC traces (Mendelson, 1985). According to the information explained, since specific TOC values were not known, gamma rays have been used as color key in LMR analysis.
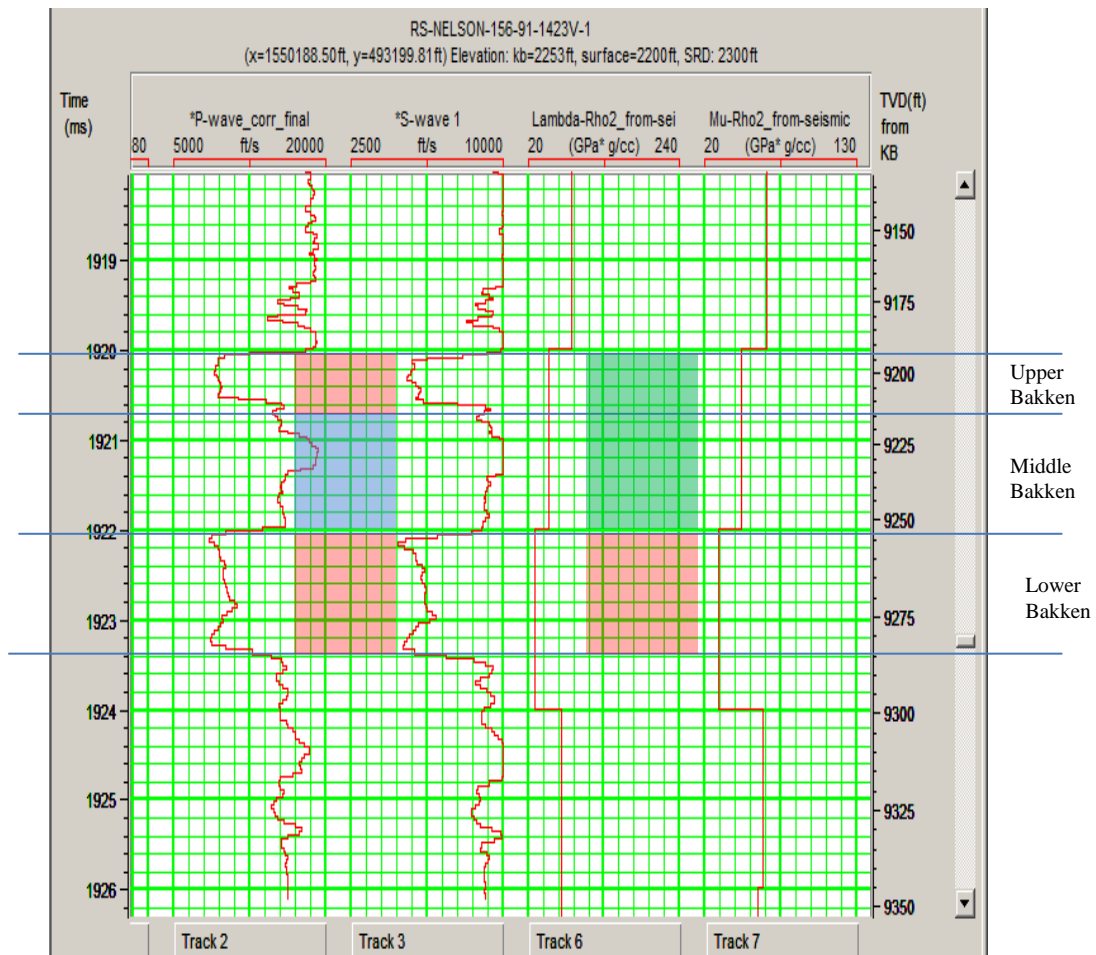
Figure 6. 3 Log results for Lambda-Rho and Mu-Rho comparing with P-and S-wave velocity.
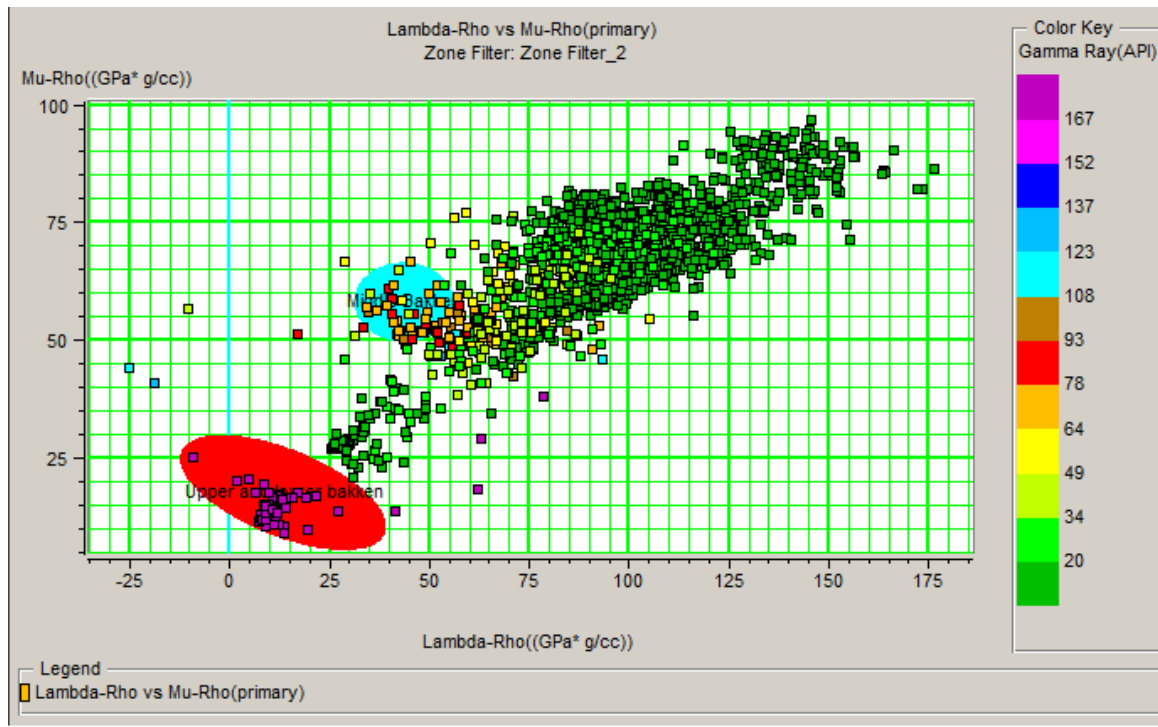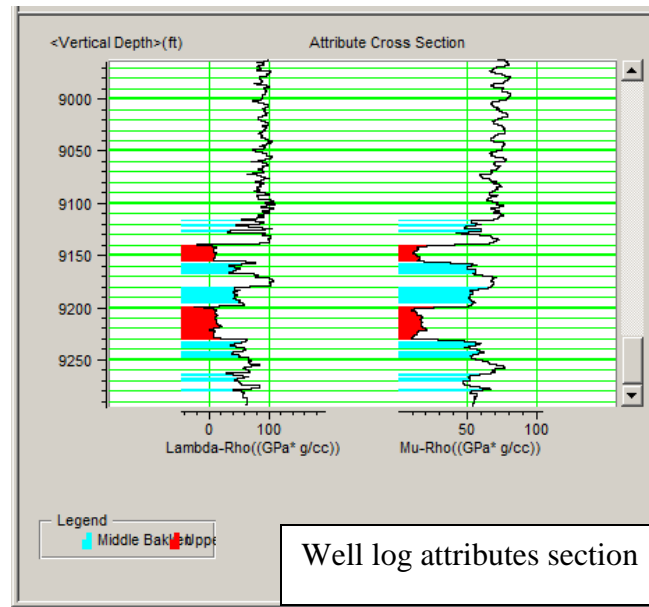
Figure 6. 4 Lambda-Rho versus Mu-Rho cross-plot from log values with color key

gamma ray.

Seismic trace attributes section
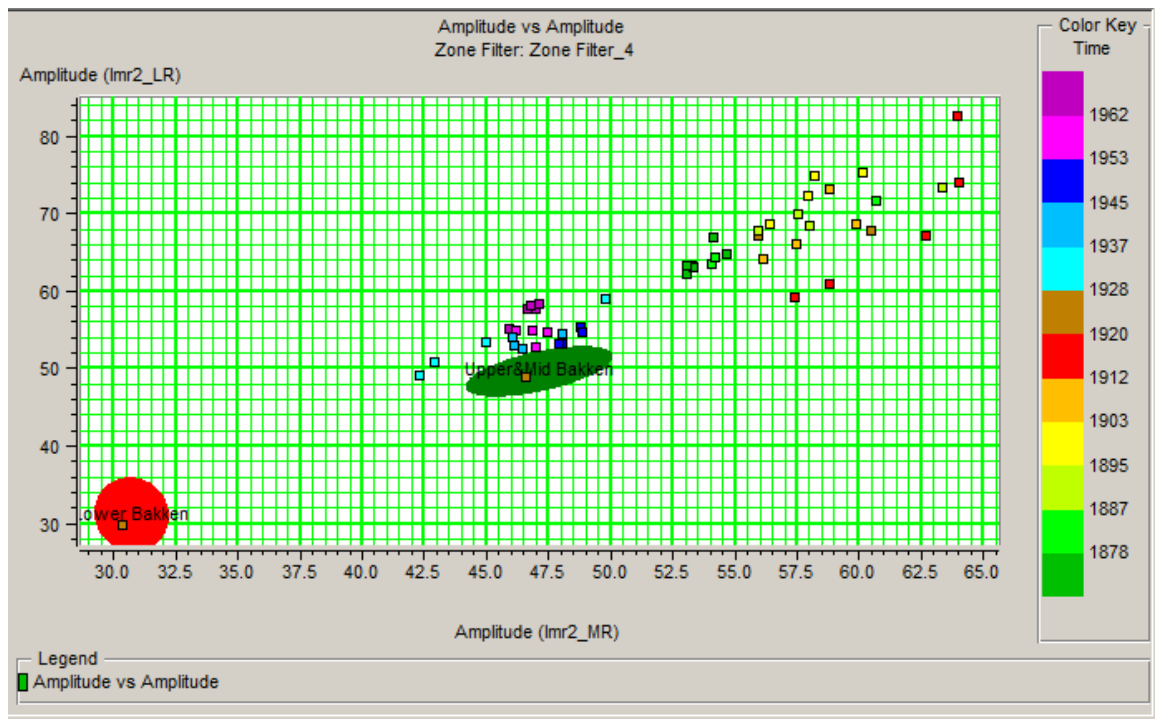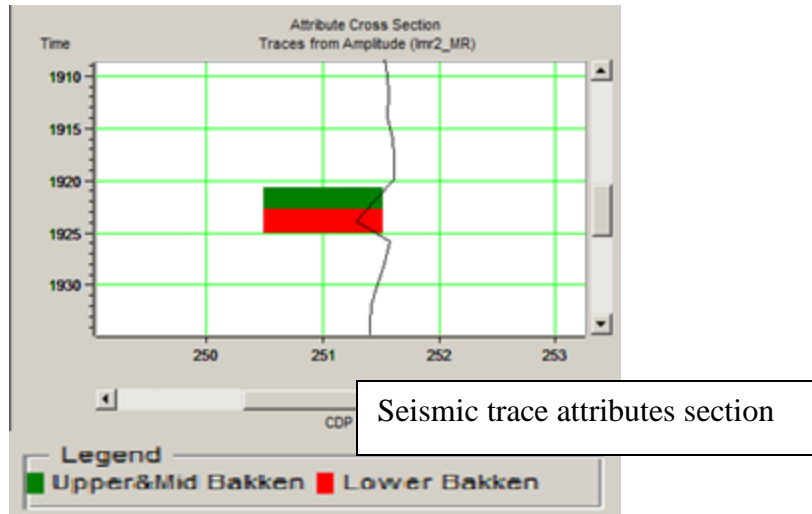

Figure 6. 5 Lambda-Rho versus Mu-Rho cross-plot from seismic values

Lambda-Rho and Mu-Rho derived from simultaneous inversion, plot attributes section
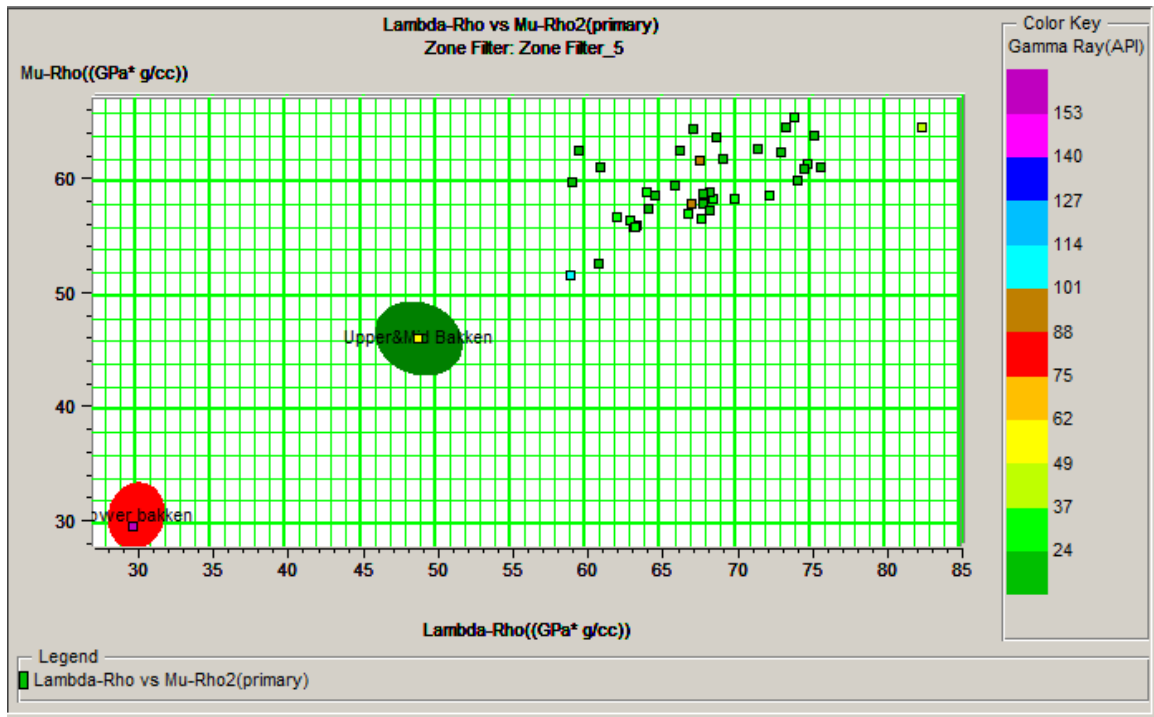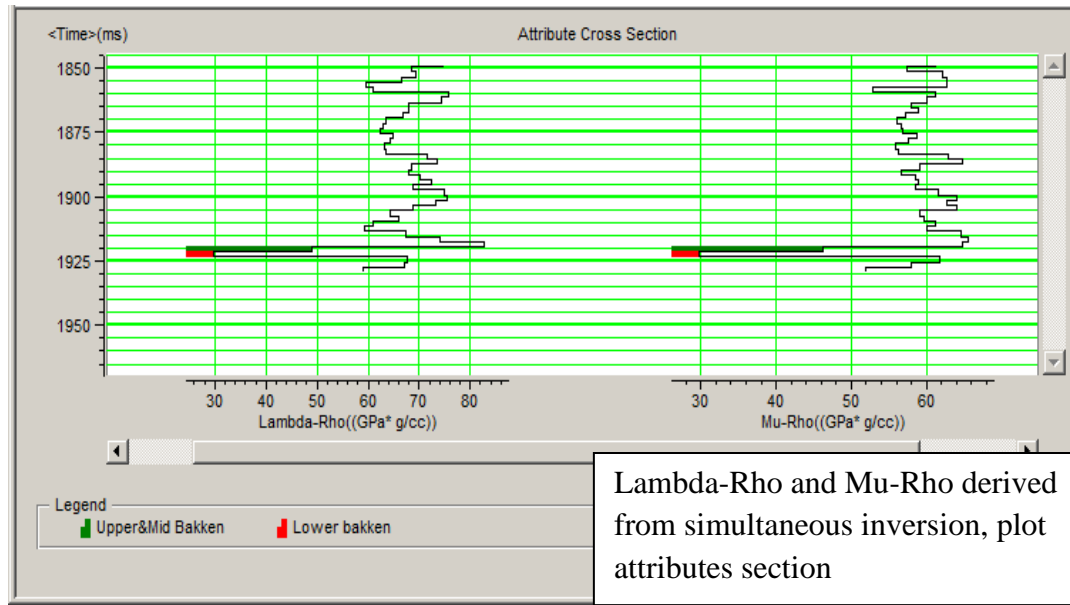

Figure 6. 6 Lambda-Rho versus Mu-Rho derived from simultaneous inversion cross-plot

Chapter 7

Results

The results of AVO analysis, pre-stack inversion, and LMR cross-plot have been interpreted in this chapter. The results obtained from different analysis have been compared.

7.1 AVO Analysis

The classification of AVO anomalies usually depend on their angle or offset change. In order to conclude a classification, intercept and gradient volumes were used. CDP gathers have been flattened by applying trim statics, which are improved by using signal-to-noise ratio. When the angle gathers have been created, it was then proven that the analysis gave similar results to the Class IV.

Since the formation is shale, dolomite, and sandstone, it would not be possible to fit it in a specific classification. However, as discussed in Chapter 4, it shows similarities to sand in AVO analysis within dolomite. Since the seismic resolution and frequency are low, the creation of intercept and gradient cross-plots corresponding to AVO volumes did not give any results. Area of the interest could not be seen in details in the cross-plot. In order to improve this process, the data analysis has been conducted with pre-stack inversion.

7.2 Pre-stack Simultaneous Inversion

The main reason for doing the pre-stack simultaneous inversion is to define each member of the Bakken Formation and to analyze the changes of rock properties by improving vertical resolution.

The performed analysis have been obtained from inverted acoustic impedance model, inverted shear wave impedance model, inverted density model, inverted P-wave model, and inverted S-wave model by using their initial models with angle gathers. The main focus was the impedance models created at the end of inversion in the area worked on.

The correlation of the inverted models and initial models, for the P-impedance, S-impedance, density, P-wave, and S-wave are high. With the results of these, the upper, middle, and lower Bakken members are differentiated well.

The inverted volumes of P-impedance, S-impedance, P-wave, and S-wave for the Bakken Formation have been determined to be lower than the underlying Three Fork formation, and the overlying Lodgepole Formation. The upper and lower formations consist of shale and have higher values than the middle member of the Bakken Formation. Even though the density volume has shown similar values, it doesn't show any results that reflect the geology.

From all the obtained results, it can be said that the Upper Member and Lower Member of the Bakken Formation is characterized by shale. However, Middle Member of the Bakken Formation is an alternation of dolomite and sandstone with lesser shale contribution.

With AVO intercept or gradient results, it was not possible to see the formation details because of the low vertical resolution. As a result AVO analysis has failed in this study. The results were compared by using LMR analysis.
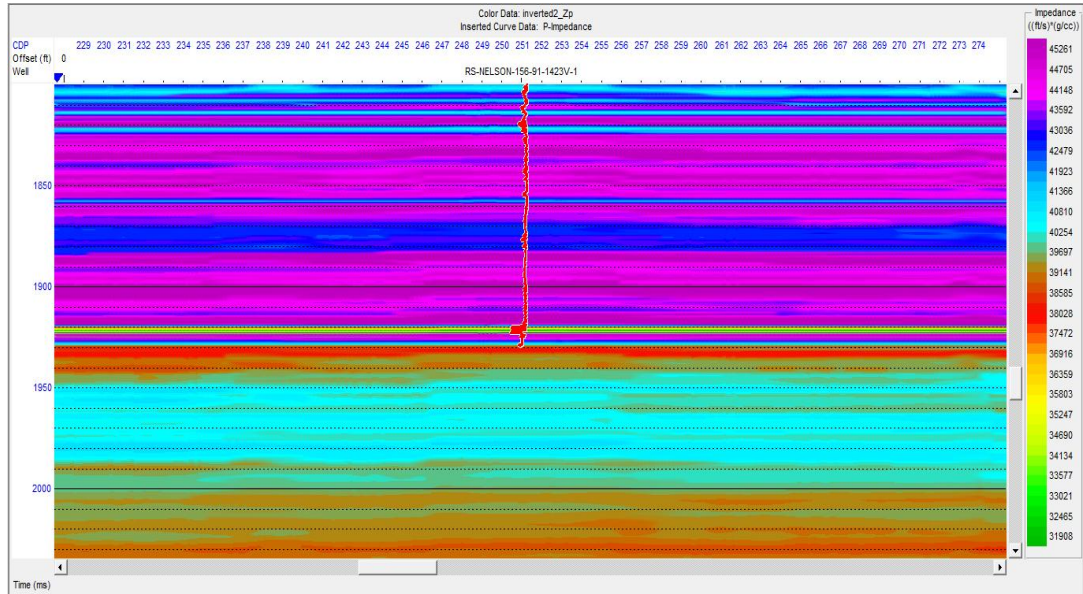

Figure 7. 1 Inverted acoustic impedance result for 2001 seismic line
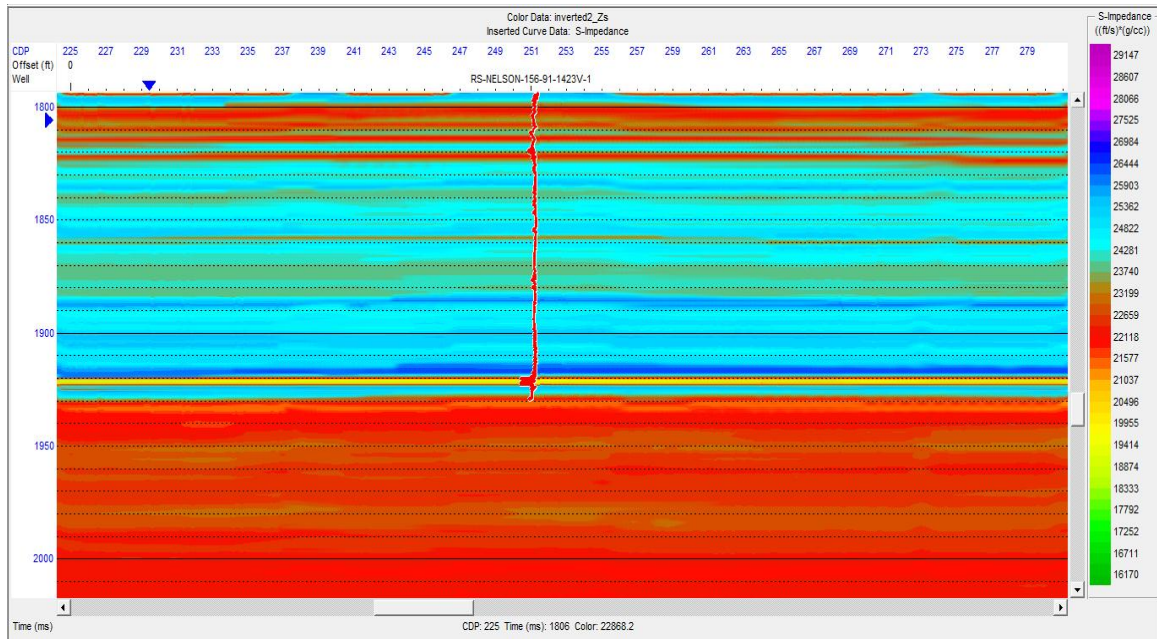
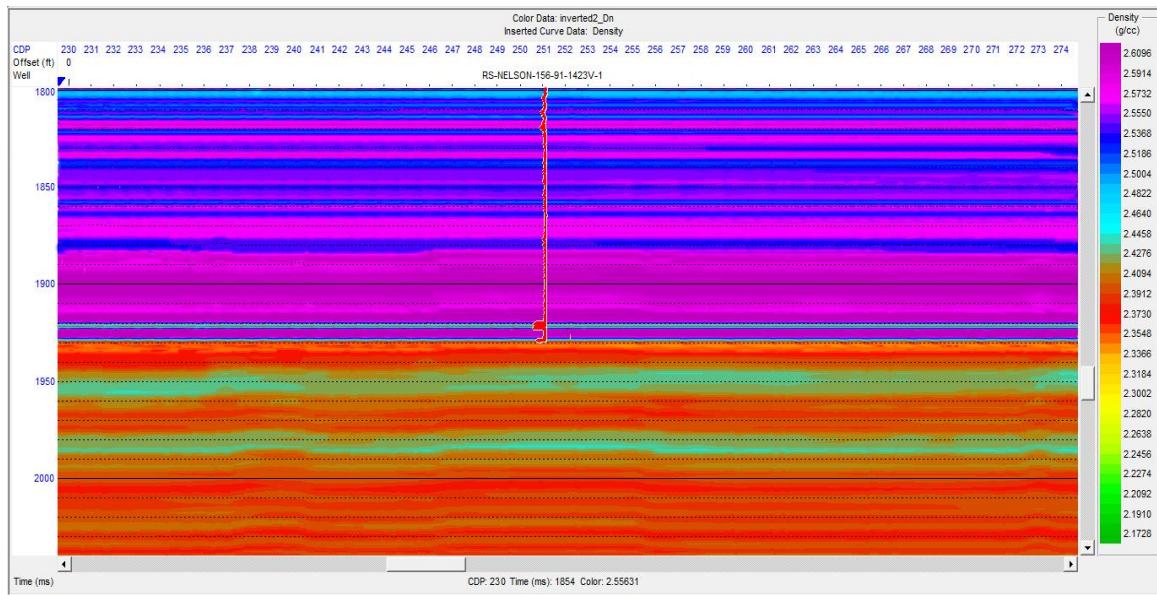Figure 7. 2 Inverted shear impedance result for 2001 seismic line

Figure 7. 3 Inverted density result for 2001 seismic line
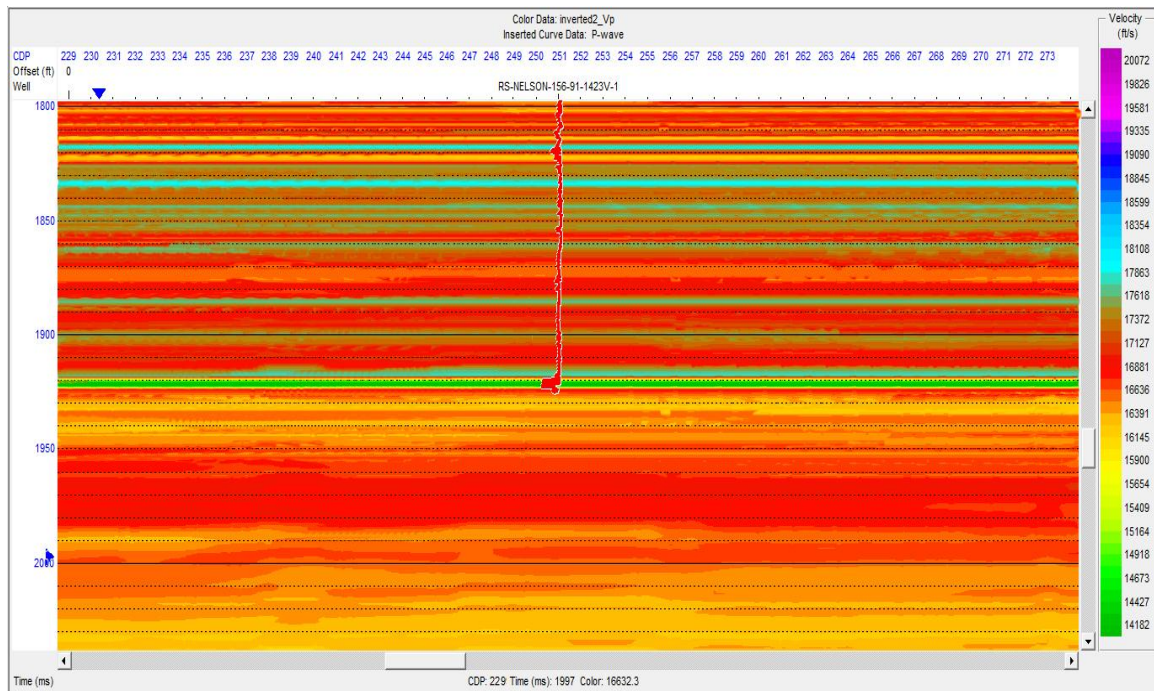
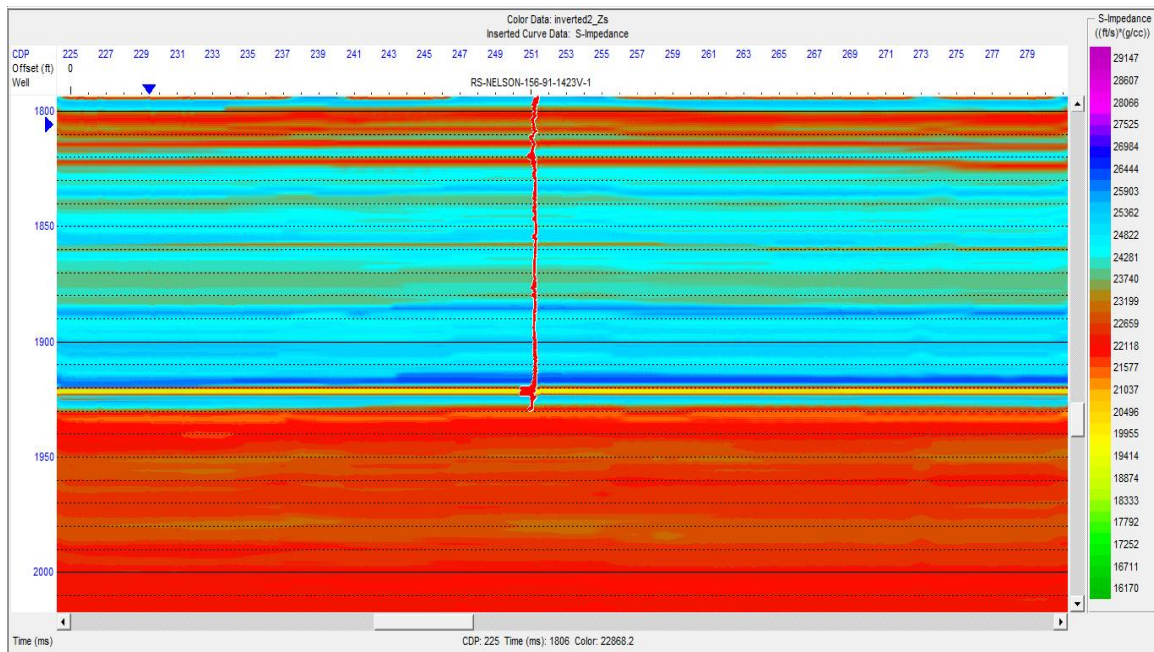Figure 7. 4 Inverted P-wave velocity result for 2001 seismic line

Figure 7. 5 Inverted S-wave velocity result for 2001 seismic line

Figure 7. 6 Inverted acoustic impedance result for 1001 seismic line
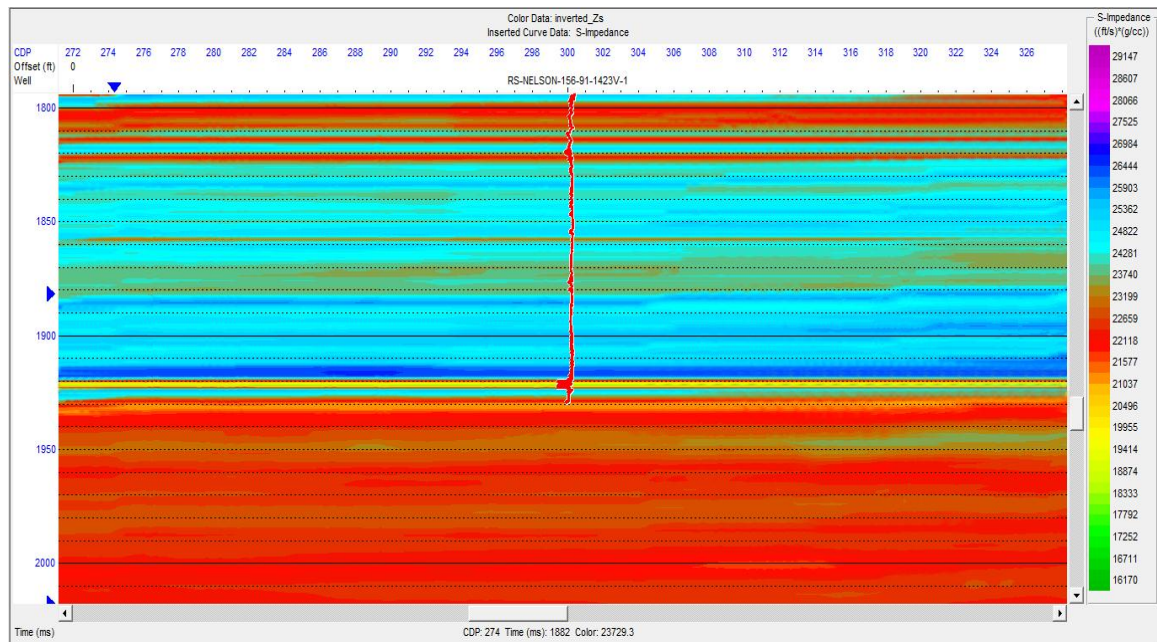
Figure 7. 7 Inverted shear impedance result for 1001 seismic line

85
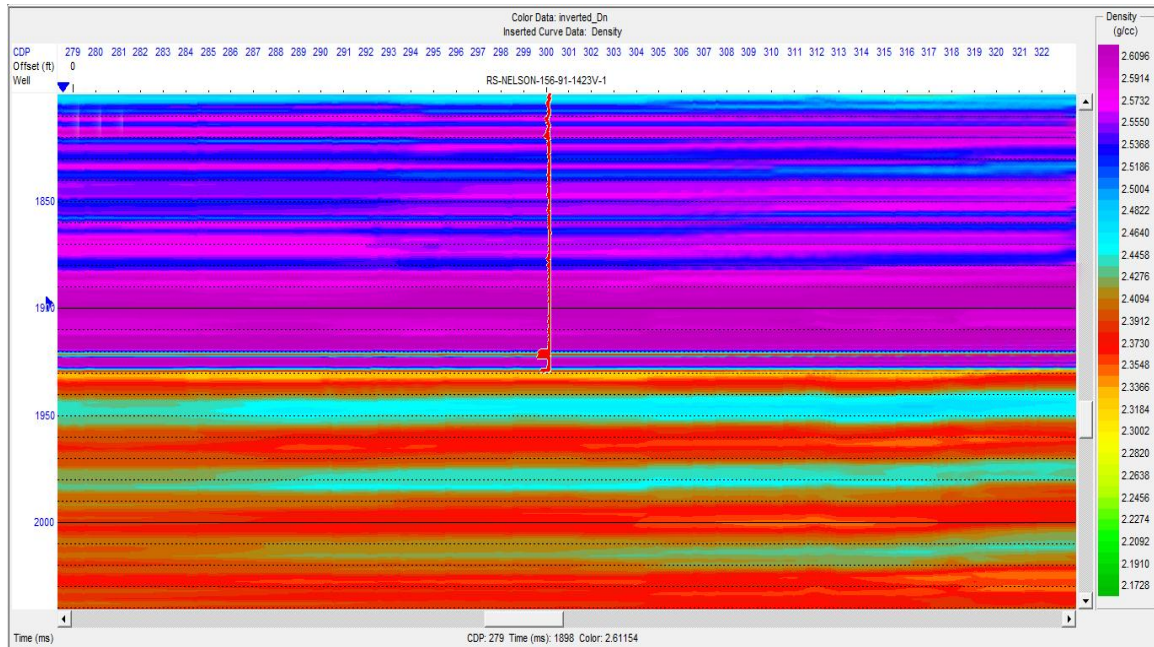
Figure 7. 8 Inverted density result for 1001 seismic line
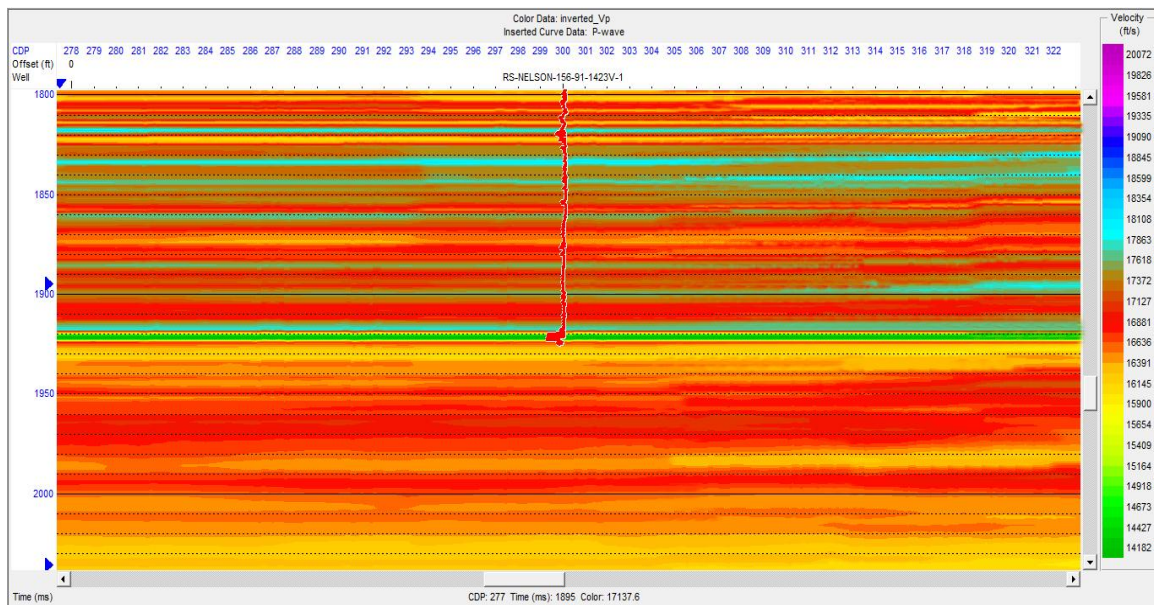
Figure 7. 9 Inverted P-wave result for 1001 seismic line
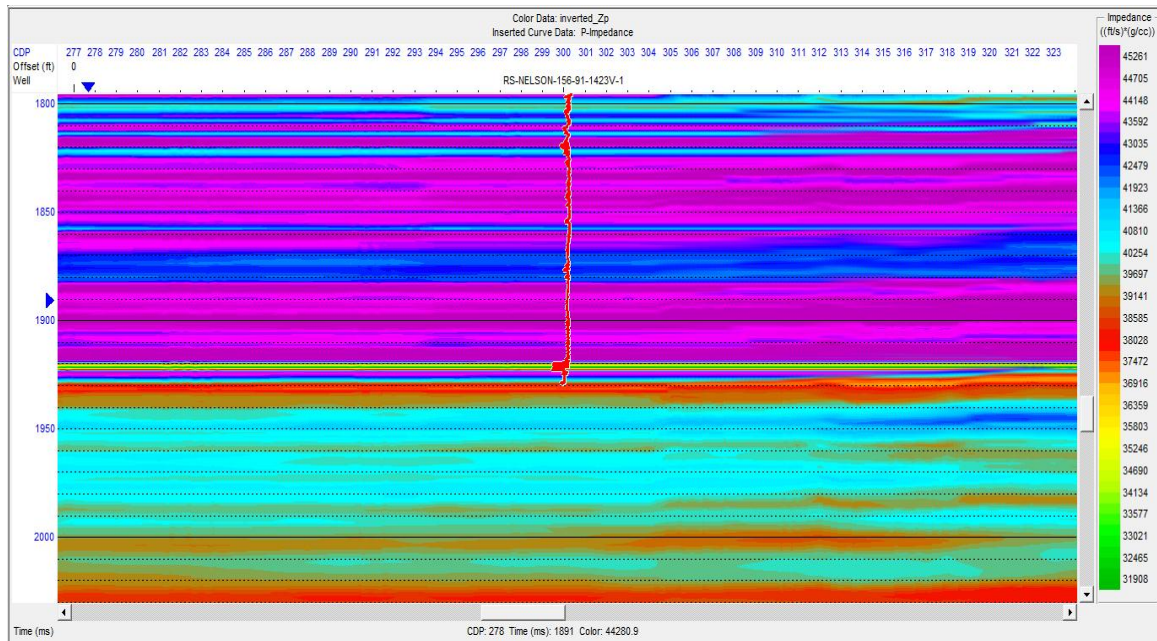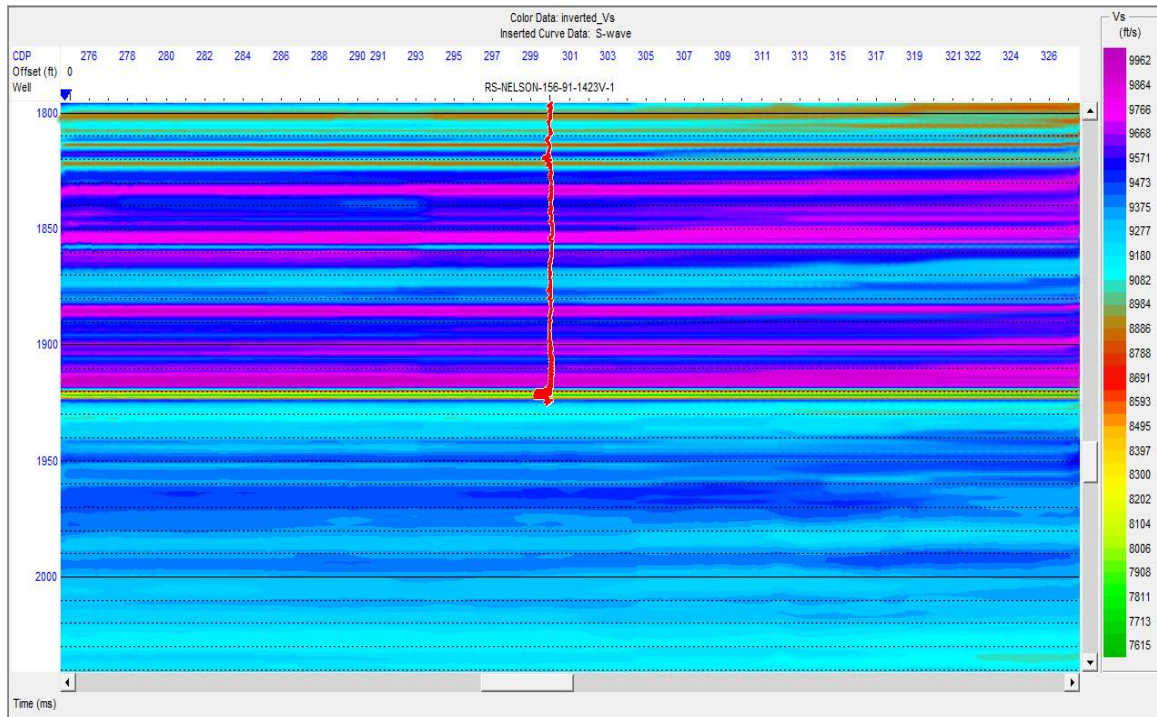
Figure 7. 10 Inverted S-wave result for 1001 seismic line

| 1001 Seismic line | 2001 Seismic line |
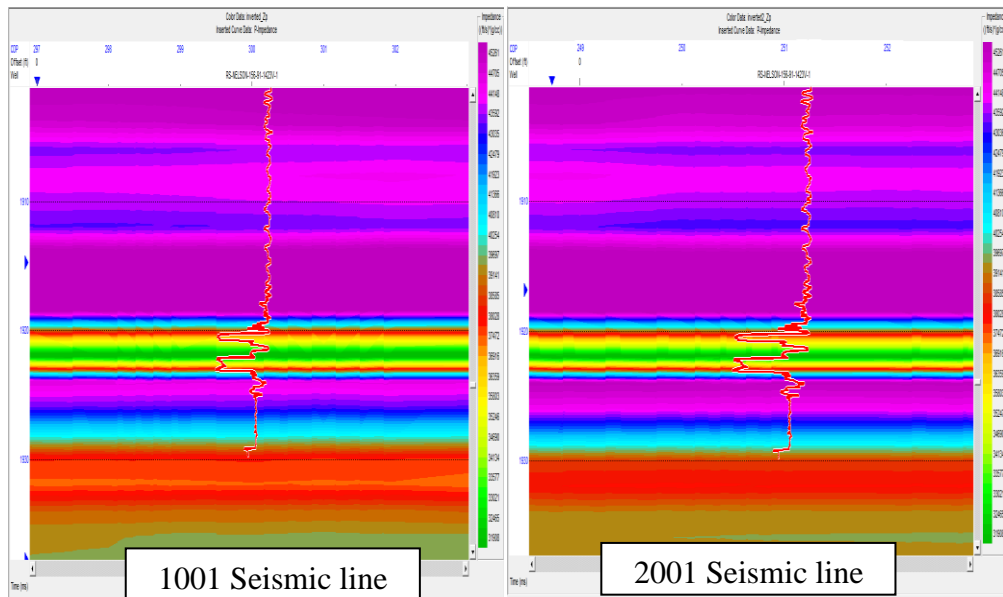
Figure 7. 11 Close-up view of the Bakken Formation's acoustic impedance inverted
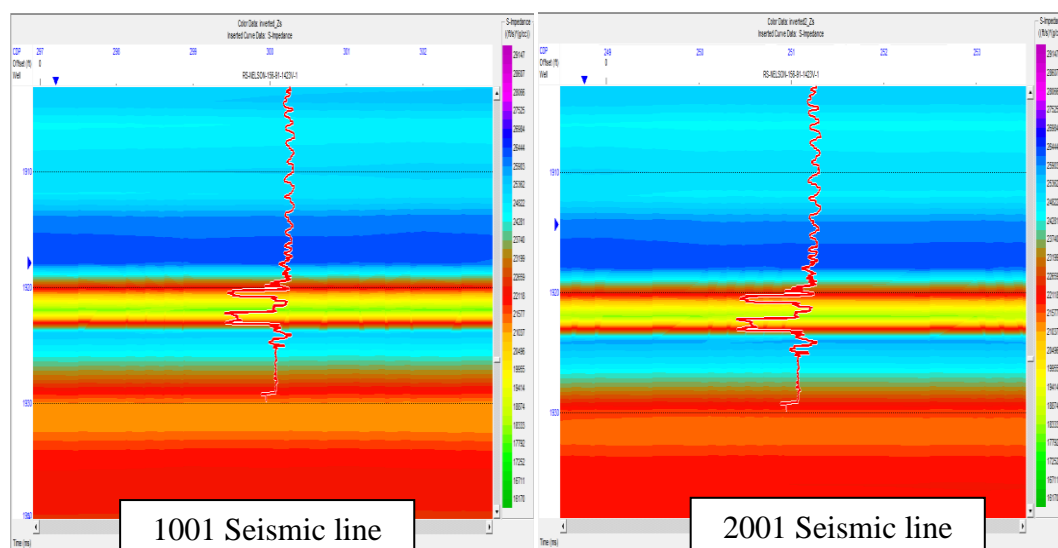
result.

Figure 7. 12 Close-up view of the Bakken Formation's shear impedance inverted results.
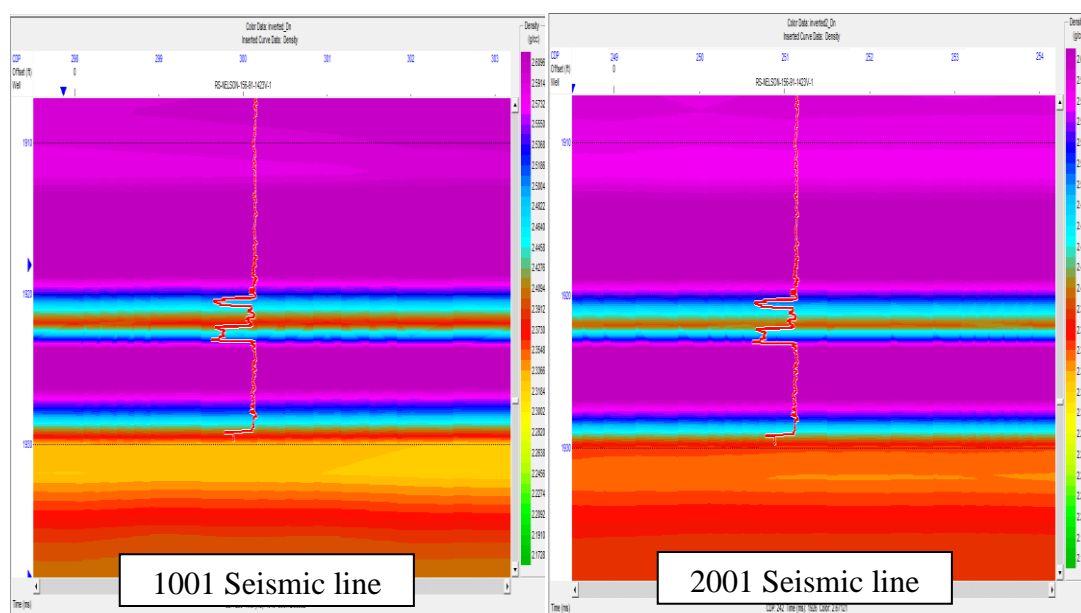
Figure 7. 13 Close-up view of the Bakken Formation's density inverted results.
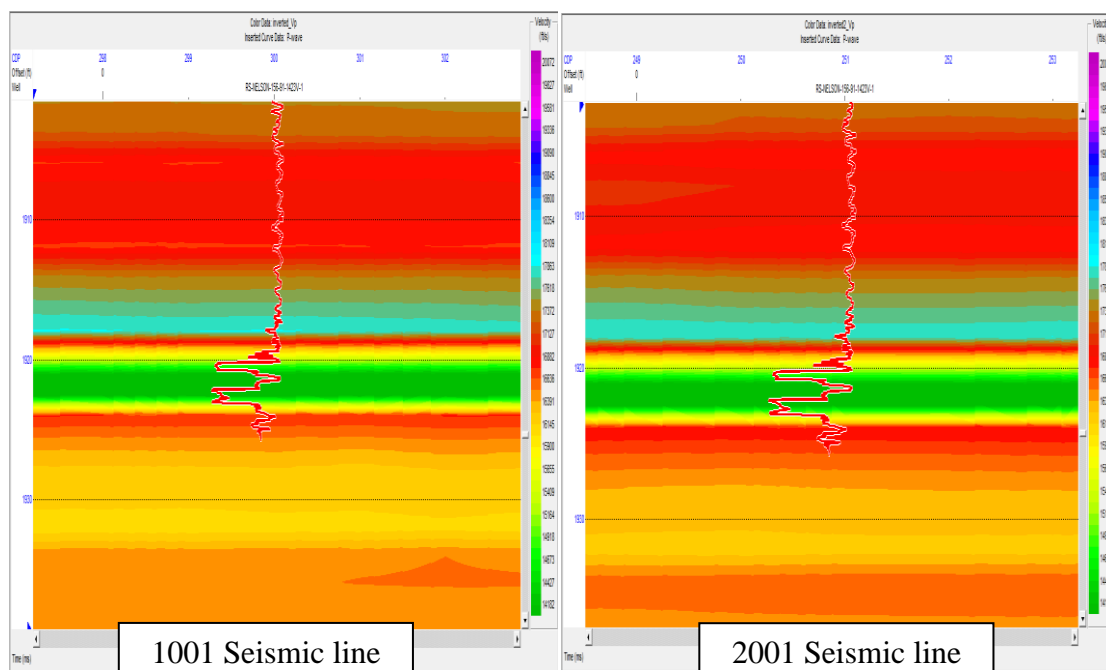
Figure 7. 14 Close-up view of the Bakken Formation's P-wave velocity inverted results.
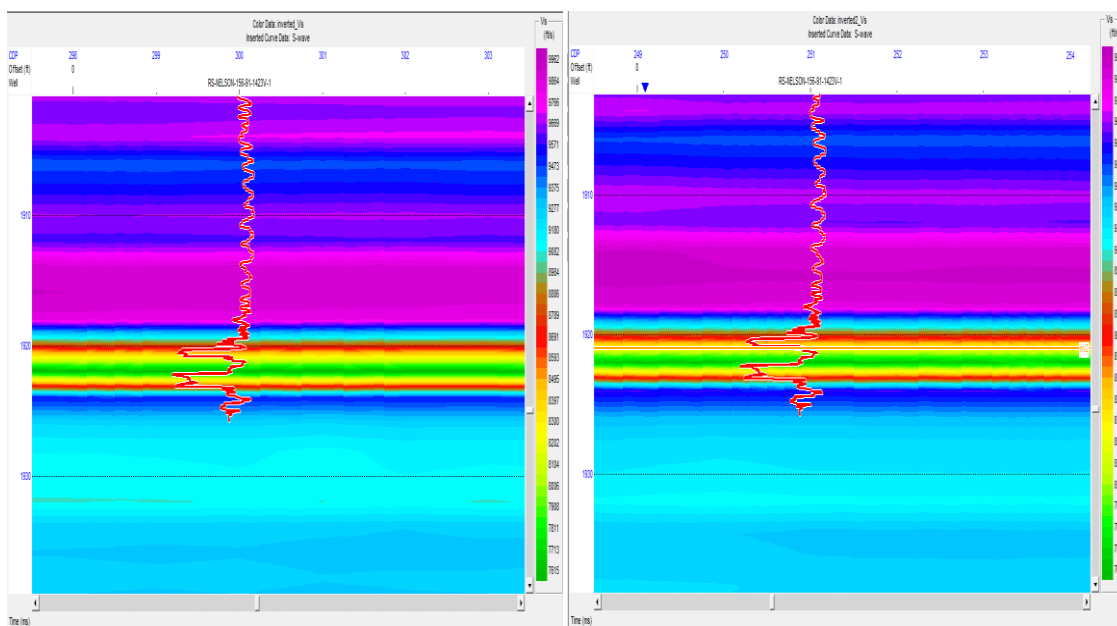
Figure 7. 15 Close-up view of the Bakken Formation's S-wave velocity inverted results.

7.3 LMR Cross-plot Results

The cross-plots of Lambda-Rho and Mu-Rho, derived from simultaneous inversion, have been used in LMR cross-plot template of Goodway (2010) and were interpreted.

The Lower Member and the Upper Member of the Bakken Formation are interpreted as shale since $\lambda/\mu=1$. We can specify it as ductile shale since the incompressibility value (λ) is low. The Middle Member of the Bakken Formation can easily be recognized as carbonate formation, since $1<\lambda/\mu<2$ and the Lambda-Rho value is high.

The LMR simultaneous inversion volume attributes were created after the cross-plot have shown bending just like pre-stack simultaneous inversion. This has shown us the change on the seismic section of the Bakken Formation.
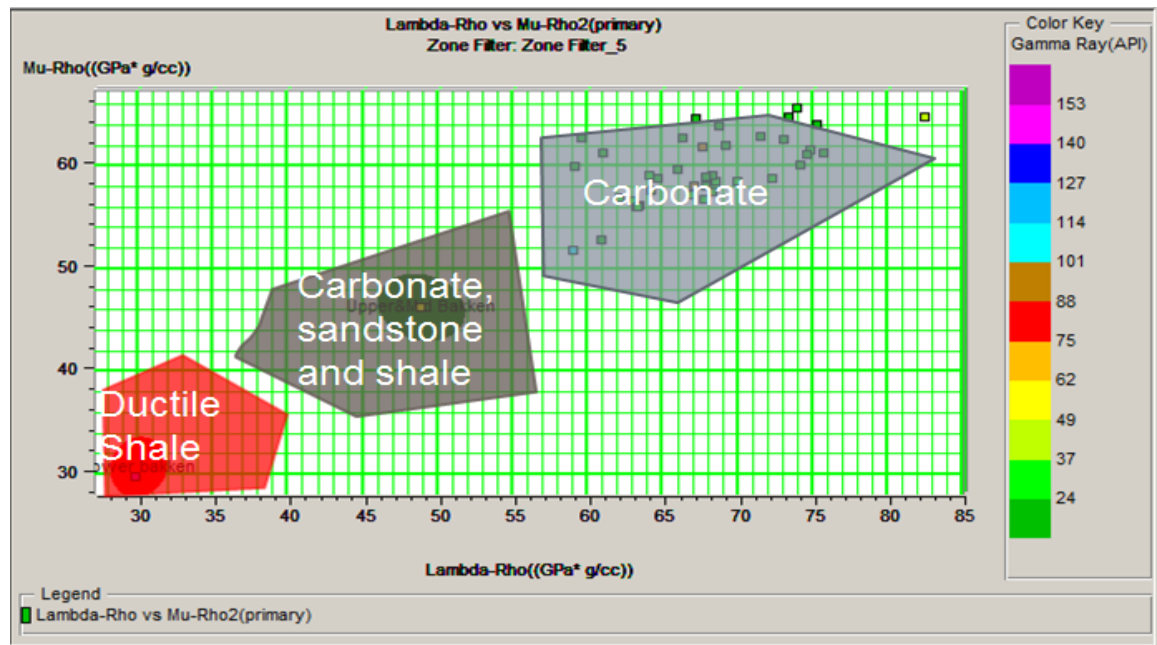
Figure 7. 16 LMR cross-plot interpretation.

Conclusion

The purpose of this study was to analyze the rock properties of the Bakken Formation which lies at 9120 ft. (2780 m) depth. The forward modeling AVO analysis to determine the rock properties was not able to give any effective results. In order to receive more reliable information, pre-stack simultaneous inversion and LMR analysis have been performed on the data.

First of all, angle gather has been created by correlating well logs with the seismic. Trim statics and bandpass filters were applied to the angle gathers, to be ready for the inversion analysis.

Even though the velocity changes follows the trends within the logs in inversion results, the values in the logs have been found to be lower than inversion values. After LMR, it has been seen that the Lower and Upper Members of the Bakken Formation are ductile, while the Middle Member is carbonate rock, sandstone, and shale.

It has been seen after all the research that the lateral offset is 1800 ft (550m) long towards east-west and north-south within the survey area of the Bakken Formation. It can be seen that the thickness of the Bakken Formation gets lesser and deeper towards the southwest direction. After concluding the information from the log data, seismic inversion and LMR cross-plotting, the Upper and Lower Bakken members contain more shale compared to the Middle Bakken. The Upper and Lower Bakken have high gamma rays and low Vp/Vs

ratio. It is also concluded in this research that it is ductile shale. However, the Middle Member is a mixed formation. It is the alternation of dolomite and sandstone with less shale contribution. It has high Vp/Vs and low gamma ray values. According to the inversion results, it can be concluded that the Bakken Formation conserves its characteristics throughout the offsets in lateral direction.

In conclusion, simultaneous inversion and LMR analysis helped to obtain useful and successful results in order to analyze the rock properties and the reservoir zone better. Achieving correct results from this analysis is imperative to conclude seismic well tie correctly. Even though the seismic resolution is low, it is possible to achieve effective information by improving resolution through inversion. 2D seismic data has been used in this study and only one well lies within the seismic section. It is possible to obtain more accurate results by using more well log information and 3D seismic data.

References

- Carl T., Michael B. Smith, & NSI Technologies (2010, December). *Hydraulic fracturing*. Retrieved from http://www.spe.org/jpt/print/archives/2010/12/10Hydraulic.pdf

- Castagna, J.P., and Swan, H.W. ,1997, Principles of AVO cross-plotting: The Leading Edge, Vol. 4, No. 16, 337-342.

- Echos-Paradigm, 2011, WSHAPE deconvolution guide.

- Goodway, B., Chen, T., & Downton, J. (1997). Improved AVO fluid detection and lithology discrimination using Lamé petrophysical parameters, SEG Technical Program Expanded Abstracts 1997: pp. 183-186.

- Goodway, B. , 2001, AVO and Lamé constants for rock parameterization and fluid detection. GSEC Recorder: Vol. 6, 39-60.

- Goodway, B., et al. , 2010, Seismic petrophysics and isotropic-anisotropis AVO methods for unconventional gas exploration. The Leading Edge: Vol. 12, 1500-1508.

- Hampson and Russell Software, CGG Veritas, Strata Workshop, June 2012.

- Hayes, M. D., 1984, Conodonts of the Bakken Formation (Devonian and Mississippian), Williston Basin, North Dakota: M.S. thesis, University of North Dakota.

- Karasinski D. R., 2006, Sedimentology and Hydrocarbon Potential of the Devonian Three Forks and Mississippian Bakken Formations, Sinclair Area,

Southeast Saskatchewan-Southwest Manitoba: M.S. Thesis, University of Manitoba (Canada).

- Li, Y., et al. , 2003, Recent advances in application of AVO to carbonate reservoirs. <u>CSEG Recorder</u>**:** 34-40.

- Manz, L. A., 2008, Deep Geothermal Resources: Estimated Temperature on Top of the Lodgepole Formation Cedar Hills Field, Bowman/Slope Counties, North Dakota. North Dakota Geological Survey Geological Investigations No. 69.

- Mason, J. (2012). Oil production potential of the North Dakota Bakken. *Oil Production Potential of the North Dakota Bakken*, <u>Oil and Gas Journal</u>: p.4

- Mavko, G., T. Mukerji, and J. Dvorkin, 2003, The Rock Physics Handbook: Tools For Seismic Analysis in Porous Media: Cambridge University Press.

- Mendelson, A. B., 1985, Petroleum Source Rock Logging. M.S. Thesis, Earth and Atmospheric and Planetary Sciences, Massachusetts Institute of Technology.

- Ostrander, W. J., 1984, Plane-wave reflection coefficients for gas sands at non-normal angles of incidence. <u>Geophysics</u>: Vol. 49, 1637-1648.

- Perez, M. and R. Tonn, 2003, Reservoir Modelling and Interpretation with Lamé's Parameters: A Grand Banks Case Study. Interpretation Templates, EnCana Corporation.

- Pitman, J., L. Price, and J, Lefever. , 2001, Diagenesis and Fracture Development in the Bakken Formation, Williston Basin, Implications on Reservoir Quality in the Middle Member. Denver: U.S. Geological Survey Professional Paper 1653, 1-19

- Russell, B.H., 1991, "Introduction to seismic inversion methods", *SEG continuing Education Short Course.*

- Russell, B., and Hampson, D., 1999, AVO theory, Hampson-Russell software services limited, 69 p.

- Russell, B., 2005, Strata workshop: Theory and exercises in seismic inversion and AVO, unpublished lecture notes.

- Rutherford, S.R., and Williams, R.H. , 1989, Amplitude versus offset variations in gas sands, Geophysics, Vol. 54, No. 6, 680 - 688.

- Savic, M., VerWest, B., Masters, R., Sena, A., and Gingrich, D., 2000, Elastic impedance inversion in practice: SEG Expanded Abstracts, Vol. 19, 689.

- Sheriff, R. E., 2002, Encyclopedic Dictionary of Applied Geophysics: Society of Exploration Geophysicists.

- Tatham, R. H., and M. D. McCormack, 1991, Multicomponent Seismology in Petroleum Exploration: Society of Exploration Geophysicists.

- U.S. Geological Survey petroleum resource assessment of the Bakken Formation, Williston Basin Province, Montana and North Dakota: U.S. Geological Survey presentation, U.S. Department of Interior, Washington, D.C., April 2008.